

ผลของการเติมผลึกเหลวโมเลกุลต่ำต่อโครงสร้างผลึกของไอโซแทกติกพอลิโพรพิลีน



นายเอกลักษณ์ สิงห์หนู

สถาบันวิทยบริการ
จุฬาลงกรณ์มหาวิทยาลัย

วิทยานิพนธ์นี้เป็นส่วนหนึ่งของการศึกษาตามหลักสูตรปริญญาวิทยาศาสตรมหาบัณฑิต

สาขาวิศวกรรมเคมี ภาควิชาวิศวกรรมเคมี

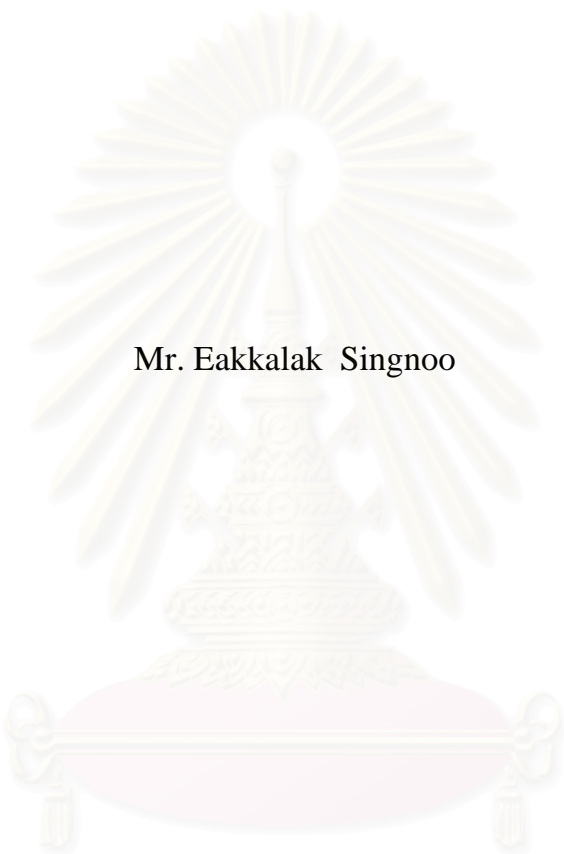
คณะวิศวกรรมศาสตร์ จุฬาลงกรณ์มหาวิทยาลัย

ปีการศึกษา 2546

ISBN 974-17-4995-3

ลิขสิทธิ์ของจุฬาลงกรณ์มหาวิทยาลัย

EFFECTS OF LOW MOLAR MASS LIQUID CRYSTAL ADDITION ON
CRYSTAL STRUCTURE OF ISOTACTIC POLYPROPYLENE



Mr. Eakkalak Singnoo

สถาบันวิทยบริการ
จุฬาลงกรณ์มหาวิทยาลัย

A Thesis Submitted in Partial Fulfillment of the requirements
for the Degree of Master of Engineering in Chemical Engineering
Department of Chemical Engineering
Faculty of Engineering
Chulalongkorn University
Academic Year 2003
ISBN 974-17-4995-3

Thesis Title EFFECTS OF LOW MOLAR MASS LIQUID CRYSTAL
 ADDITION ON CRYSTAL STRUCTURE OF
 ISOTACTIC POLYPROPYLENE

By Mr. Eakkalak Singnoo

Field of Study Chemical Engineering

Thesis Advisor Assistant Professor ML. Supakanok Thongyai , Ph.D.

Accepted by the Faculty of Engineering , Chulalongkorn University
in Partial Fulfillment of the Requirements for the Master's Degree.

..... Dean of the Faculty of Engineering
(Professor **Direk Lavansiri** , Ph.D.)

THESIS COMMITTEE

..... Chairman
(Associate Professor Suttichai Assabumrungrat , Ph.D.)

..... Thesis Advisor
(Assistant Professor ML. Supakanok Thongyai , Ph.D.)

..... Member
(Assistant Professor Seeroong Prichanont , Ph.D.)

..... Member
(Bunjerd Jongsomjit , Ph.D.)

เอกฉัตรชัย สิงห์หนู : ผลของการเติมผลึกเหลวมวลโมเลกุลต่ำ ต่อโครงสร้างผลึกของไอโซแทกติกพอลิโพรพิลีน (EFFECTS OF LOW MOLAR MASS LIQUID CRYSTAL ADDITION ON CRYSTAL STRUCTURE OF ISOTACTIC POLYPROPYLENE).อาจารย์ที่ปรึกษา : ผศ.ดร.มล. ศุภกนก ทองใหญ่ ,116 หน้า ISBN 974-17-4995-3.

งานวิจัยนี้ มุ่งเน้นที่จะศึกษาเกี่ยวกับลักษณะโครงสร้างผลึกของพอลิเมออร์ผสมระหว่าง พอลิโพรพิลีน และ สารผลึกเหลวมวลโมเลกุลต่ำ หรือ กลีเซอรอลโมโนสเตียเรท โดยใช้กล้องจุลทรรศน์อิเล็กตรอนแบบส่องกราด Scanning Electron Microscope (SEM) ในการศึกษาโครงสร้างผลึก และใช้เทคนิค small angle light scattering (SALS) ในการศึกษาพฤติกรรมการกระเจิงแสง อีกทั้งการใช้เทคนิค X-ray Diffraction (XRD) ในการหาค่าเปอร์เซ็นต์ความเป็นผลึกจากพื้นที่ได้กราฟ ตลอดจนหาอุณหภูมิหลอมเหลวผลึก (Tm) และ อุณหภูมิตกผลึก (Tc) โดยการวิเคราะห์ Differential Scanning Diffraction (DSC) เพื่อนำมาใช้ในการสนับสนุนพฤติกรรมการตกผลึกของพอลิเมออร์ผสม จากผลวิเคราะห์ที่กล่าวมานี้ พบว่า มีความสัมพันธ์กันระหว่างแต่ละผลการทดลอง กล่าวคือผลวิเคราะห์ Small angle light scattering (SALS) จะมีความสอดคล้องกับ ผลวิเคราะห์ X-ray Diffraction (XRD) โดยที่ พอลิเมออร์ผสมที่มี เปอร์เซ็นต์ความเป็นผลึกมากกว่า จะสามารถ กระเจิงแสงเลเซอร์ได้ดีกว่า แต่เฉพาะในกรณีของพอลิโพรพิลีนที่สังเคราะห์จากตัวเร่งปฏิกิริยาเมทัลโลซีน จากการวิเคราะห์ DSC สารผลึกเหลวมวลโมเลกุลต่ำ และ กลีเซอรอลโมโนสเตียเรท สามารถลด อุณหภูมิหลอมเหลวผลึก เพราะสารทั้งสอง ไปลดความหนืดหลอมเหลวของพอลิเมออร์ผสม ทำให้ผลึกหลอมเหลวได้ในอุณหภูมิต่ำกว่า อีกทั้งสารผลึกเหลวมวลโมเลกุลต่ำ และ กลีเซอรอลโมโนสเตียเรท ยังไปเพิ่มอุณหภูมิตกผลึกของพอลิเมออร์ผสม แต่เฉพาะพอลิโพรพิลีนที่สังเคราะห์จากตัวเร่งปฏิกิริยาซีเกลอร์-แนตตา เนื่องจากสารผลึกเหลวมวลโมเลกุลต่ำ และ กลีเซอรอลโมโนสเตียเรททำให้โมเลกุลเคลื่อนที่ได้เร็วขึ้น ส่งผลให้เกิดการตกผลึกได้ที่อุณหภูมิต่ำกว่า

สถาบันวิทยบริการ
จุฬาลงกรณ์มหาวิทยาลัย

ภาควิชา วิศวกรรมเคมี
สาขาวิชา วิศวกรรมเคมี
ปีการศึกษา 2546

ลายมือชื่อนิสิต.....
ลายมือชื่ออาจารย์ที่ปรึกษา.....

##4570665421: MAJOR CHEMICAL ENGINEERING

KEY WORD: STATIC LIGHT SCATTERING / POLYPROPYLENE / LOW MOLAR MASS LIQUID CRYSTAL / CRYSTALLIZATION

EAKKALAK SINGNOO : EFFECTS OF LOW MOLAR MASS LIQUID CRYSTAL ADDITION ON CRYSTAL STRUCTURE OF ISOTACTIC POLYPROPYLENE. THESIS ADVISOR: ASSISTANT PROFESSOR ML. SUPAKANOK THONGYAI, Ph.D. , 116 pp. ISBN 974-17-4995-3.

This research is concerned with studying the crystallization and the morphologies of polymer blends between isotactic polypropylene and low molar mass liquid crystal chemical (LCC) or glycerol monostearate (GMS). Propylene polymerization was carried out using the ansa-metallocene $\text{Et}[\text{Ind}]_2\text{ZrCl}_2$ as catalyst and methylaluminoxane (MAO) as cocatalyst and Ziegler-Natta - synthesized polypropylenes were purchased . The blends were investigated by Small Angle Light Scattering (SALS) , X-ray Diffraction (XRD) , Differential Scanning Calorimetry (DSC) and Scanning Electron Microscope (SEM). The correlative results of each analytically characteristic techniques were observed. Comparation between light scattering results obtained from SALS technique and crystallinity results from XRD technique are corresponded in the case of metallocene-synthesized polypropylene , namely better light scattering come from higher crystallinity. LCC and GMS can also slightly decrease melting temperature of the blends because they reduce **melt viscosity** of the blends ,therefore melting phenomena can occur at lower temperature. In the case of Ziegler-Natta - synthesized polypropylene, crystallization temperature of the GMS and LCC blends significantly increase because LCC and GMS are able to enhance molecular mobility, therefore crystallization is able to occur at higher temperature .

Department Chemical Engineering Student's signature.....

Field of study Chemical Engineering Advisor's signature.....

Academic year 2003

Acknowledgement

I would like to express my deeply gratitude to my advisor : Assistant Professor ML. Supakanok Thongyai , Ph.D. to his continuous guidance , enormous number of invaluable discussions , helpful suggestions and warm encouragement. I am grateful to Associate Professor Suttichai Assabumrungrat , Ph.D. , Assistant Professor Seeroong Prichanont , Ph.D. and Bunjert Jongsomjit , Ph.D. for serving as chairman and thesis committees , respectively , whose comments were constructively and especially helpful.

Sincere thanks are made to the Scientific and Technological Research Equipment Center , Chulalongkorn University for using scanning electron microscope (SEM) , the Central Instrument Facility (CIF) , Mahidol University for using differential scanning calorimetry measurement (DSC) and the Metallurgy and Materials Science Research Institute , Chulalongkorn University for using high temperature X-ray diffraction (XRD) in this study.

Sincere thanks to all my friends and all members of the Center of Excellence on Catalysis and Catalytic Reaction Engineering Research Laboratory and all members of the polymer Engineering Research Laboratory , Department of Chemical Engineering , Chulalongkorn University , for their assistances and friendly encouragement.

Finally , I would like to dedicate this thesis to my parents and families , who generous supported and encouraged me through the year spent on this study.

Contents

	Page
Abstract (in Thai).....	iv
Abstract (in English).....	v
Acknowledgement.....	vi
Contents.....	vii
List of Tables.....	x
List of Figures.....	xi
 Chapter	
I Introduction.....	1
1.1 General Introduction.....	1
1.2 The objectives of this research.....	3
1.3 The scope of this research.....	3
II Theories.....	4
2.1 Metallocene Catalysts.....	4
2.1.1 Tailoring of metallocene catalysts.....	5
2.1.2 Isotactic polymers using metallocene catalysts.....	6
2.1.3 Single-Center Catalysts.....	7
2.1.4 Cocatalytic Systems for Metallocene-Based Catalysis (MBC)....	9
2.2 Polymer Morphology.....	10
2.2.1 The Amorphous State.....	10
2.2.2 Glass Transition Temperature , T _g	10
2.2.3 The Crystalline Polymer.....	11
2.2.4 Liquid crystal.....	13
2.2.4.1 Introduction to the liquid crystal.....	13
2.2.4.2 Structure of liquid Crystals.....	14
2.2.4.2.1 Smectic structure.....	14
2.2.4.2.2 Nematic structure.....	15
2.2.4.2.3 Cholesteric or chiral nematic structure.....	15
2.2.4.2.4 Discotic structure.....	16
2.2.4.2 Mesophasic Transition Temperature.....	17
2.3 Melting Phenomena.....	18
2.4 Thermal Properties.....	18
2.5 Structure of Crystalline Polymers.....	19
2.6 Crystal Structure in polymers.....	20

Contents (continued)

	Page
2.6.1 Crystallization from dilute solution.....	20
2.6.1.1 Polymer Single Crystals.....	20
2.6.1.2 The Folded Chain Model.....	21
2.6.1.3 The Switchboard Model.....	21
2.6.2 Crystallization From the Melt.....	21
2.6.2.1 Spherulitic Morphology.....	21
2.6.2.2 Mechanism of Spherulite Formation.....	23
2.6.2.3 Spherulites in Polymer Blends.....	23
2.6.2.4 Effect of Crystallinity on Tg.....	24
2.7 Light Scattering Theory.....	24
2.8 Polymer Blends.....	26
2.8.1 The Blends Preparations.....	26
2.8.1.1 Melt Mixing.....	26
2.8.1.2 Solvent Casting.....	26
2.8.1.3 Freeze Drying.....	27
2.8.1.4 Emulsions.....	27
2.8.1.5 Reactive Blend.....	28
2.9 Permanganic etching.....	28
III Literature Reviews.....	29
IV Experiments.....	35
4.1 Materials and Chemicals.....	35
4.1.1 Synthesis Part.....	35
4.1.2 Polymer Blend Part.....	36
4.2 Equipments.....	37
4.2.1 Synthesis Part.....	37
4.2.2 Polymer Blend Part.....	40
4.3 Polymerization Procedure.....	40
4.4 Sample Preparations.....	41
4.4.1 Sample preparation for light scattering (SALS).....	41
4.4.2 Sample preparation for scanning electron microscope (SEM)....	41
4.4.3 Sample preparation for X-ray Diffraction (XRD).....	42
4.4.4 Sample preparation for Differential Scanning Calorimetry (DSC).....	42
4.5 Characterization Instruments.....	43
4.5.1 Small Angle Light Scattering (SALS).....	43
4.5.2 Scanning Electron Microscopy (SEM).....	44
4.5.3 Differential Scanning Calorimetry (DSC).....	45

Contents (continued)

	Page
4.5.4 X-Ray Diffraction (XRD).....	45
V Results and Discussions.....	46
5.1 Polymerization of Propylene.....	46
5.1.1 The Effect of Polymerization Time on Catalytic Activity.....	46
5.2 Light Scattering Measurement.....	48
5.2.1 Scattered light photographs.....	48
5.2.2 Digital Intensity data.....	55
5.2.2.1 Smoothing Digital Intensity Data.....	57
5.2.2.2 Removing the beam stop.....	66
5.3 Differential Scanning Calorimetry (DSC).....	68
5.4 Scanning Electron Microscopy (SEM).....	71
5.5 X-Ray Diffraction (XRD).....	76
VI Conclusions and Recommendations.....	85
References.....	87
Appendices.....	90
Appendix A : The light scattering measurement and etching	91
Appendix B : The data of DSC characterization	92
Appendix C : The data of XRD characterization	107
Vita.....	116

List of Tables

	Page
Table 5.1 : Yields and catalytic activities of polypropylene produced at different polymerization time	46
Table 5.2 : Properties of polypropylene that synthesized by metallocene catalyst and Ziegler-Natta catalyst.....	48
Table 5.3 : Melting temperature and Crystallization temperature of Polypropylene and their blends.....	68
Table 5.4 : Melting lattice energy and Lattice energy of polypropylene and their blends.....	69
Table 5.5 : % Crystallinity of polypropylenes and their blends.....	83



สถาบันวิทยบริการ
จุฬาลงกรณ์มหาวิทยาลัย

List of Figures

	Page
Figure 2.1 : The mechanism of olefin polymerization using metallocene catalysts.....	4
Figure 2.2 : Different types of polymer tacticity.....	6
Figure 2.3 :The production of isotactic polymers using chiral metallocene catalysts.....	7
Figure 2.4 : Organometallic complexes employed in olefin polymer.....	8
Figure 2.5 : Three different configurations of a polypropylene.....	12
Figure 2.6 : (a) Smectic structure. (b)liquid crystal chemical structures of Smectic structure.....	15
Figure 2.7 : (a) Nematic structure. (b) liquid crystal chemical structures of Nematic structure.....	15
Figure 2.8 : (a) Cholesteric structure. (b) liquid crystal chemical structures of Cholesteric structure.....	16
Figure 2.9 : (a) Discotic structure. (b) liquid crystal chemical structures of Discotic structure.....	16
Figure 2.10 : Phase transition of Liquid Crystal.....	17
Figure 2.11 : The fringed micelle model. Each chain meanders from crystallite to crystallite, binding the whole mass together.....	19
Figure 2.12 : Model of spherulitic structure.....	22
Figure 2.13 : A typical photographic light scattering apparatus.....	25
Figure 4.1 : Schlenk line.....	38
Figure 4.2 : Schlenk tube.....	39
Figure 4.3 : Glove box.....	39
Figure 4.4 :A schematic diagram of static light scattering equipment.....	43
Figure 5.1 : Yield of polypropylene produced at different polymerization times.....	46
Figure 5.2 : Catalytic activity of polypropylene produced at different polymerization times.....	47
Figure 5.3 : Scattering light photographs of pure polypropylene 1 and their blends of LC and GMS.....	49
Figure 5.4 : Scattering light photographs of pure polypropylene 2 and their blends of LC and GMS.....	50

List of Figures (continued)

	Page
Figure 5.5 : Scattering light photographs of pure polypropylene 3 and their blends of LC and GMS.....	51
Figure 5.6 : Scattering light photographs of pure polypropylene 4 and their blends of LC and GMS.....	52
Figure 5.7 : Scattering light photographs of pure polypropylene 5 and their blends of LC and GMS.....	53
Figure 5.8 : Scattering light photographs of pure polypropylene 6 and their blends of LC and GMS.....	54
Figure 5.9 : Scattered light contour graphs of (a) Pure Polypropylene 1 , (b) Polypropylene 1/1% LC and (c) Polypropylene 1/1% GMS.....	55
Figure 5.10 : Schematic diagram of smoothing procedure.....	56
Figure 5.11 : Contour graphs of trial and error in smoothing intensity data...	59
Figure 5.12 : Smoothed contour graphs of (a) pure polypropylene 1 , (b) polypropylene1 /1% LC and (c) polypropylene 1 / 1% GMS blends.....	60
Figure 5.13 : Smoothed contour graphs of (a) pure polypropylene 2 , (b) polypropylene2 /1% LC and (c) polypropylene 2 / 1% GMS blends.....	61
Figure 5.14 : Smoothed contour graphs of (a) pure polypropylene 3 , (b) polypropylene 3 /1% LC and (c) polypropylene 3 / 1% GMS blends.....	62
Figure 5.15 : Smoothed contour graphs of (a) pure polypropylene 4 , (b) polypropylene4 /1% LC and (c) polypropylene 4 / 1% GMS blends.....	63
Figure 5.16 : Smoothed contour graphs of (a) pure polypropylene 5 , (b) polypropylene5 /1% LC and (c) polypropylene 5 / 1% GMS blends.....	64
Figure 5.17 : Smoothed contour graphs of (a) pure polypropylene 6 , (b) polypropylene6 /1% LC and (c) polypropylene 6 / 1% GMS blends.....	65
Figure 5.18 : Contour graphs of (a) pure polypropylene 4 (b) polypropylene 4 / 1% LC and (c) polypropylene 4 / 1%GMS.....	66
Figure 5.19 : SEM Photograph of polypropylene that synthesized by metallocene.....	71

List of Figures (continued)

	Page
Figure 5.20 : SEM Photograph of polypropylene that synthesized by metallocene and their blends.....	72
Figure 5.21 : SEM Photograph of spherulites of polypropylene 4 and their blends.....	73
Figure 5.22 : SEM Photograph of spherulites of polypropylene 5 and their blends.....	74
Figure 5.23 : SEM Photograph of spherulites of polypropylene 6 and their blends.....	75
Figure 5.24 : X-ray diffractograms of amorphous reflection of Polypropylene.....	76
Figure 5.25 : X-ray diffractogram of pure polypropylene 1.....	77
Figure 5.26 : X-ray diffractograms of polypropylene 1 / 1% LCP.....	77
Figure 5.27 : X-ray diffractograms of polypropylene 1 / 1% LCP	77
Figure 5.28 : X-ray diffractogram of pure polypropylene 2.....	78
Figure 5.29 : X-ray diffractograms of polypropylene 2 / 1% LCP.....	78
Figure 5.30 : X-ray diffractograms of polypropylene 2 / 1% LCP	78
Figure 5.31 : X-ray diffractogram of pure polypropylene 3.....	79
Figure 5.32 : X-ray diffractograms of polypropylene 3 / 1% LCP.....	79
Figure 5.33 : X-ray diffractograms of polypropylene 3 / 1% LCP	79
Figure 5.34 : X-ray diffractogram of pure polypropylene 4.....	80
Figure 5.35 : X-ray diffractograms of polypropylene 4 / 1% LCP.....	80
Figure 5.36 : X-ray diffractograms of polypropylene 4 / 1% LCP	80
Figure 5.37 : X-ray diffractogram of pure polypropylene 5.....	81
Figure 5.38 : X-ray diffractograms of polypropylene 5 / 1% LCP.....	81
Figure 5.39 : X-ray diffractograms of polypropylene 5 / 1% LCP	81
Figure 5.40 : X-ray diffractogram of pure polypropylene 6.....	82
Figure 5.40 : X-ray diffractograms of polypropylene 6 / 1% LCP.....	82
Figure 5.40 : X-ray diffractograms of polypropylene 6 / 1% LCP	82
Figure B-1 : DSC curve of Pure Polypropylene 1.....	92
Figure B-2 : DSC curve of Pure Polypropylene 2.....	92
Figure B-3 : DSC curve of Pure Polypropylene 3.....	93
Figure B-4 : DSC curve of Pure Polypropylene 4.....	93
Figure B-5 : DSC curve of Pure Polypropylene 5.....	94
Figure B-6 : DSC curve of Pure Polypropylene 6.....	94
Figure B-7 : DSC curve of Polypropylene 1/ 1% LCC.....	95
Figure B-8 : DSC curve of Polypropylene 2/ 1% LCC.....	96
Figure B-9 : DSC curve of Polypropylene 3/ 1% LCC.....	97

List of Figures (continued)

	Page
Figure B-10 : DSC curve of Polypropylene 4/ 1% LCC.....	98
Figure B-11 : DSC curve of Polypropylene 5/ 1% LCC.....	99
Figure B-12 : DSC curve of Polypropylene 6/ 1% LCC.....	100
Figure B-13 : DSC curve of Polypropylene 1/ 1% GMS.....	101
Figure B-14 : DSC curve of Polypropylene 2/ 1% GMS.....	102
Figure B-15 : DSC curve of Polypropylene 3/ 1% GMS.....	103
Figure B-16 : DSC curve of Polypropylene 4/ 1% GMS.....	104
Figure B-17 : DSC curve of Polypropylene 5/ 1% GMS.....	105
Figure B-18 : DSC curve of Polypropylene 6/ 1% GMS.....	106
Figure C-1 : Amorphous curve of pure polypropylene1.....	107
Figure C-2 : Amorphous curve of polypropylene1/ 1%LCC.....	107
Figure C-3 : Amorphous curve of polypropylene1/ 1%GMS.....	108
Figure C-4 : Amorphous curve of pure polypropylene2.....	108
Figure C-5 : Amorphous curve of polypropylene2/ 1%LCC.....	109
Figure C-6 : Amorphous curve of polypropylene2/ 1%GMS.....	109
Figure C-7 : Amorphous curve of pure polypropylene3.....	110
Figure C-8 : Amorphous curve of polypropylene3/ 1%LCC.....	110
Figure C-9 : Amorphous curve of polypropylene3/ 1%GMS.....	111
Figure C-10 : Amorphous curve of pure polypropylene4.....	111
Figure C-11 : Amorphous curve of polypropylene4/ 1%LCC.....	112
Figure C-12 : Amorphous curve of polypropylene4/ 1%GMS.....	112
Figure C-13 : Amorphous curve of pure polypropylene5.....	113
Figure C-14 : Amorphous curve of polypropylene5/ 1%LCC.....	113
Figure C-15 : Amorphous curve of polypropylene5/ 1%GMS.....	114
Figure C-16 : Amorphous curve of pure polypropylene6.....	114
Figure C-17 : Amorphous curve of polypropylene6/ 1%LCC.....	115
Figure C-18 : Amorphous curve of polypropylene6/ 1%GMS.....	115

CHAPTER I

Introduction

1.1 General Introduction

Most ordinary people have been familiar with polymers, since the first synthetic polymer was made in the beginning of 20th century. Their development and commercialization has been spectacular. Regarding where we are or whatever we are doing, the probability of having something made by plastic around us is really high, for example, toys, pipes, many parts of cars and planes, are made from polymeric materials. Their easy processing and cheap price have been the key to their success.

Polyolefins are the most common and at the same time simplest polymer group. The basic polymers of this group are polyethylene and polypropylene. They were synthesized for the first time in 1933 in the laboratories of Imperial Chemical Industries (ICI), England, under high pressure conditions, and their industrial production began 10 years later in the United States. Since then, various processes for their production have been developed.

Polypropylene (PP) is one of the most important plastics nowadays. Its properties depend largely on the microstructure, the molecular weight and the molecular weight distribution and can be tuned over a wide range. The most commercial form of polypropylene is isotactic polypropylene which features good stiffness, high melting temperature and tensile strength, good chemical resistance and excellent moisture barrier properties (Del Duca, D. *et al.* 1996). Polypropylene is for example used in packaging (films, containers etc.), domestic appliances and automotive applications (Wolfsberger, A. *et al.* 2002) (Oertel, C.G. *et al.* 1996).

Commercially available polypropylene is usually synthesized with Ziegler-Natta type catalysts, but also metallocene-polypropylene is now commercially available (Sherman, L.M. 2002). The advantage of metallocene-polypropylene is the possibility to fine-tune the properties by varying the metallocene structure. It is common knowledge that it is possible to synthesize

not only isotactic but also syndiotactic polypropylene with a broad range of molar masses with metallocene/MAO catalysts (Busico, V. *et al.* 2001)

It has been known for a long time that the properties of polymers can be improved by the addition of organic or inorganic fillers. It is interesting to further alter and improve the properties of polypropylene by the addition of fillers to create new materials and thereby extend its area of application.

There are three principal routes to produce filled polymers (Bergman, J.S. 1999)(Morgan, A.B. 2001). In solution blending, the filler is treated with a polymer in solution, and the solvent is then evaporated to yield the filled polymer. They can also be prepared by a melt mixing process, in which molten polymer and filler are mixed under the influence of shear forces, and by the in-situ polymerization, in which the polymer is synthesized directly in the presence of the filler.

The light scattering technique provides information about structure having size of the order of the wavelength of visible light such as fluctuations in density and fluctuations in refractive index of anisotropic regions. For morphology observation, using highly powerful microscopes, it can reveal the internal morphology which is impossible to see with bare eyes. The normal technique is optical microscope. However, as some blends have very tiny components, other more powerful techniques are required such as scanning electron microscope, SEM. It should be noted that in order to see the morphology clearly, preliminary treatments are sometimes necessary, for example, etching.

To enable the study of crystallization of polypropylene, the high temperature X-ray diffraction technique was used. And differential scanning calorimetry was used to estimate melting temperature and crystallization temperature. Two techniques of XRD and DSC were used to facilitate correlation with SALS technique.

1.2 The Objectives of this Research

The objectives of this research are to investigate effects of low molar mass liquid crystal chemical (LCC) and glycerol monostearate (GMS) addition on crystal structure of isotactic polypropylene blend by using small angle light scattering (SALS), X-ray diffraction (XRD), scanning electron microscope (SEM) and differential scanning calorimetry (DSC) techniques for characterization.

1.3 The Scope of this Research

1.3.1 Synthesize isotactic polypropylene by using metallocene catalyst in amount of three **samples** with varying polymerization times.

1.3.2 Operate polymer blending between isotactic polypropylene and low molar mass liquid crystal chemical (LCC) or glycerol monostearate (GMS) by using melt mixing method.

1.3.3 Investigate melting temperature (T_m) and crystallization temperature (T_c) of polymer blends by using differential scanning calorimeter (DSC) technique.

1.3.4 Create light scattering database of polymer blends between polypropylene and low molar mass liquid crystal chemical (LCC) or glycerol monostearate (GMS) by using the static light scattering apparatus (SALS) which is modified to increase the efficiency. This modified apparatus can provide the light scattering photograph and its digital intensity data at every angles of the light scattering photograph.

1.3.5 Operate X-ray diffraction (XRD) in order to estimate % crystallinity of polymer and its blends.

1.3.6 Observe the morphology of these polymers by using scanning electron microscope (SEM) to find the radius of spherulite which is the required information for the study of crystallization.

CHAPTER II

Theories

2.1 Metallocene Catalysts

The first catalytic studies of metallocene complexes provided detail information on the ability of Cp_2TiCl_2 / DEAC and Cp_2TiCl_2 / TEA to polymerize ethylene (Natta *et al.*, 1957). Due to their marginal activity and inability to polymerize propylene, these system received little attention. However, since the advent of polymethylalumoxane (MAO) as a cocatalyst in 1980, they have found renewed interest (Sinn and Kaminsky, 1980). Dramatic improvements in activity along with the discovery of stereospecific metallocene systems have fueled numerous intense research efforts in the field. The proposed mechanism of metallocene-catalyzed polymerization is shown in [Figure 2.1](#)

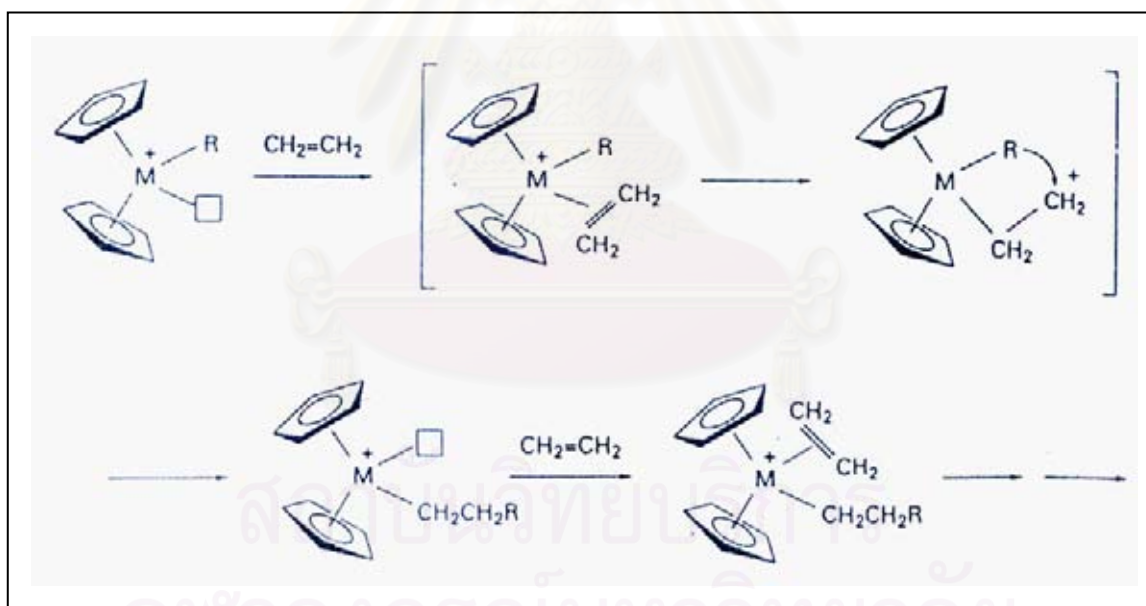


Figure 2.1 : The mechanism of olefin polymerization using metallocene catalysts.

(Long, 1998)

2.1.1 Tailoring of metallocene catalysts

Catalytic tailoring via the ligand modification of the catalyst system is one of the modifications. This leads to the specific changes in the catalytic activity and properties of the product. The important factors affecting catalytic performance are as follow :

- (a) Transition metal-olefin interactions. The olefin has a Lewis basic character with respect to the metal and therefore acts as an electron donor. The σ - and π -bonds formed between the metal and olefin destabilize and activate the olefin for insertion into the polymer propagating chain. Olefin co-ordination also destabilizes the M-R (M= metal, R= alkyl) bond. The stability of olefin co-ordination to M decreases with increasing olefin size.
- (b) Metal-alkyl bond stability. Fine adjustment of the M-R bond is possible by variation of ligand electronic effects. The M-R bond should be relatively weak to permit facile opening and olefin insertion to form a new metal-alkyl bond but also strong enough to favor catalytic lifetimes. The strength of this bond depends on R itself and the stability decreases in the order $\text{Me} > \text{Et} > (\text{CH}_2)_n\text{CH}_3$. Olefin coordination is also another method of weakening the M-R bond in preparation for migratory insertion.
- (c) Influence of other ligands. Considering the Cp rings and substituents attached to them, then if the ligand system used is a good electron donor it will reduce the positive charge on the metal. This weakens the bonding between the metal and all other ligands, particularly the already relatively weak M-R bond, making insertion more facile. Conversely, this will also stabilize high oxidation state complexes and make co-ordinate of the incoming olefin more unfavorable and so a balance must be found between these effects.
- (d) Steric effects of the other ligands. Bulky ligands will aid stereospecific olefin coordination and polymerization (Figure 2.2). Steric effects influence the position of bulky monomers when coordinated with the metal center therefore the stereospecific insertion can be obtained throughout the polymerization time. The coordination site can be opened or closed by controlling the angle that the cyclopentadienyl rings tilt away from each other. Shortening or lengthening the bridge in ansa-metallocenes can lead to much improved monomeric stereoselectivity (Long,1988)

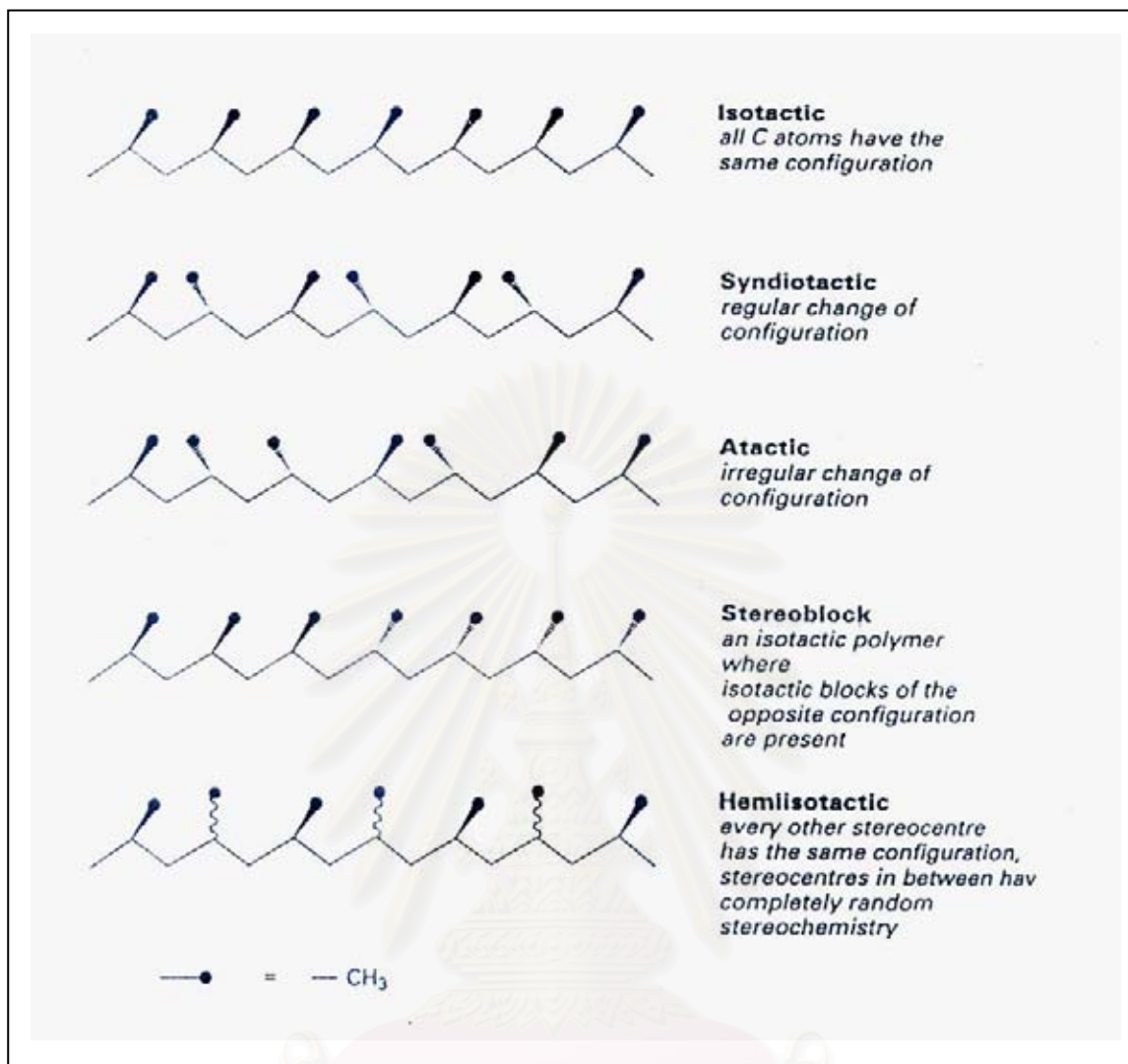


Figure 2.2 : Different types of polymer tacticity. (Long , 1998)

2.1.2 Isotactic polymers using metallocene catalysts

The modification of group 4 metallocenes to produce catalysts capable of isospecific is possible. Polymerization developed slowly however dramatic successes were reported in the mid-1980s, Prior to this time, catalysts using achiral $[\text{Cp}_2\text{MCl}_2]$ systems could only produce atactic polypropylene. Then Ewen (1984) reported the use of metallocene-based catalysts for the isospecific polymerization of propylene using Brintzinger chiral ansa-metallocenes. It was shown that using a combination of meso and racemic ansa-metallocenes, a mixture of atactic and isotactic polymer chains were produced and soon it was recognized that the isotacticity of the polymer was directly related to the chirality of the metallocene that produced it. This was

confirmed when isotactic polypropylene was formed using an isomerically pure sample of a chiral zirconocene analogue.

Corradini has carried out studies on conformational modeling and found that the polymer chain is forced into an open region of the metallocene thus relaying the chirality of the metallocene to the incoming monomer through the orientation of the β -carbon of the alkyl chain (Corradini et al.,1995). These chiral metallocenes have C_2 symmetry with both possible reaction sites being homotopic and therefore selective for the same alkene enantioface. The result is a polymerization reaction that yields an isotactic polyalkene (Figure 2.3).

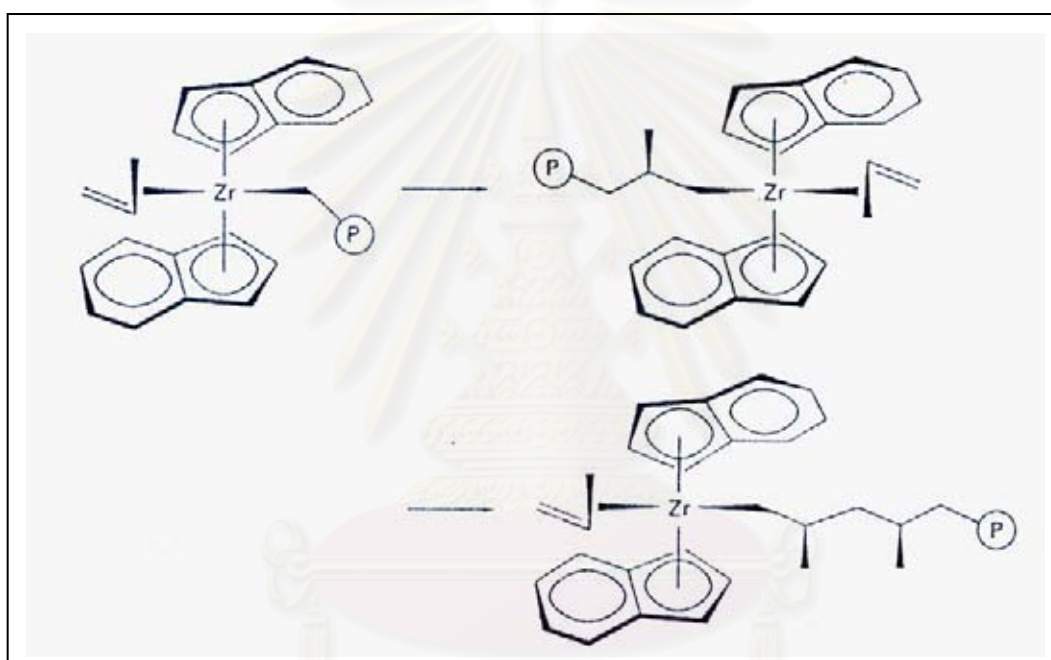


Figure 2.3 :The production of isotactic polymers using chiral metallocene catalysts. (Long,1998)

2.1.3 Single-Center Catalysts

The demonstrated potential of the metallocene/MAO system has paved the way to the discovery of many other organometallic complexes suitable for olefin polymerization. They are represented in Figure 2.4.

The catalytic systems based on these complexes are : (1) single-center i.e. the catalytic centers responsible for the chain propagation have the same nature, (2)

soluble in most aliphatic and aromatic solvents and, nevertheless, active also in liquid monomers and in the gas phase and (3) in many cases endowed with high catalytic activity. Furthermore, (4) the organometallic complexes have a well-defined chemical structure and (5) the π ligands remain coordinated to the transition metal atom during the course of the polymerization.

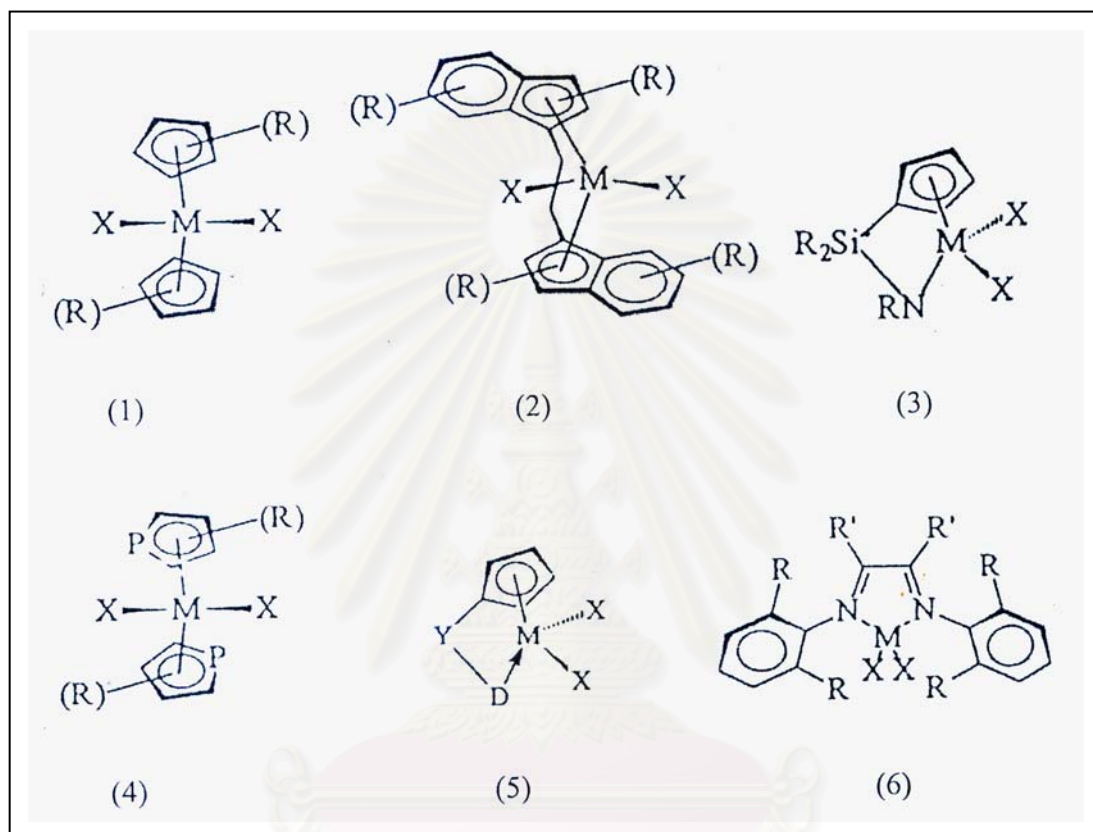


Figure 2.4 : Organometallic complexes employed in olefin polymerization.

(Scheirs,1999,p.310)

Nowadays, all these families of single-center catalysts are used for the preparation of polyolefins, to a different extent also on the industrial scale. As far as the performances of the single-center catalysts are concerned, it is possible to say that (1) only metallocenes are, at present, mature catalysts for the synthesis of stereoregular polyolefins and (2) any of the single-center catalysts can be in principle suitable for preparing ethylene-based homo- and copolymers. In fact, in this case the catalyst need not necessarily be stereospecific. This explains the wide application of

complexes other than metallocenes e.g. (3) and (5) in **Figure 2.5.**, for the preparation of ethylene-based polymers, from HDPE (high-density polyethylene) to **EP(DM)** (elastomeric copolymers of ethylene and propylene with a diene).

2.1.4 Cocatalytic Systems for Metallocene-Based Catalysis (MBC)

Cocatalyst alternatives to MAO have appeared on the scene and have been proved able to Promote the homo- and copolymerization of ethylene and 1-olefins, e.g., in the first instance, boron containing compounds (Hlatky, 1989). Montell scientists have discovered and developed cocatalysts based on AlR_3 and H_2O (Resconi et al., 1993). They can be prepared and isolated as a tetraalkylalumoxane or can be formed in situ, during the process, adopting a suitable Al : H_2O ratio.

In the scientific literature, the performances of different metallocenes are usually compared adopting MAO-based polymerization tests. AS a consequence, any difference, for example, as far as the catalytic activity, is completely attributed to the structure of the metallocene. Different aluminium-based cocatalysts give rise to different catalytic activities and an MAO-based system is not necessarily the most active one. This suggests the need for the new approach to the evaluation of the metallocene-based results.

สถาบันวิทยบริการ
จุฬาลงกรณ์มหาวิทยาลัย

2.2 Polymer Morphology

Generally, there are two morphologies of polymers; (a) amorphous and (b) crystalline. The former is a physical state characterized by almost complete lack of order among the molecules. The crystalline refers to a situation where polymer molecules are oriented, or aligned. Because polymers for all practical purposes never achieve 100% crystallinity, it is more practical to categorize their morphologies as amorphous and semi-crystalline.

2.2.1 The Amorphous State

Some polymers do not crystallize at all. Therefore they remain in an amorphous state throughout the solidification. The amorphous state is characteristic of those polymers in the solid state that, for reasons of structure, exhibit no tendency toward crystallinity. In the amorphous state, the polymer resembles as a glass.

We can imagine the amorphous state of polymers like a bowl of cooked spaghetti. The major difference between the solid and liquid amorphous states is that with the former, molecular motion is restricted to very short-range vibrations and rotations, whereas in the molten state there is considerable segmental motion or conformational freedom arising from rotation about chemical bonds. The molten state has been likened on a molecular scale to a can of worms, all intertwined and wriggling about, except that the average worm would be extremely long relative to its cross-sectional area. When an amorphous polymer achieves a certain degree of rotational freedom, it can be deformed. If there is sufficient freedom, the polymer flows when the molecules begin to move past one another. At low temperatures amorphous polymers are glassy, hard and brittle. As temperature is raised, they go through the glass-rubber transition characterized by the glass transition temperature T_g .

2.2.2 Glass Transition Temperature, T_g

One of the most important characteristics of the amorphous state is the behavior of a polymer during its transition from solid to liquid. If an amorphous glass is heated, the kinetic energy of the molecules increases. Motion is still restricted, however, to short-range vibrations and rotations so

long as the polymer retains its glasslike structures. As temperature is increased further, there comes x_0 , a point where a decided change takes place; the polymer loses its glasslike properties and assumes those more commonly identified with a rubber. The temperature at which this takes place is called the glass transition temperature, T_g . If heating is continued, the polymer will eventually lose its elastomeric properties and melt to a flowable liquid. The glass transition temperature is defined as the temperature at which the polymer softens because of onset of long-range coordinated molecular motion. The amorphous parts of semicrystalline polymers also experience glass transition at a certain temperature T_g .

The importance of the glass transition temperature cannot be overemphasized. It is one of the fundamental characteristics as it relates to polymer properties and processing. The transition is accompanied by more long-range molecular motion, greater rotational freedom and consequently more segmental motion of the chains. It is estimated that between 20 and 50 chain atoms are involved in this segmental movement at the T_g . Clearly for this increased motion to take place, the space between the atoms (the free volume) must increase, which gives rise to an increase in the specific volume. The temperature at which this change in specific volume takes place, usually observed by dilatometry (volume measurement), may be used as a measure of T_g . Other changes of a macroscopic nature occur at the glass transition. There is an enthalpy change, which may be measured by calorimetry. The modulus, or stiffness, decreases appreciably, the decrease readily detected by mechanical measurements. Refractive index and thermal conductivity have also been changed.

2.2.3 The Crystalline Polymer

Polymers crystallized in the bulk state are never totally crystalline, because of a consequence of their long-chain nature and subsequent entanglements. The melting temperature of the polymer, T_m , is always higher than the glass transition temperature, T_g . Thus the polymer may be either hard and rigid or flexible. For example, polypropylene which has a glass transition temperature of about -5°C and a melting temperature of about 175°C . At room temperature it forms a leathery product as a result. Factors that control the T_m include polarity, hydrogen bonding and packing capability.

The development of crystallinity in polymers depends on the regularity of structure in the polymer, the tacticity of the polymer. The different possible spatial arrangements are called the tacticity of the polymer. If the R groups on successive pseudochiral carbons all have the same configuration, the polymer is called isotactic. When the pseudochiral centers alternate in configuration from one repeating unit to the next, the polymer is called syndiotactic. If the pseudochiral centers do not have any particular order, but in fact are statistical arrangements, the polymer is said to be atactic.

Thus isotactic and syndiotactic structure are both crystallizable, because of their regularity along the chain but their unit cells and melting temperatures are not the same. On the other hand, atactic polymers are usually completely amorphous unless the side group is small or so polar as to permit some crystallinity.

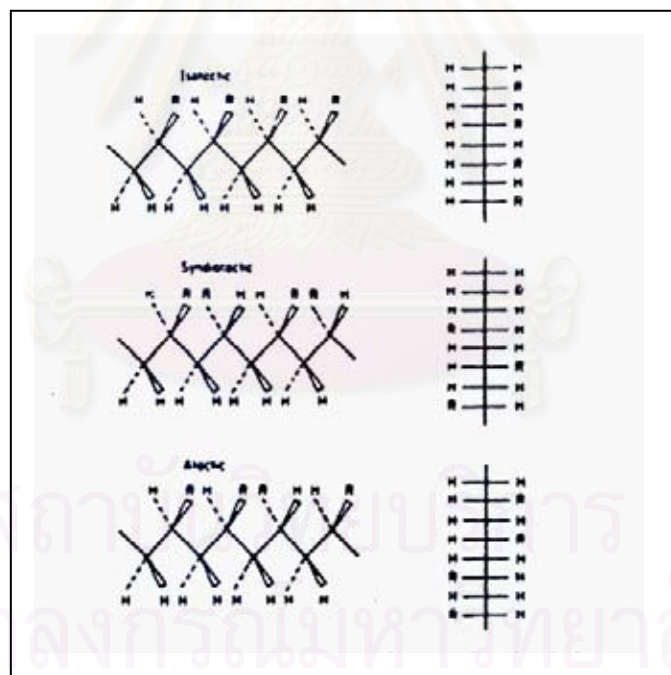


Figure 2.5 : Three different configurations of a polypropylene [Sperling, L.H. 2001]

Nonregularity of structure first decreases the melting temperature and finally prevents crystallinity. Mers of incorrect tacticity tend to destroy crystallinity. Thus statistical copolymers are generally amorphous. Blends of

isotactic and atactic polymers show reduced crystallinity, with only the isotactic portion crystallizing. Furthermore, the long-chain nature and the subsequent entanglements prevent total crystallization.

2.2.4 Liquid crystal

2.2.4.1 Introduction to the liquid crystal

Liquid crystals were discovered more than a hundred years ago. They are defined as liquid material, which also have the high degree of anisotropy. One of the important manifestations of LCs is their melting behavior. When heating normal crystalline solid, it changes from solid phase directly to isotropic liquids at its crystalline melting point (T_m). In liquid crystalline materials, several different mesophases may form after their T_m and the mesophases will become isotropic at the higher transition temperature called clearing temperature. The transition properties of liquid crystals come from the rigid parts of their molecules, which are called mesogens. Mesogens may consist of low molecular weight compounds. They may be arranged along the main polymer chain or on side branches of the graft molecules.

The liquid crystalline state can be discovered as small molecules or polymers and generally requires special chemical structures. The chemical structures are composed of the central core comprising aromatic or cycloaliphatic units joined by rigid links or either polar or flexible alkoxy terminal groups.

The mesophase may exist in solution state (Lyotropic liquid crystal) or in a melting state (Thermotropic liquid crystal). The ability of the polymers to form Lyotropic or thermotropic liquid crystalline mesophases depends on the chemical structure of the molecules.

The formation of a Lyotropic liquid crystalline mesophase can be present alone or in equilibrium with an isotropic liquid phase. At higher polymer concentrations the liquid crystalline mesophases depends on the chemical structure of the molecules.

The presence of mesogenic groups is important for the anisotropic formation of liquid crystals in solutions and melt, but the occurrence of the liquid crystals also depends on many other factors such as temperature. Liquid crystals form only in a certain temperature range which lies between the melting point, T_m and the upper

transition temperature at which a liquid crystalline phase changes into an isotropic liquid or clearing point, T_i . This temperature is also called the temperature of isotropisation or the solution point. If the material being tested does not crystallize, liquid crystals are formed between the glass transition temperature, T_g , and temperature of isotropisation T_i .

In order to use liquid crystals, it is essential that the range of the mesophase extends over a wide temperature range. However, compounds containing a mesophase, particularly polymer, have a high melting point, and the melting point of crystals is often a limiting factor, since the range of the liquid crystalline transition may be located in the range of thermal decomposition.

2.2.4.2 Structure of liquid Crystals

Many kinds of mesophases can be classified by the different ways of the molecular arrangements. The anisotropic region ends at the clearing temperature because of the completely disordering of the molecules. There are many different types of liquid crystals. However, the major liquid crystal mesophase topologies are shown in [Figure 2.6](#) to [Figure 2.9](#).

2.2.4.2.1 Smectic structure

In the smectic structures, long molecules are arranged side by side in layers much like those in soap films. The term smectic (soap like) derives from the Greek word for grease or slime. The layers are not strictly rigid, but they are flexible. Two dimensional molecular sheets can slide past each other ([Figure 2.6](#)). Molecular motion is rather slow, so smectic mesophases are quite viscous.

Optically smectic layers behave like uniaxial, birefringent crystals. The intensity of light transmitted parallel to the molecular layer is greater than that transmitted perpendicularly. The temperature dependence of smectic interval tested by birefringence has slightly small effect to internal order.

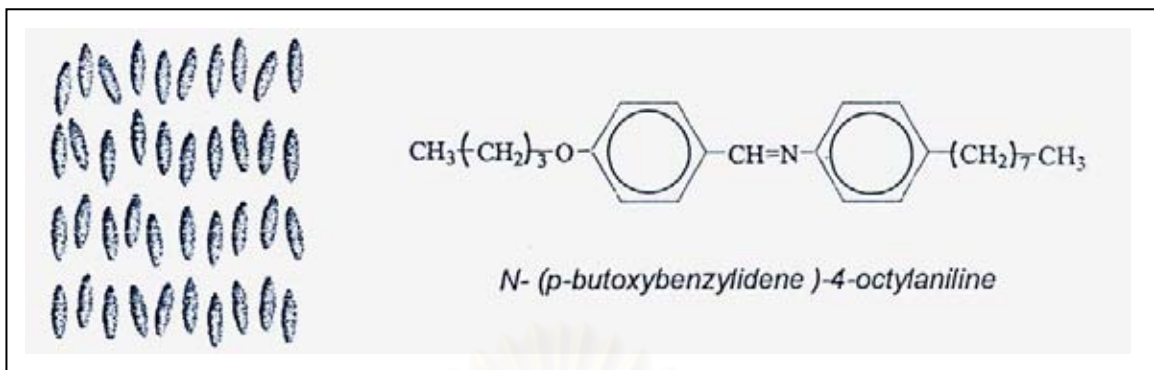


Figure 2.6 : (a) Smectic structure. (b)liquid crystal chemical structures of Smectic structure.[Sperling,2001]

2.2.4.2.2 Nematic structure

The molecular organization, classified as a nematic mesophase, involves in the irregular alignment in one dimension. Molecules remain parallel to each other in the nematic structure (Figure 2.7), but the position of their gravitational centers are disorganized. Molecules of nematic liquid crystals can be oriented in one dimension. Their mobilities can be reduced by the attraction to supporting surfaces. For examples, nematic molecules tend to lie parallel to the rough surface of a glass slide. A bright satin-like texture is observed when nematic liquid crystals are viewed between crossed polaroids. Characteristic dark threads appear at lines of optical discontinuity. These wavering filaments give the mesophase its name; take from the Greek word *nematos*, meaning fiber.

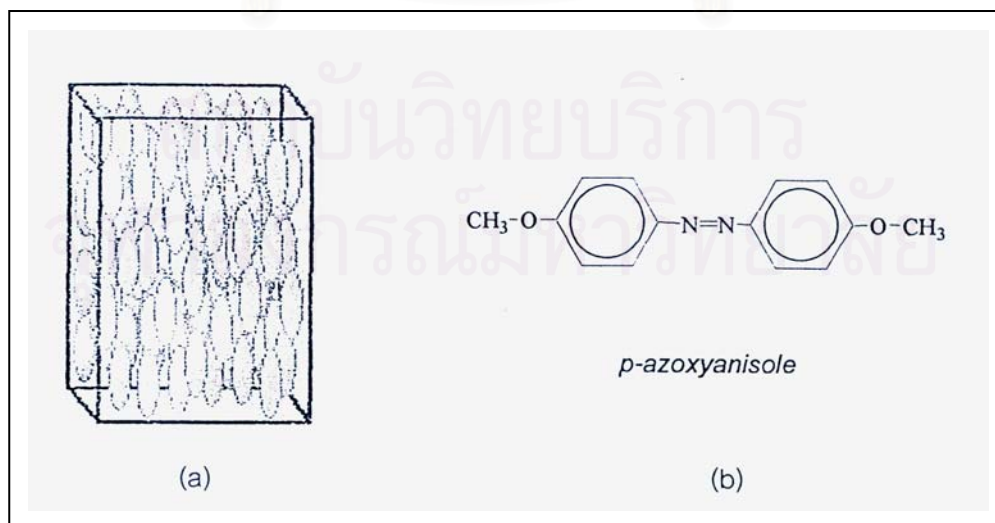


Figure 2.7 : (a) Nematic structure. (b) liquid crystal chemical structures of Nematic structure.[Sperling,2001]

2.2.4.2.3 Cholesteric or chiral nematic structure

The cholesteric structure is the third type of liquid crystal behaviors. It is so named because many compounds that form this mesophase are the derivatives of cholesterol. A cholesteric structure (Figure 2.8) is the shape of a nematic phase which is periodically wrapped around the axis. When chiral groups are present, the basic structure is helicoidal.

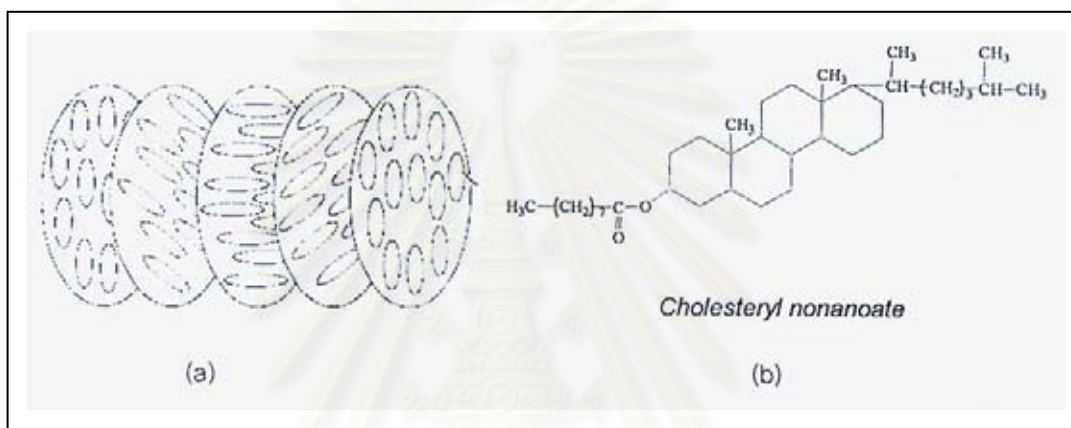


Figure 2.8 : (a) Cholesteric structure. (b) liquid crystal chemical structures of Cholesteric structure.[Sperling,2001]

2.2.4.2.4 Discotic structure

The discotic structure is the fourth type of liquid crystal behaviors. The discotic mesophase resemble stacks of dishes or coins (Figure 2.9)

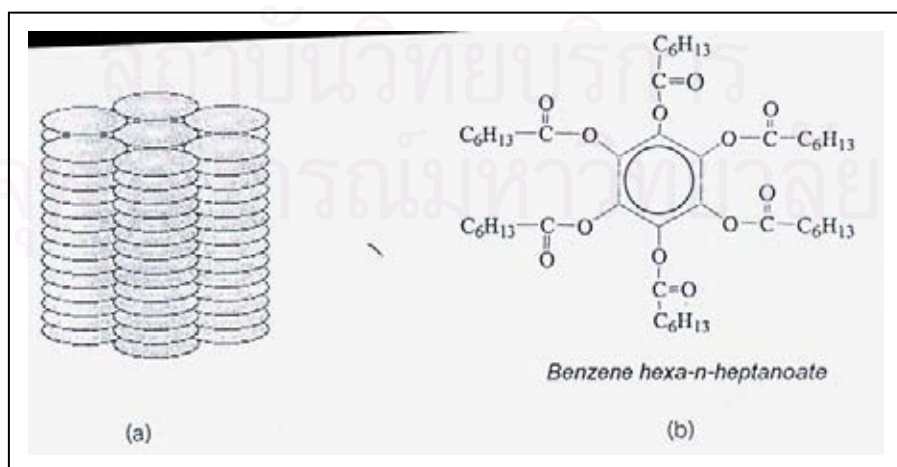


Figure 2.9 : (a) Discotic structure. (b) liquid crystal chemical structures of Discotic structure.[Sperling,2001]

2.2.4.3 Mesophasic Transition Temperature

Liquid crystals can undergo various phase transitions as the temperature increases from the ordered to the least ordered states, can be shown as **Figure 2.10**.

The temperature, when liquid crystal changes form crystal to the first liquid crystalline phase, is called “crystalline melting temperature” (T_3).

The temperature, when liquid crystal changes form smectic phase to nematic phase, is called “S \rightarrow N transition temperature” (T_4).

The temperature, when the last (or only) liquid crystalline phase gives way to the isotropic melt or solution, is called “clearing temperature” (T_5).

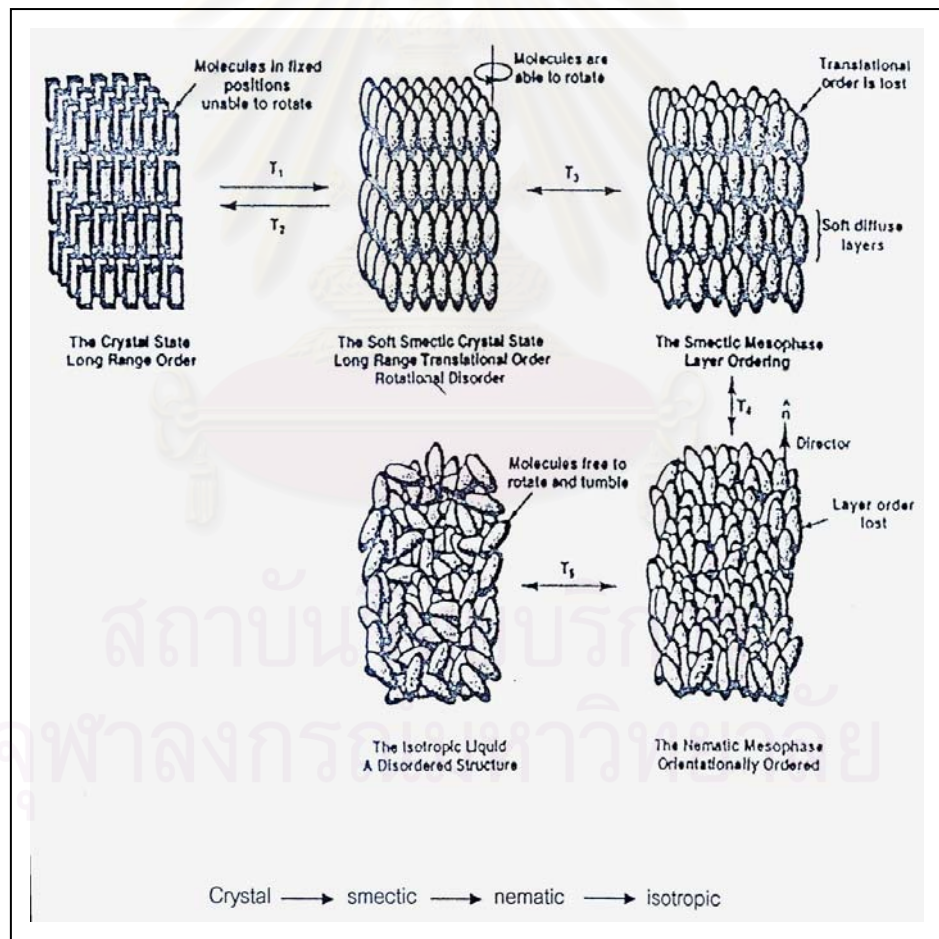


Figure 2.10 : Phase transition of Liquid Crystal [Demas, et. Al., 1998]

2.3 Melting Phenomena

The melting of polymers may be observed by any of several experiments. For linear or branched polymer, the melting cause the samples to becomes liquid and flows. First of all, simple liquid behavior may not be immediately apparent because of the polymer's high viscosity. If the polymer is cross-linked, it may not flow at all. It must also be noted that amorphous polymers soften at their glass transition temperature, T_g , which is emphatically not a melting temperature. If the sample does not contain colorants, it is usually hazy in the crystalline state because of the difference in refractive index between the amorphous and crystalline portions. On melting, the sample becomes clear, or more transparent.

Ideally, the melting temperature, T_m , should give a discontinuity in the volume, with a concomitant sharp melting point. In fact, because of the very small size of the crystallites in bulk crystallized polymers, most polymers melt over a range of several degrees. The melting temperature is usually taken as the temperature at which the largest and / or most perfect crystals are melting.

2.4 Thermal Properties

The existence of a polymeric system as a rigid glassy liquid, a mobile liquid, a microcrystalline solid or a liquid crystalline mesophase depends on the temperature and the chemical structure of the polymer. Changes from a microcrystalline state to a liquid crystalline or isotropic liquid state takes place at the equilibrium melting temperature.

T_m and T_g of crystallizable polymers vary widely with a change in the chemical structure. The presence of amide and of aromatic groups in the chain raise T_m and T_g . The morphology of a thermoplastic crystallizable homopolymer at a particular forces. If the usage temperature depends on T_m , which is in turn dependent on the intermolecular forces. If the usage temperature is greater than T_m for a crystallizable polymer, only a rubbery liquid morphology will be realized. At temperatures below T_m but above T_g such a material will be partially crystalline, when crystallized quiescently, with rubbery interlayers. Below T_g , the interlayers between crystallites will be glassy.

In various kind of the polymers, the melting points refer to the melting of the crystal form with the highest T_m . Changes from one form to another at easily attained temperatures and pressures can be reversible or involve melting of one form and crystallization of the other.

Some polymers with few chain irregularities, although intrinsically crystallizable, can be easily supercooled, without appreciable crystallizable, into a glassy amorphous state upon rapid cooling from the melt to a temperature below T_g . Polymers showing this type of behavior usually contain rings in the main or side chains. Examples are poly(ethylene terephthalate) and various polymers that form liquid crystalline mesophases. These supercooled materials can be crystallized by heating to a temperature where the polymer is below T_m but above T_g . Sufficient time for the various portions of the chains to adopt the conformation necessary for crystallization is then supplied.

2.5 Structure of Crystalline Polymers

Very early studies on bulk materials showed that some polymers were partly crystalline. X – ray line broadening indicated that the crystals were either very imperfect or very small. Because of the known high molecular weight, the polymer chain was calculated to be even longer than the crystallites. Hence it was reasoned that they passed in and out of many crystallites and many unit cells. These findings led to the fringed micelle model.



Figure 2.11 : The fringed micelle model. Each chain meanders from crystallite to crystallite, binding the whole mass together. [Sperling , L.H. 2001]

According to the fringed micelle model, the crystallites are about 100 Å long. The disordered regions separating the crystallites are amorphous. The chains wander from the amorphous region through a crystallites, binding them together.

The fringed micelle model was used with great success to explain a wide range of behaviour in semi-crystalline plastics and also in fibers. The amorphous regions, if glassy, yielded a stiff plastic. However, if they were above T_g , then they were rubbery and were held together by the hard crystallites. This model explains the leathery behaviour of ordinary polyethylene plastics. The greater tensile strength of polyethylene over that of low molecular-weight hydrocarbon waxes was attributed to amorphous chains wandering from crystallite to crystallite, holding them together by primary bonds. However, the exact stiffness of the plastic was related to the degree of crystallinity, or fraction of the polymer that was crystallized.

2.6 Crystal Structure in polymers

2.6.1 Crystallization from dilute solution

2.6.1.1 Polymer Single Crystals

Although the formation of single crystals of polymers was observed during polymerization many year ago, such crystals could not be produced from polymer solution because of molecular entanglement. In several laboratories, the phenomenon of growth has been reported for so many polymers, including polyethylene, polypropylene and other poly(α -olefins), that it appears to be quite general and universal.

All the structures described as polymer single crystals have the same general appearance, being composed of thin, flat platelets (lamellae) about 100 angstroms thick and often many micrometers in lateral dimensions. They are usually thickened by the spiral growth of additional lamellae from screw dislocations.

The size, shape, and regularity of the crystals depend on their growth conditions, such as solvent, temperature, and growth rate being important. The thickness of the lamellae depends on crystallization temperature and any subsequent annealing treatment. Electron – diffraction measurements indicated that the polymer chains are oriented very nearly normal to the plane of the lamellae. Since the

molecules in the polymers are at least 1000 angstroms long and the lamellae are only about 100 angstroms thick, the only reasonable description is that the chains are folded.

2.6.1.2 The Folded Chain Model

Ideally, the molecules fold back and forth with hairpin turns building a lamellar structure by regular folding. The chain folding is perpendicular to the plane of the lamellar. While adjacent reentry has been generally confirmed by small – angle neutron scattering and infrared studies for single crystals. For many polymers the single crystals are not simple flat structures. The crystals often occur in the form of hollow pyramids, which collapse on drying. If the polymer solution is slightly more concentrated, or if the crystallization rate is increased, the polymers will crystallize in the form of various twins, spirals, and dendritic structures, which are multilayered.

2.6.1.3 The Switchboard Model

In the switchboard model, the chains do not have a reentry into the lamellae by regular folding, but rather reentry more or less randomly. Both the perfectly folded chain and switchboard models represent limiting cases. Real system may combine elements of both.

2.6.2 Crystallization From the Melt

2.6.2.1 Spherulitic Morphology

When polymer samples are crystallized from the bulk of an unstained melt, the most obvious of the observed structures are the spherulites are sphere – shaped crystalline structure that form in bulk. Usually the spherulites are really spherical in shape only during the initial stages of crystallization. During the latter stages of crystallization, the spherulites impinge on their neighbours. When the spherulites are nucleated simultaneously, the boundaries between them are straight. However, when the spherulites have been nucleated at different times, so that they are different in size

when impinging on one another, their boundaries form hyperbolas. Finally, the spherulites form structures that pervade the entire mass of the material.

Electron microscopy examination of the spherulitic structure shows that the spherulites are composed of individual lamellar crystalline plates. The lamellar structures sometimes resemble staircases, being composed of nearly parallel lamellae of equal thickness.

The growth and structure of spherulites may also be studied by small-angle light scattering. The sample is placed between polarizers, a light beam is passed through, and the resultant scattered beam is photographed. Two types of scattering patterns are obtained, depending on polarization condition. When the polarization of the incident beam and that of the analyser are both vertical, it is called a Vv type of pattern. When the incident radiation is vertical in polarization but the analyser is horizontal (polarizers crossed), an Hv pattern is obtained.

These patterns arise from the spherulitic structure of the polymer, which is optically anisotropic, with the radial and tangential refractive indices being different.

A model of the spherulite structure is illustrated in [Figure 2.13](#)

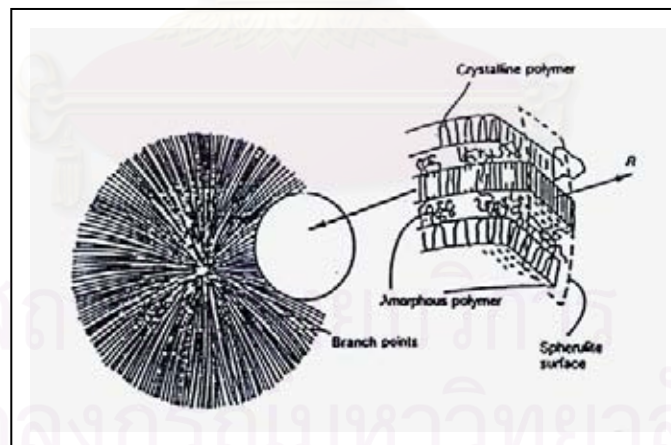


Figure 2.12 : Model of spherulitic structure. [Sperling, L.H. 2001]

The chain direction in the bulk crystallized lamellae is perpendicular to the broad plane of the structure, just like the dilute solution crystallized material. The spherulite lamellae also contain low – angle branch points, where new lamellar structures are initiated. The new lamellae tend to keep the spacing between the

crystallites constant. While the lamellar structures in the spherulites are the analogue of the single crystals. In between the lamellar structures lies amorphous material. This portion is rich in components such as atactic polymers, low – molecular – weight material, or impurities of various kinds.

The individual lamellae in the spherulites are bonded together by tie molecules, which lie partly in one crystallite and partly in another. Sometimes these tie molecules are actually in the form of what are called intercrystalline links, which are long, threadlike crystalline structures. These intercrystalline links are thought to be important in the development of the great toughness characteristic of semi-crystalline polymers. They serve to tie the entire structure together by crystalline regions and / or primary chain bonds.

2.6.2.2 Mechanism of Spherulite Formation

On cooling from the melt, the first structure that forms is the single crystal. These rapidly degenerate into sheaflike structures during the early stages of the growth of polymer spherulites. These sheaflike structures have been variously called axialites or hedrites. These transitional, multilayered structures represent an intermediate stage in the formation of spherulites.

2.6.2.3 Spherulites in Polymer Blends

There are two cases to be considered. Either the two polymers composing the blend may be miscible and form one phase in the melt, or they are immiscible and form two phases. If the glass transition of the noncrystallizing component is lower than that of the crystallizing component (i.e., its melt viscosity will be lower, other things being equal) , then the spherulites will actually grow faster, although the system is diluted. The crystallization behavior is quite different if the two polymers are immiscible in the melt. On spherulite formation, the droplets, which are non-crystallizing, become ordered within the growing arms of the crystallizing component.

2.6.2.4 Effect of Crystallinity on T_g

Semi-crystalline polymers such as polyethylene or polypropylene types also exhibit glass transitions, though only in the amorphous portions of these polymers. The T_g is often increased in temperature by the molecular – motion restricting crystallites. Sometimes T_g appears to be masked, especially for high crystalline polymers.

2.7 Light Scattering Theory

The phenomenon of light scattering is encountered widely in everyday life. For example, light scattering by airborne dust particles causes a beam of light coming through a window to be seen as a shaft of light, the poor visibility in a fog results from light scattering by airborne water droplets, and laser beams are visible due to scattering of the radiation by atmospheric particles. Also, light scattering by gas molecules in the atmosphere gives rise to the blue color of the sky and the spectacular colors that can sometimes be seen at sunrise and sunset. These are all examples of static light scattering since the time-averaged intensity of scattered light is observed.

In general, interaction of electromagnetic radiation with a molecule results in scattering of the radiation. Scattering results from interaction of the molecules with the oscillating electric field of the radiation, which forces the electrons to move in one direction and the nuclei to move in the opposite direction. Thus a dipole is induced in the molecules, which for isotropic scatters is parallel to, and oscillates with, the electric field. Since an oscillating dipole is a source of electromagnetic radiation, the molecules emit light, the scattered light, in all directions. Almost all of the scattered radiation has the same wavelength (and frequency) as the incident radiation and results from elastic scattering, that is zero energy change. Additionally, a small amount of the scattered radiation has a higher, or lower, wavelength than the incident radiation and arises from inelastic scattering, that is non-zero energy change. Inelastically scattered light carries information relating to bond vibrations and is the basis of Raman spectroscopy, a technique which increasingly is being used in studies of polymer structure and polymer deformation micromechanics.

The scattering of light from crystalline polymeric films has been studied for a long time. This scattering arises principally from orientation fluctuations among aggregates of crystals. The scattering patterns are complex, especially with polarized

light and oriented samples. This technique described involved photometric measurement of the scattered intensity as a function of sample and scattering angle. The photographic technique like the photographic X-ray diffraction except that a laser is used as a radiation source as a substitute for an X-ray tube. A typical photographic light scattering is shown in [Figure 2.14](#).

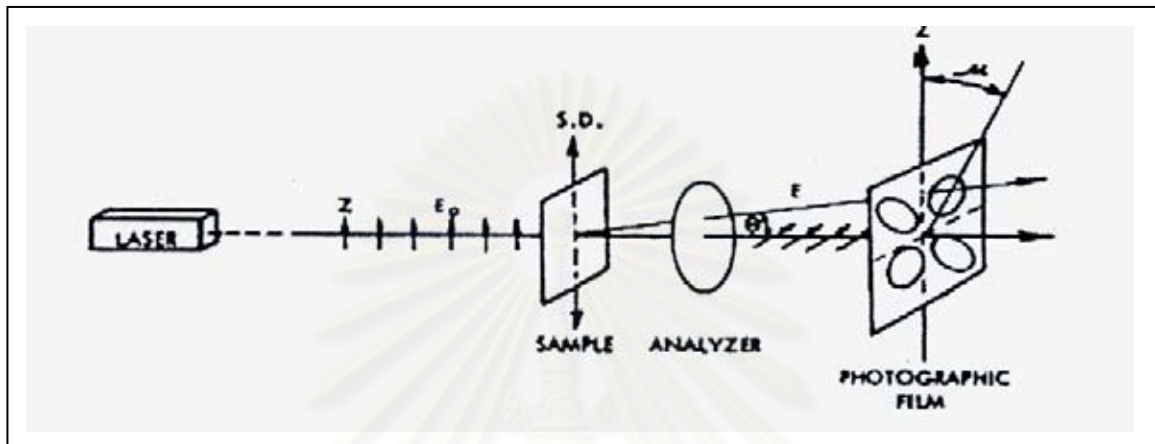


Figure 2.14 : A typical photographic light scattering apparatus. [Stein, R.S. 1964]

The intensity depends upon the scattering angle θ between the incident and scattered ray and the azimuthal angle μ . The range of θ that may be recorded in a picture depends upon the sample to film distance, d since $\tan \theta = (x/d)$, where x is the distance from the center of the photographic film to the point where the intensity is recorded.

Polypropylene crystallites are known to be arranged in spherical aggregates called spherulites with differing radial and tangential refractive indexes. This optical anisotropy is a consequence of the arrangement of the anisotropic crystallites within the spherulites.

It is also apparent that in isotropic spherulites, the induced dipole will be oriented in the direction of polarization of the incident light, and no scattered light will be transmitted through an analyzer perpendicular to polarizer. Consequently, the H_v component of scattering for isotropic spherulites will be zero.

2.8 Polymer Blends

Polymer blends are the mixtures of at least two or more polymers. The mixing of two or more existing polymers may obtain the new properties of the blend. By using these techniques the designed properties can be explored without synthesizing the new polymer which have the designed properties. The results of blending polymers have many advantages, for example, lower cost than synthesizing the desired properties of new polymer. The new properties can also be under controlled.

2.8.1 The Blends Preparations

There are many methods to mix each polymer together, such as by using heat (melt mixing), by using solvent (solution casting, freeze drying) or by in situ reaction, etc.

2.8.1.1 Melt Mixing

Melt mixing of thermoplastics polymer is performed by mixing the polymers in the molten state under shear in various mixing equipments. The method is popular in the preparation of polymer blends on the large commercial scale because of its simplicity, speed of mixing and the advantage of being free from foreign components (e.g. solvents) in the resulted blends. A number of are available for laboratory – scale mixing such as internal mixer, electrically - heated two – roll mill, extruder, rotational rheometer.

The advantages of this method are the most similar to the industrial practice. The commercial compounding or adding additives into base polymers are applied by melt mixing. So the investigations of polymer blends by melt mixing method are the most practical methods in industrial applications.

2.8.1.2 Solvent Casting

This method group is performed by dissolving polymers in the some solvent. The solution is then cast on a glass plate into thin films and the removal of solvent from the films is performed by evaporating the solvents from the casing polymer films, the condition of high temperature is invariably needed, and protection

of the polymer in case of degradation is essential. The inert gas or lower down the pressure (vacuums) is typically used. In the vacuum conditions, the vapor pressure can be reduced and thus allows the solvents to evaporate more easily. However, too fast evaporation rate of solvent will result in the bubble in the final films produced.

Solvents casting is the simplest mixing method available and is widely practiced in academic studies, usually when the experiments need a very small quantities of polymers.

2.8.1.3 Freeze Drying

In the freeze drying processes, the solution of the two polymers is quenched down immediately to a very low temperature and the solution is frozen. Solvent is then removed from the frozen solution by sublimation at a very low temperature. Dilute solutions must be used and the solution volume must have as large surface area as possible for good heat transfer.

An advantage of this method is that the resulted blend will be independent of the solvent, if the single phase solution is freezed rapidly enough. However, there are many limitations of this method. Freeze drying method seems to work best with solvents having high symmetry, i.e. benzene, naphthalene, etc. The powdery form of the blend after solvent removal is usually not very useful and further shaping must be performed. While not complex, freeze drying does require a good vacuum system for low - boiling solvents and it is not a fast blending method. After solvent removal, the blend is in the powdery form, which usually needs further shaping. The advantage of this method is the simplicity. However, this method needs a good fume trap, vacuum line for the sublimation solvent and it takes to complete the sublimation process.

2.8.1.4 Emulsions

The advantages of the emulsion polymer mixing are the easy handling and all the other advantages as the solvent casting. The mixing or casting of the film requires neither expensive equipment nor high temperature. However, emulsions of polymers are an advantage technique and not always applicable to all monomers.

2.8.1.5 Reactive Blend

Co – crosslinking and interpenetrating polymer networks (IPN) formations are the special methods for forming blends. The ideas of these methods is to enforce degree of miscibility by reactions between the polymer chains. Other methods involve the polymerization of a monomer in the presence of polymer and the introduction of interface graft co – polymer onto the polymer chains.

2.9 Permanganic etching

The macroscopic properties of crystalline polymers are controlled in large measure by their physical microstructure. Since there is substantial texture in crystalline polymers below the resolution of the optical microscope and for nearly thirty years attempts have been made by using a wide variety of techniques to relate this texture to presumed lamellar structures whose precise arrangement must strongly affect mechanical and other properties. It is only recently, however, that it has become possible to use transmission electron microscopy and scanning electron microscopy to study actual lamellar organization representative of the interior morphology of melt – crystallized polymers. Permanganic etching of various polyolefins and other polymers offer alternative and complementary means of studying polymer lamellae and their organization within spherulites and other textural entities. This technique confirms not only that crystalline polymer, even when of only moderate crystallinity, are profusely lamellar, but also show that there is a hierarchy of lamellae with a systematic spatial distribution through a sample. Permanganic etching offers additional information on differences between different components of the morphology through differential etching. It has been appreciated from the introduction of this technique that etching could be differential between many regions, revealing various differences, including those of polymeric components in blends, lamellar thickness and related segregation, as well as deformed regions representing differences underlying such differential etching.

CHAPTER III

Literature Reviews

Synthesis of polypropylene by using metallocene and crystallization of polypropylene have been studied in many researches. The reviews cover light scattering and X-ray diffraction behavior of polypropylene and its blends.

N. Kawahara *et al.* [2004]. carried out studies on propylene homopolymerizations by using three kinds of metallocenes: Cp_2ZrCl_2 , $\text{En}(\text{Ind})_2\text{ZrCl}_2$ and $i\text{-Pr}(\text{Cp})(\text{Flu})\text{ZrCl}_2$, all of which were activated with methylaluminoxane. It is found that $\text{En}(\text{Ind})_2\text{ZrCl}_2$ has the highest activity. The results described characteristic of each metallocene for the mechanism of polymerization.

G.Farrow [1961] investigated method for the measurement of crystallinity in oriented polypropylene fibers by an X-ray technique. The general level of crystallinity is higher than in similar oriented poly(ethylene terephthalate) fibers. The results also show that the crystallinity so measured is lower than values inferred from density measurement and that no correlation exists between the two methods. A possible method is suggested for the determination of the atactic content of polypropylene polymer by X-ray diffraction.

A.E.M. Keijzers, J.J. van Aartsen, and W. Prins [1967] investigated light scattering by crystalline polystyrene and polypropylene, which can yield valuable information regarding the crystallization behavior and the resulting crystalline morphology if (i) quantitative measurements are carried through and (ii) these are analyzed by using a physically realistic model. It is found that isotactic polystyrene and polypropylene samples can be adequately described as containing imperfect spherulites in which a number of perfectly spherulitic and a number of "random orientation" crystallites are present. Growth rates, sizes, and the number of spherulites follow easily from the scattering data. The internal structure of the imperfect spherulites can be characterized by the birefringence of the perfectly spherulitic crystallites plus a density correlation distance, two orientation correlation distances, and the mean polarizability and isotropy fluctuations of the "random orientation" crystallites. It is found that in isotactic polystyrene the crystallinity of the spherulites is a decreasing function of the radius. In the case of isotactic polypropylene it could be shown that the secondary crystallization is not spherulitical, in contradistinction to the primary crystallization.

D.Hlavata' and Z.Hora'k [1993] investigated the character of the polypropylene crystalline phase and polypropylene- high impact polystyrene blends by using combination of wide angle and small angle X-ray scattering. It was found that addition of a copolymers slightly reduces the crystallinity of polypropylene but the degree of crystallinity of polypropylene in blend with HIPS does not change with the HIPS content. In the absence of the compatibilizer no miscibility of the components was observed. In all samples polypropylene maintains its α - crystalline phase.

S.Vleeshouwers [1995] studied the recrystallization and melting behaviour of the α and β form of iPP by simultaneous in-situ WAXS/SAXS and DSC. It was found that melting behaviour depended on the formation history. In samples formed at high cooling rates , best comparable to processing conditions, the melting of β crystals is followed by an absolute increase in α crystallinity. In the slowly cooled samples , α and β crystal lamellae melt independently on heating.

Stein, R.S., Cronauer, J., and Zachmann, H.G. [1996] studied the crystallization of a single polymer component and polymer blends by using the small angle light scattering technique. They found that this technique can be a convenient method for quantitatively following spherulitic crystallization. Moreover , it provides information about the number and size of spherulites as well as their internal crystallinity. From this technique , they observed that most polymers crystallize by a nucleation – and – growth mechanism in which spherulites develop as a consequence of the radial growth of branching crystalline lamellae from heterogeneous nuclei. The amorphous component is included within the spherulites. These grow until they **impling** and become filling. The primary crystallization occurs at the expanding interface of the spherulite with the amorphous polymer. Sometime the secondary crystallization may occur within the spherulite.

Stein, R.S. , Jacob, K. ,*et al.*[2001] studied light scattering of the crystallization of polymers. They explained that the realtime light scattering measurements during polymer crystallization can be interpreted in terms of the number, size and anisotropy of crystallizing species. Such observations have been used to show the lack of ordered regions in amorphous polymers. It is very

sensitive for detecting the early stages of crystallization. While the crystals are too small at early stages to affect the angular dependence of scattering, they can appreciably contribute to its intensity, which depends upon their number and size. The subsequent changes in intensity and polarization can be fitted to parameters for a nucleation and growth model. Ultimately, when the dimensions of the growing species become sufficiently large, angularly dependent scattering results, which may be interpreted in terms of their size and state of aggregation. The technique of light scattering may be extended to study of crystallization of oriented polymers. It is rapid and may be used to follow the crystallization of films during their processing.

Zhi-Gang Wang , Benjamin S. Hsiao , *et al.* [2001] investigated the transformation of mesomorphic phase to α - monoclinic crystal phase in quenched isotactic polypropylene by using TEM , DSC and time-resolved SAXS and WAXD methods. It is found that even though the initial appearance of the cluster structure in mesomorphic i-PP seems to support the model of a multi-step process for polymer crystallization , results indicate that the transformation is not spontaneous. In the cluster domains, a significant fraction of chain segments must undergo a reorganization process in order to establish the correct registration of helical hands for crystallization. In addition , a fraction of the ordered chains with correct registration of helical hands should also serve as primary nuclei to initiate crystallization. However , the entire cluster domains should not be considered as 'precursors'. The growth process via secondary nucleation eventually transforms the cluster structure to the lamellar structure.

Jerome Maugey , Patrick Navard [2002] studied the curing of a homogeneous mixture of a nematic liquid crystal and an acrylate UV curable prepolymer by small angle light scattering , varying temperature and UV intensity. For all the conditions except at elevated temperature , the phase separation occurs with a spinodal decomposition which phases can be more or less easily recognised. Whatever the temperature below the clearing point of the liquid crystal and the UV intensity , the isotropic-to-nematic transition that occurs in the liquid crystal rich region is easily seen as a strong decrease of the light scattering intensity. For all the conditions tested , the final morphology is in the form of droplet morphology. At high UV intensity , there are two scattering peaks that are appearing in the scattering pattern which was tentatively interpreted as a double spinodal decomposition.

Sayant Saengsuwan *et al.* [2002] investigated in situ composite films were prepared by a two-step method. First, polypropylene and thermotropic liquid crystalline polymer (TLCP), Rodrun LC5000 (80 mol% p-hydroxy benzoic acid (HBA)/20 mol% polyethylene terephthalate (PET)), were melt blended in a twin-screw extruder and then fabricated by extrusion through a mini-extruder as cast film. Rheological behavior of the blends, morphology of the extruded strands and films, and tensile properties of the in situ composite films were investigated. Rheological behavior of the blends at 295 °C studied using a plate-and-plate rheometer revealed a substantial reduction of the complex viscosity with increasing TLCP content, and all specimens exhibited shear thinning behavior. Over the angular frequency range of 0.6–200 rad/s, the viscosity ratio (dispersed phase to matrix phase) was found to be very low, in the range of 0.03–0.07. Morphologies of the fracture surfaces of the blend extrudates and the film surfaces etched in permanganic solution were investigated by scanning electron microscope (SEM). The TLCP droplets in the extruded strands were seen with a progressive deformation into fibrillar structure when TLCP content was increased up to 30 wt%. In the extruded films, TLCP fibrils with increasing aspect ratio (length to width) were observed with increasing TLCP concentration. Orientation functions of each component were determined by X-ray diffraction using a novel separation technique. It was observed that the Young's modulus in machine direction of the extruded film was greatly improved with increasing TLCP loading, due to the increase in fiber aspect ratio and also molecular orientation.

Kilwon Cho *et al.* [2002] investigated structural changes in β -isotactic polypropylene (β -iPP) during the heating were studied by means of differential scanning calorimetry and real-time in situ X-ray diffraction using a synchrotron source. Crystalline phase transformation and the memory effect caused by residual nuclei of α -iPP were observed during the heating of β -iPP. The memory effect observed in β -iPP during heating and crystallization is believed to be due to the existence of locally ordered α -form in the melt. The effect of local α -form order was probed by studying the behavior under heating of samples with a range of thermal histories. Samples were heated above the equilibrium melting temperature of iPP to remove all residual local order and the memory effect associated with this local order. The samples crystallized isothermally at different temperatures exhibited a significantly different melting and phase transformation behavior during heating. β -iPP is found to be an excellent material for the study of polymorphism, phase transformations, and characteristic memory effects in semicrystalline polymers.

Shaofeng Ran *et al.* [2002] investigated the structure and morphology development during the deformation of metallocene based ethylene-propylene copolymers with dominant propylene moiety (C3 M-EP) and its isotactic polypropylene (M-iPP) blends were investigated by simultaneous small-angle X-ray scattering (SAXS) and wide-angle X-ray diffraction (WAXD) using synchrotron radiation, high temperature tensile testing and differential scanning calorimetry (DSC). X-ray results showed that the structure and morphology in the blends of M-iPP/C3 M-EP are dictated by the M-iPP component. During stretching at room temperatures, both pure M-iPP and polymer blends exhibited the same transition from the a-form crystal to the mesophase. However, the a-form was found to be unchanged during the deformation of C3 M-EP copolymer, which indicated that the effect of local stress on the crystal domain in pure copolymer was too small to induce the phase transition. Although the DSC results showed that the blends in their isotropic state were immiscible with each other, the mechanical properties of the blends at high temperature (70 °C) indicated that they follow the conventional rule of mixing.

F. Javier Torre *et al.* [2003] investigated the isothermal crystallization behavior and morphology of blends of isotactic polypropylene, iPP, and a liquid crystal polymer, Vectra A950, by using differential scanning calorimetry, optical microscopy and simultaneous WAXS and SAXS in real-time measurements using synchrotron radiation. It has been observed that Vectra domains act as sites for the nucleation of iPP, and the rate of crystallisation is enhanced with increasing Vectra content in the blend. The presence of the a crystalline form in pure iPP, and both a and b forms for iPP in iPP/Vectra blends has been found. The SAXS patterns for iPP/Vectra blends containing b iPP are characterized by two different long period values that were related to the a and b lamellae. The secondary crystallisation mechanism has been investigated by SAXS/WAXS experiments. It is shown that, in contrast to primary crystallisation, secondary crystallisation of iPP is not affected by the presence of the thermotropic liquid crystalline polymer. As already known from pure iPP, the main process of secondary crystallisation is the growth of new lamellar stacks within remaining amorphous regions in the iPP spherulites.

Sayant Saengsuwan *et al.* [2003] investigated the effects of composition and compatibilizers on the molecular orientation in thermotropic liquid crystalline polymer (TLCP)/PP in situ composite films by using wide angle X-ray scattering (WAXS) techniques. The degree of preferred orientation for each component was evaluated using a novel separation technique based on a description of the scattering through spherical harmonic functions. The evaluated orientation

parameters $kP2l$ and $kP4l$ of TLCP phase were found to increase up to 0.76 and 0.53, respectively, with increasing TLCP content and film draw ratio. In contrast, the PP component in all films exhibits a very low orientation ($kP2l$, 0.01) i.e. essentially isotropic. The PP component exhibits the so-called smectic phase which can be transformed to the more stable crystalline phase (α -form) by annealing at 110 °C for 2 h, with a small increase in the level of preferred orientation. The inclusion of particular polystyrene-based compatibilizers was observed to have a substantial effect on the modulus of the composite and in some cases this is reflected in the level of preferred orientation in the TLCP. We deduce that the orientation parameters are largely insensitive to the fibril morphology once a certain aspect ratio has been exceeded.

T. Xu et al. [2003] investigated the effect of nucleating agent on the crystalline morphology under different structure levels of polypropylene (PP) materials. From the analysis, increasing nucleating agent has an effect on both high and low levels of the crystalline structure. Nucleating agent showed a heterogeneous nucleation effect. The results showed that at the level of the aggregation structure, crystallinity increases and spherulite size tends to decline with increasing nucleating agent. At the same time, the nucleating agent also has an effect on both the crystal grain structure and the unit cell structure.

CHAPTER IV

Experiments

In this chapter , the materials and chemicals , equipments , polymerization procedure , characterization instruments and sample preparations will be explained.

4.1 Materials and Chemicals

4.1.1 Synthesis Part

4.1.1.1 Propylene gas (99.96%) was donated from National Petrochemical Co.,Ltd. Thailand (NPC) .

4.1.1.2 Hydrochloric acid (Fuming 37 %) was purchased from Merck.

4.1.1.3 Methanol (Commercial grade) was purchased from SR Lab

4.1.1.4 Argon gas (Ultra high purity grade , 99.999 %) was purchased from Thai Industrial Gas Co.,Ltd. (TIG) and further purified by passing through columns packed with copper catalyst , NaOH , P₂O₅ and molecular sieve 4A to remove traces of oxygen and moisture.

4.1.1.5 Methylaluminoxane (MAO) 2.857 M in toluene was donated from Tosoh Akzo , Japan. Dried MAO was prepared by drying MAO in vacuum at room temperature.

4.1.1.6 Ethylene bis-indinyl zirconium dichloride (Et[Ind]₂ZrCl₂) was purchased from Aldrich

4.1.1.7 Toluene Commercial grade was donated from Exxon Chemical Ltd.,Thailand. This solvent was dried over dehydrated CaCl₂ and distilled over sodium/benzophenone under argon atmosphere before use.

4.1.2 Polymer Blend Part

Polypropylene (PP) is the one of the polyolefins. The basic structure of polypropylene is the chain, $\text{—(CH}_2\text{C}_2\text{H}_4\text{)—}$, which has no substituent groups. Moreover PP is a crystalline solid, somewhat flexible, whose properties are strongly influenced by the relative amounts of crystalline and amorphous phases.

This research studied about light scattering behavior, morphology, melting temperature, % crystallinity, molecular weight and molecular weight distribution of polymer blend between polypropylene and low molar mass liquid crystal and GMS.

4.1.2.1 Isotactic Polypropylene (iPP)

1100RC, 1100NK and 1102H Polypropylene that synthesized by Ziegler-Natta catalyst was purchased from Thai Petrochemical Industry Public Co.,Ltd. Their melt flow index are 20, 11 and 2, respectively.

4.1.2.2 Cyclohexylbiphenylcyclohexane (CBC-33)

Cyclohexylbiphenylcyclohexane (CBC-33) is the low molar mass thermotropic liquid crystal that was used in this study and manufactured by Merck Co.,Ltd. Germany. The molecular weight of CBC-33 is 402.67. The melting temperature (T_m) is 158°C . Smectic to Nematic temperature is 223°C and the clearing temperature is 327°C .

4.1.2.3 Glycerol monostearate (GMS)

Glycerol monostearate (GMS) is in the form of ivory white beads as received. It was manufactured by RIKEVITA (Malaysia) SDN.BHD. It can be used as an additive for internal lubricant and as an anti-static agent in various polymers. The molecular weight of GMS is 361. The melting temperature (T_m) is 65°C .

4.2 Equipments

4.2.1 Synthesis Part

All equipments , used in the catalyst preparation and polymerization , were listed as follows :

4.2.1.1 Schlenk line

Schlenk line consists of vacuum and argon lines. The vacuum line was equipped with the solvent trap and pump , respectively. The argon line was connected to the mercury bubbler that was a manometer tube and contain enough mercury to provide a seal from the atmosphere when argon line was evacuated. The Schlenk line was Show in [Figure 4.1](#).

4.2.1.2 Schlenk tube

A tube with a ground glass joint and a side arm which was three way glass valve as shown in [figure 4.2](#). Size of the Schlenk tubes were 50 ,100 and 200 ml used to prepare catalyst and collect materials which were sensitive to oxygen and moiture.

4.2.1.3 Glove box

Glove Box System 30905C manufactured by Vacuum Atmospheres Company , USA as shown in [figure 4.3](#).

4.2.1.4 Reactor

A 100 ml Stainless steel autoclave was used as the polymerization reactor.

4.2.1.5 Magnetic stirrer and Hot plate

The magnetic stirrer and hot plate Model RCT Basic from IKA Labortechnik were used.

4.2.1.6 Vacuum pump

The Vacuum pump model 195 from Labconco Corporation was used. A pressure of $10^{-1} - 10^{-3}$ mmHg was adequate for the vacuum supply to the vacuum line in the Schlenk line.

4.2.1.7 Inert gas supply

The inert gas (argon) was passed through columns of supported copper metal catalyst as oxygen scavenger, NaOH, P₂O₅ and molecular sieve 4A to remove moisture. The oxygen scavenger was regenerated by treatment with hydrogen at 300 °C for 2 hours before flowing the argon gas through all of the above columns.

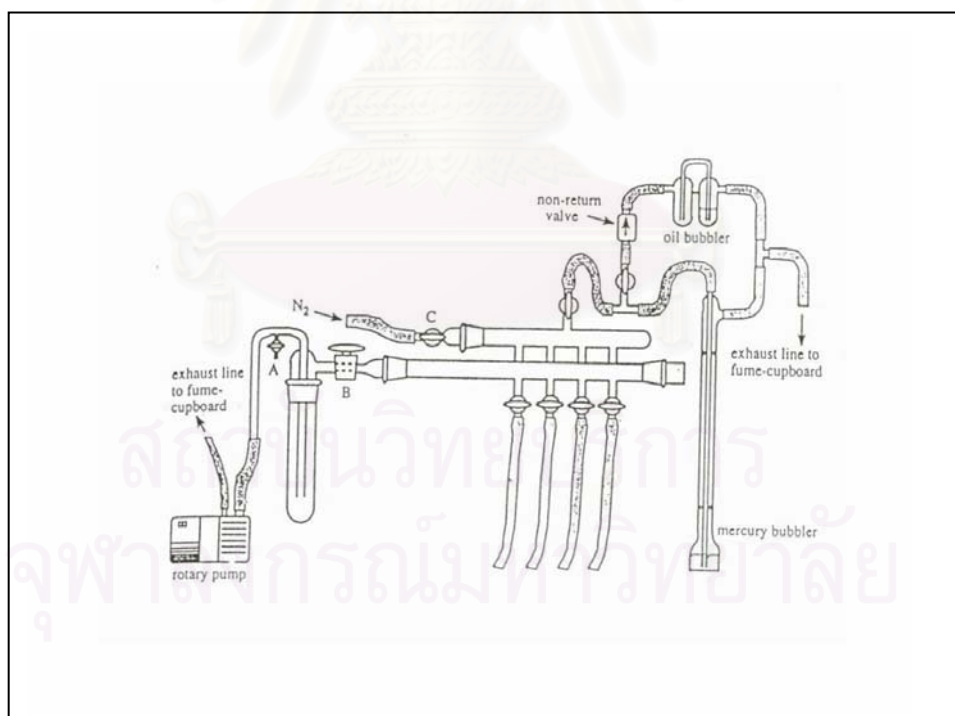


Figure 4.1 : Schlenk line



Figure 4.2 : Schlenk tube

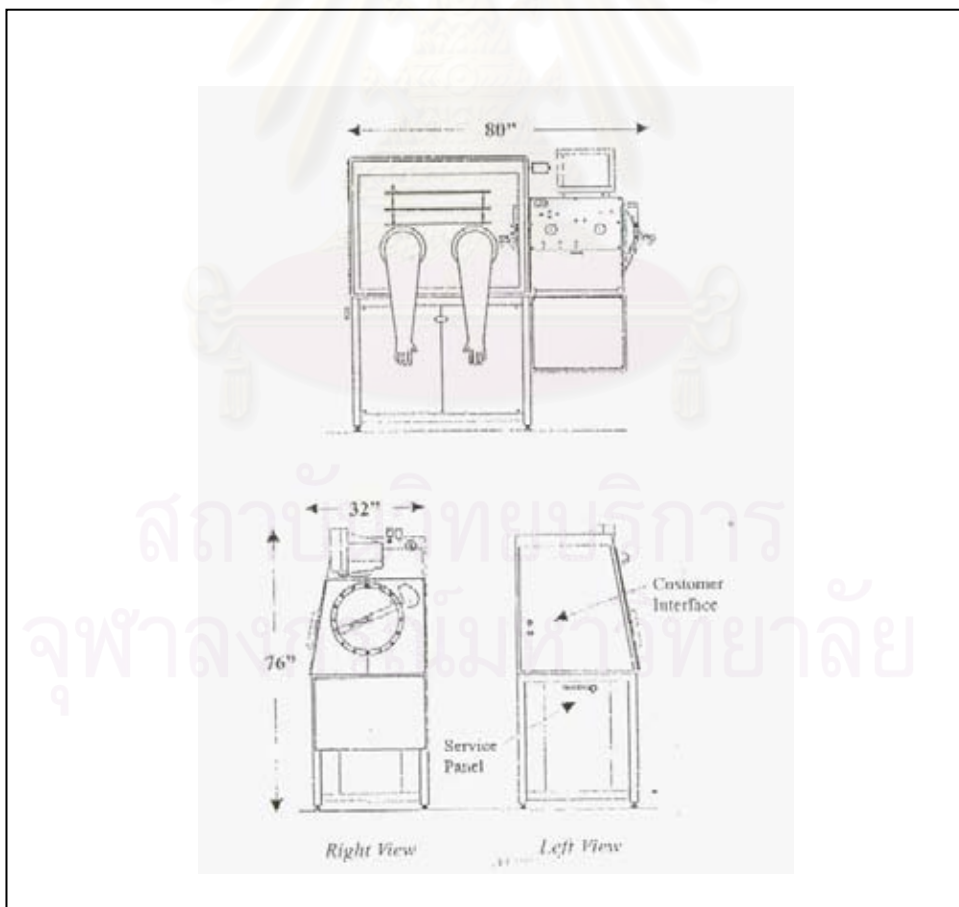


Figure 4.3 : Glove box

4.2.2 Polymer Blend Part

4.2.2.1 Digital hot plate stirrer

A Cole-Parmer digital hot plate stirrer was used for mixing the polymers with additives. This hot plate stirrer is programmable. All functions can be set from digital panel and display their status on LCD. The plate temperature, stirrer speed and time are controllable.

4.2.2.2 Hydraulic hot press

A local made hydraulic hot plate was used in these experiments. The maximum working temperature of this machine is 600 °C and the maximum pressure is 5,000 psi. This equipment was used for prepare the sample for rheology test.

4.3 Polymerization Procedure

The propylene polymerization reactions were carried out in a 100 ml stainless steel autoclave equipped with a magnetic stirrer. The autoclave and magnetic bar were dried in oven at 110 °C for 30 minutes and purged with argon 5 times by Schlenk line before used in the polymerization of propylene. Toluene and mixture of a prescribed amount of Et[Ind]₂ZrCl₂ and MAO stirred for 5 minutes at room temperature were introduced into the autoclave, respectively under argon atmosphere. The total volume of mixture solution was 30 ml. The whole mixture was allowed to aging for 10 minutes at room temperature. The reactor was frozen in liquid nitrogen to stop reaction, and then **autoclave was degassed**. The polymerization was started by feeding propylene gas at 40 °C. The reaction of polymerization was terminated by addition of acidic methanol. The precipitated polymer was washed with methanol and dried in the oven at 110 °C for 6 hours. Each polymerization was repeated to ensure reproducibility.

4.4 Sample Preparations

4.4.1 Sample preparation for light scattering

In this study we use melt mixing method to blend isotactic polypropylene and low molar mass liquid crystal chemical (LCC) or glycerol monostearate (GMS) because this method is most similar to the industrial practice. The blends of isotactic polypropylene and low molar mass liquid crystal chemical (LCC) or glycerol monostearate (GMS) were prepared at the composition of 1% by weight of isotactic polypropylene. Isotactic polypropylene and low molar mass liquid crystal chemical or glycerol monostearate were mixed on a digital hotplate that was covered by Teflon sheet, which was operated at temperature between 180-200 °C and mixed together for 15 minutes in order to have a uniform mixture. After that, the mixed blends were cut into small pellets and then pressed at 180 °C and 5000 psi for 5 minutes to form a thin with approximated thickness of 0.08 – 0.10 mm on a glass cover-slip by using a hydraulic hot press machine. And then, the samples were annealed and quenched at the temperatures of 200 °C and 100 °C, respectively and the range of time of each step is 10 minutes.

4.4.2 Sample preparation for scanning electron microscope (SEM)

The pellets of each blend were placed into a perforated plate stainless mould with the diameter of 20 mm. and 1 mm. thickness. The mould was placed between two releasing plates and heated for about 3 minutes until the polymer was almost all melted, then compressed at 200 °C and 5000 psi. for 10 minutes by a hydraulic hot press machine at polymer engineering laboratory, the Department of Chemical Engineering, Chulalongkorn University. After that, the samples were quenched at the temperatures of 100 °C for 10 minutes. And then, the pieces of sample were removed from the mould and then etched surfaces by permanganic etching which is a technique of removing material selectively to reveal lamellae in crystalline polymers. In this work, we use 3.5 % weight by volume solution of potassium permanganate in a concentrated sulfuric acid as the etchant [Marsha, S. 1998]. The samples were immersed and stirred in the etchant at 60 °C for 10 minutes in first etching. After that, samples were washed by water for 5 minutes and then washed by acetone for

5 minutes. Second etching , samples were stirred in the new prepared etchant at 60 °C for 10 minutes . Then the samples were washed by water for 10 minutes and washed by acetone for 10 minutes. Finally , samples were dried at room temperature and taken to investigate morphologies by scanning electron microscope.

4.4.3 Sample preparation for X-ray Diffraction (XRD)

Similar to sample preparation for small angle light scattering.

4.4.4 Sample preparation for Differential Scanning Calorimetry (DSC)

Similar to sample preparation for small angle light scattering.



สถาบันวิทยบริการ
จุฬาลงกรณ์มหาวิทยาลัย

4.5 Characterization Instruments

4.5.1 Small Angle Light Scattering (SALS)

This experiment was performed using the static light scattering apparatus at the polymer laboratory, the Department of Chemical Engineering, Chulalongkorn University. The equipment is schematically shown in Figure 3.

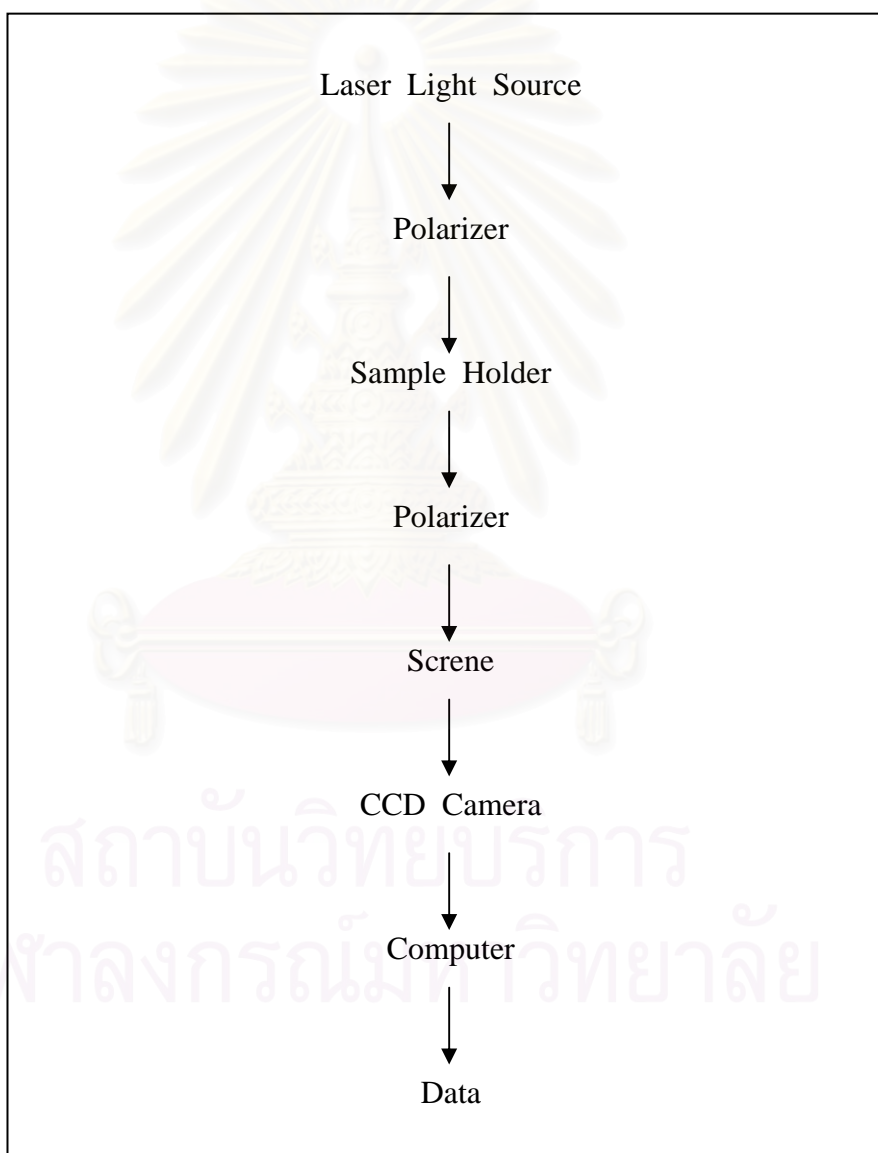


Figure 4.4 : A schematic diagram of static light scattering equipment

A He/Ne laser ($\lambda = 632.8 \text{ nm}$) is used as an incident light source. Samples were placed inside a holder, which was mounted between two polarizers where the polarization direction of the polarizer near the incident light was vertical and the other was horizontal. Light scattering photographs were detected by CCD Camera with exposure times 2 minutes, and the illumination of laser light source was set at no.6 (gain 6) and no.10 (gain10) by using the computer program which was connected to the apparatus. Then these photographs were transferred to analyze using the computer.

4.5.2 Scanning Electron Microscopy (SEM)

In scanning electron microscope, a fine beam of electron is first scanned across the surface of an opaque specimen. Once such as electron beam touches the surface, a difference of electron density in the specimen results a variety of scattering electron and photon emission. Those electrons are detected, modified and used to modulate the brightness of second beam scanned synchronously in cathode ray tube (CRT). A big collected signal produces a bright spot on the CRT while a small signal produces a dimmer spot. Details of this technique can be found elsewhere.

Crystalline morphologies of the etched surfaces of crystalline polymers in this research were observed by using a scanning electron microscope JSM – 5410 at the Scientific and Technological Research Equipment Center, Chulalongkorn University.

Since this technique requires the sample to be good at electron conducting, it is necessary to provide conduction to specimens by coating a thin metal layer. Thin film of gold was coated on specimens and then they were kept in a dry place before experiment. SEM was operated at 1.5 kV. This is considered to be suitable condition since too high energy can cause burning to sample.

4.5.3 Differential Scanning Calorimetry (DSC)

A Perkin-Elmer DSC-7 equipped with a robot at Central Instrument Facility (CIF), Mahidol University was used for the DSC measurements. The temperature calibration of the DSC was performed using the melting peak of indium, at 10 °C/min. The DSC was used for preparation of samples for the XRD experiments and, besides, for (conventional) DSC experiments. Samples were prepared by melting discs cut out of the extrudate in the DSC at 200 °C during 15 min, followed by controlled cooling at 10 °C/min and recovering the polymer discs from the pans. Part of the samples were analysed by DSC. About 5 mg was measured at a heating rate of 10 °C/min. Nitrogen was used as a flow gas.

4.5.4 X-Ray Diffraction (XRD)

Philips Expert PW 3710 Based HT 10 X-ray Diffractometer (XRD) at the Metallurgy and Materials Science Research Institute, Chulalongkorn University was utilized for phase analysis and estimating the crystallinity of the polymers and chemicals. At first the sample was operated and the crystalline reflections being measured over the range $2\theta = 5^\circ$ to $2\theta = 30^\circ$ at room temperature in order to obtain crystalline background. And then the sample was heated from room temperature to the temperature above the melting point at a heating rate of 20 °C/min and intensities were recorded in order to obtain non-crystalline background.

X-ray photographs of polypropylene samples at high temperatures in the melt were obtained and used for determined crystallinity. The samples were held in the inner chamber of the X-ray furnace (in vacuum) in a small cylindrical container made of aluminium foil with a thermocouple placed in contact with one end of the sample.

The crystallinity is determined by measuring the integrated area of the crystalline reflections and the integrated of the non-crystalline background and comparing the two [G. Farrow, 1961].

CHAPTER V

Results and Discussion

5.1 Polymerization of Propylene

5.1.1 The Effect of Polymerization Time on Catalytic Activity

The effects of different polymerization times on propylene polymerization using $\text{Et}[\text{Ind}]_2\text{ZrCl}_2$ as catalyst and methylaluminoxane (MAO) as cocatalyst, were investigated. Polymerization was operated in three different polymerization times viz., 1.0, 1.5 and 2.0 hour(s). The experimental results indicated the relationship of polymerization time, yield and catalytic activity of polypropylene produced are shown in Table 5.1, Figure 5.1 and Figure 5.2, respectively.

Table 5.1 : Yields and catalytic activities of polypropylene produced at different polymerization time ^a

Sample	Polymerization Time (hour)	Yield (g)	Catalytic activity (g PP / mmol Zr-hr)
PP1	1.0	0.7331	488.7333
PP2	1.5	2.2314	991.7333
PP3	2.0	3.0921	1,030.700

^a Polymerization conditions : $[\text{Et}[\text{Ind}]_2\text{ZrCl}_2] = 5 \times 10^{-5}$ mol/L, $[\text{MAO}] = 2.598$ mol/L, pressure of propylene gas = 100 psi, Al/Zr = 2,000, polymerization temperature = 40 °C

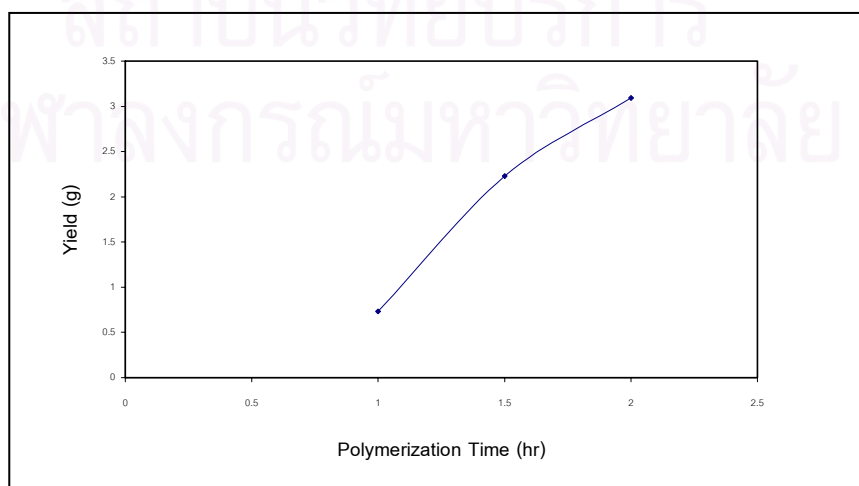


Figure 5.1 : Yield of polypropylene produced at different polymerization times

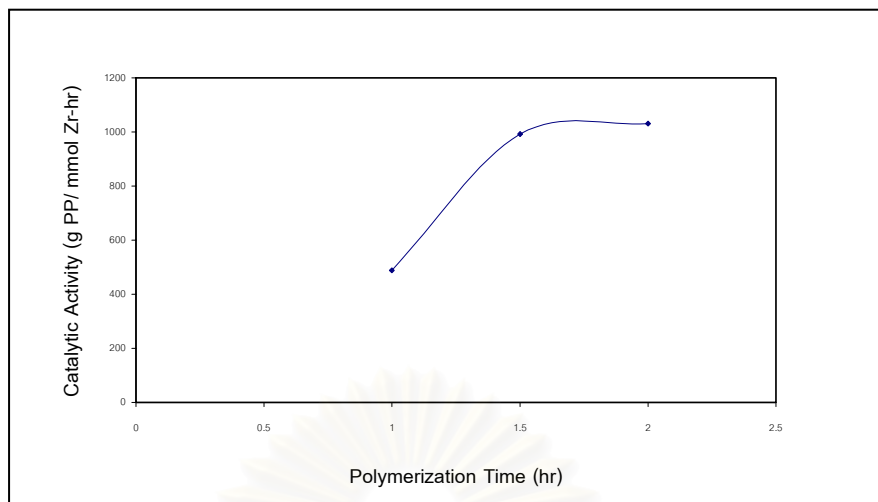


Figure 5.2 : Catalytic activity of polypropylene produced at different polymerization times

As shown in Figure 5.1, yield of polypropylene rapidly increases at the polymerization time between 1.0 and 1.5 hours and it begins to slightly increase between 1.5 and 2.0 hours of polymerization time. According to a slight increase of yield of polypropylene after polymerization time of 1.5 hours, it was indicated that the yield increases in reducing rate.

Similar to the result of yield, from Figure 5.2, the catalytic activity considerably increases with increasing polymerization time. Reaching the polymerization time of 1.5 hours, activity slightly increases. It probably concerns with steric effect of the production of polymer for the propene polymerization, that is to say the active species formed by reaction of $\text{Et}[\text{Ind}]_2\text{ZrCl}_2$ and MAO were shielded with the produced polypropylene.

5.2 Light Scattering Measurement

There are two parts of results from light scattering experiment , scattered light photographs and digital intensity data.

5.2.1 Scattered light photographs

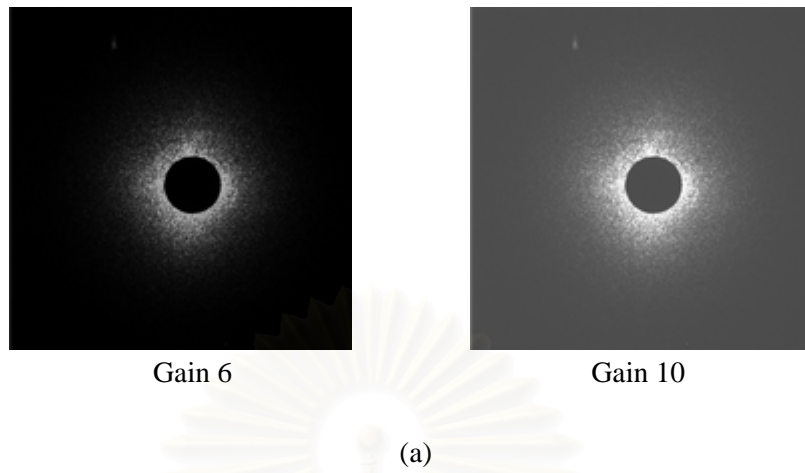
Light scattering behaviors of the systems of polymer blends between polypropylene and low molar mass liquid crystal chemical (LCC) and polymer blends between polypropylene and glycerol monostearate (GMS) were investigated by using the modified light scattering apparatus with the illumination of light at gain 6 and gain 10. This apparatus will show the scattered light photographs which are both the single image and successive images. Furthermore it can provide digital intensity data at every angle of scattering. This modification are different from the original apparatus which use only the photographic light scattering technique and cannot save the light scattering photograph into the computer. Unlike the modified apparatus, the original apparatus can measure intensity at some angle of scattering. Therefore there are many information from the modified apparatus. Figure 5.3 shows scattered light photographs of pure component and the blends at 1% of low molar mass liquid crystal chemical and glycerol monostearate compositions from gain 6 and gain 10 .

The property of each polypropylene are shown in Table 5.2 ,so that use to compare light scattering behavior.

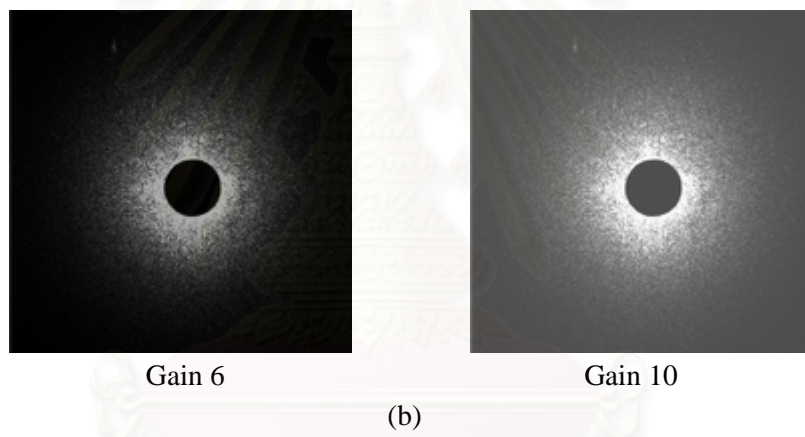
Sample	Catalyst	Polymerization time (min)	Melt flow index
PP1	Metallocene	60	n.d.
PP2	Metallocene	90	n.d.
PP3	Metallocene	120	n.d.
PP4	Ziegler-Natta	n.d.	20
PP5	Ziegler-Natta	n.d.	11
PP6	Ziegler-Natta	n.d.	2

Table 5.2 : Properties of polypropylene that synthesized by metallocene catalyst and Ziegler-Natta catalyst.

Pure Polypropylene 1



Polypropylene 1 / 1% LCC



Polypropylene 1 / 1% GMS

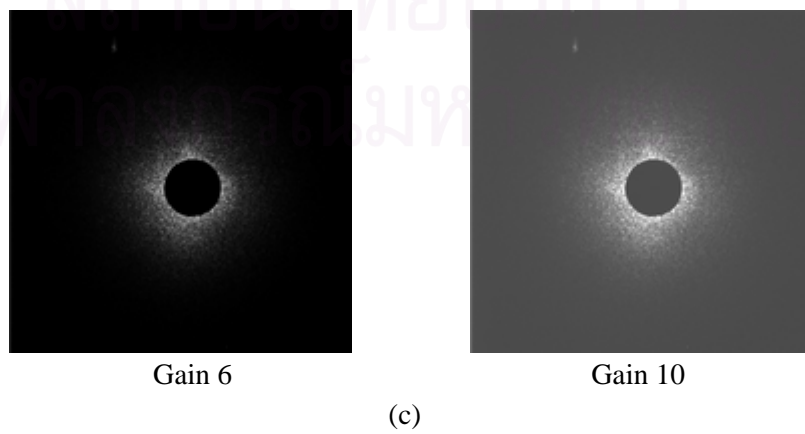
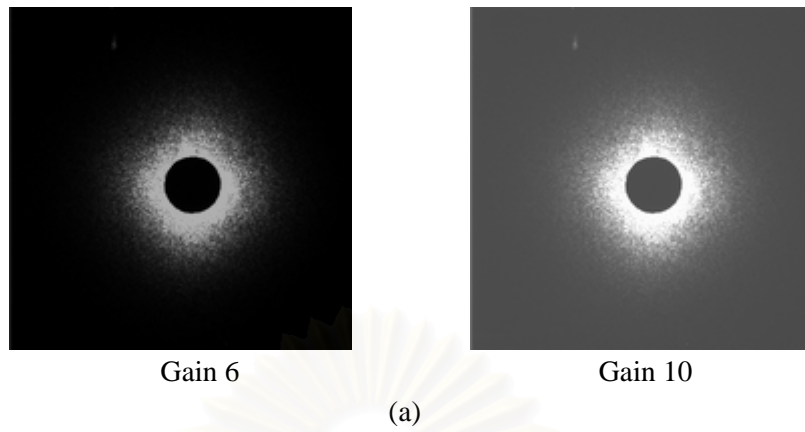
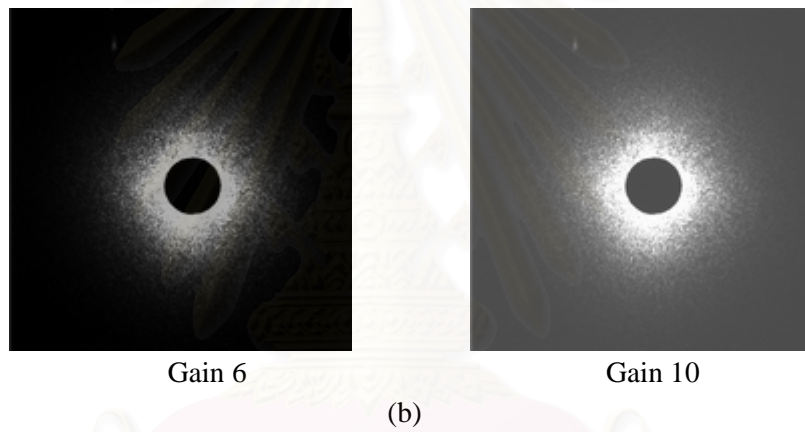


Figure 5.3 : Scattering light photographs of pure polypropylene 1 and their blends of LCC and GMS.

Pure Polypropylene 2



Polypropylene 2 / 1% LCC



Polypropylene 2 / 1% GMS

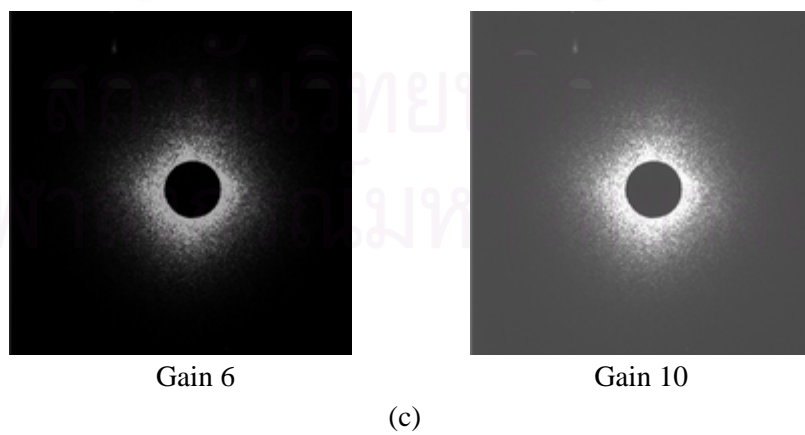
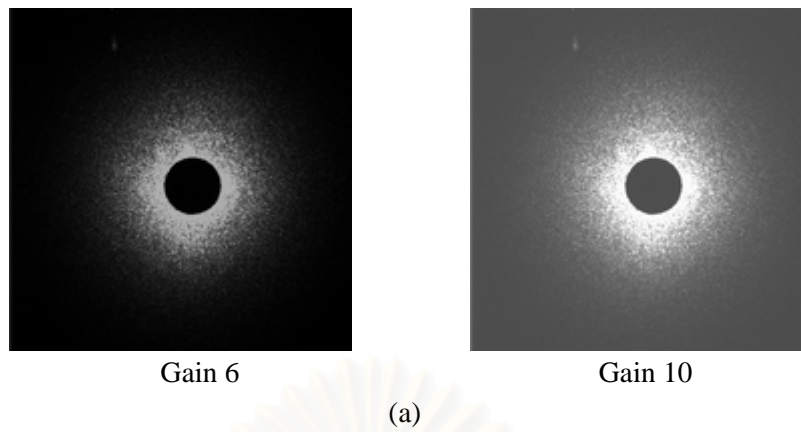
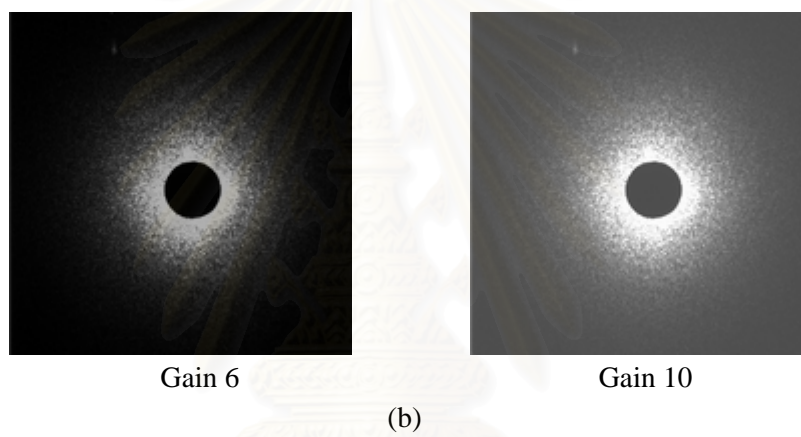


Figure 5.4 : Scattering light photographs of pure polypropylene 2 and their blends of LCC and GMS.

Pure Polypropylene 3



Polypropylene 3 / 1% LCC



Polypropylene 3 / 1% GMS

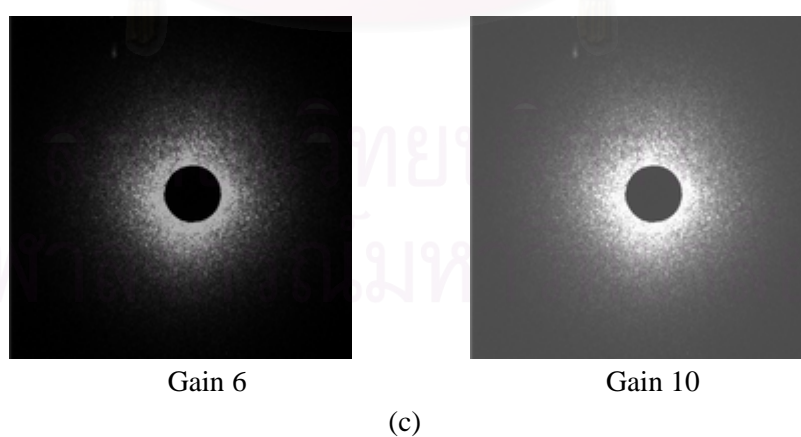
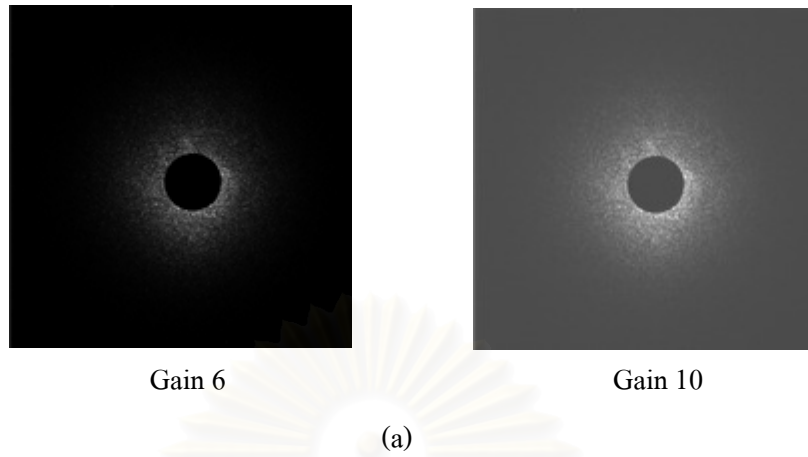
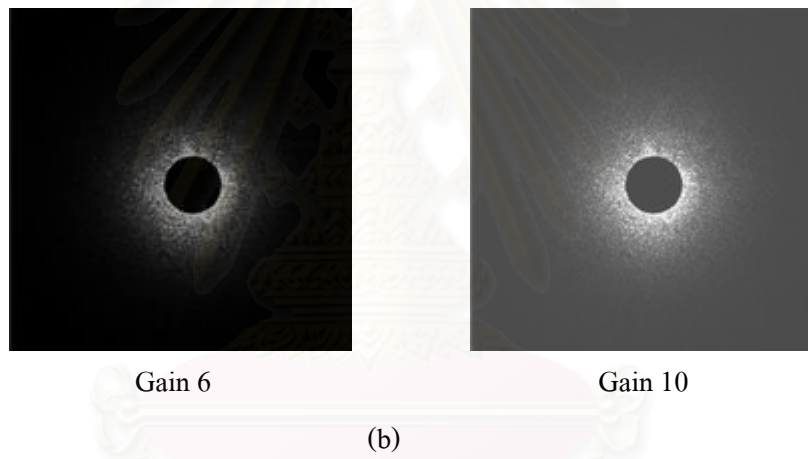


Figure 5.5 : Scattering light photographs of pure polypropylene 3 and their blends of LCC and GMS.

Pure Polypropylene 4



Polypropylene 4 / 1% LCC



Polypropylene 4 / 1% GMS

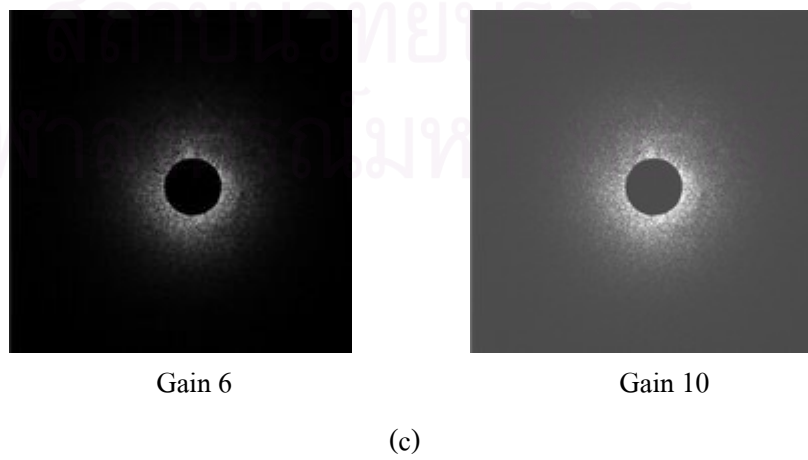
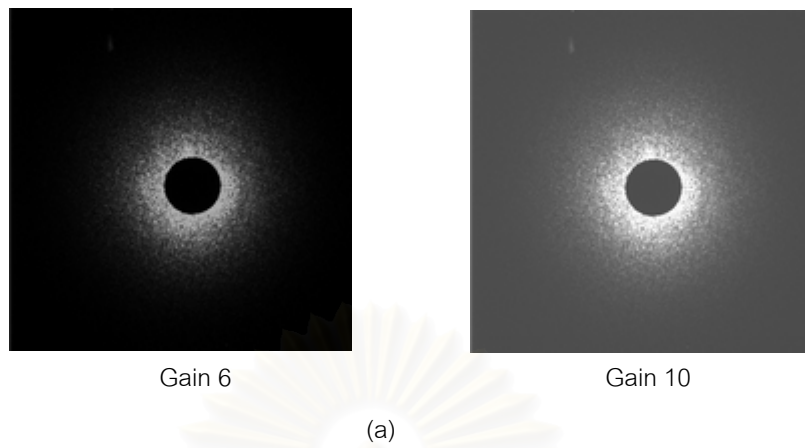
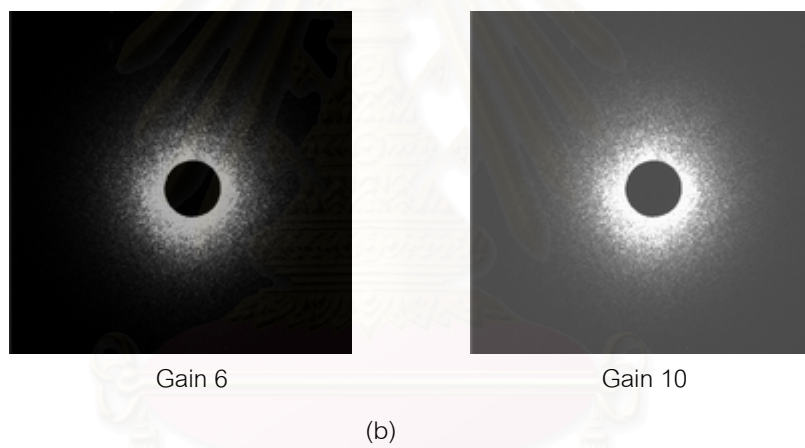


Figure 5.6 : Scattering light photographs of pure polypropylene 4 and their blends of LCC and GMS.

Pure Polypropylene 5



Polypropylene 5 / 1% LCC



Polypropylene 5 / 1% GMS

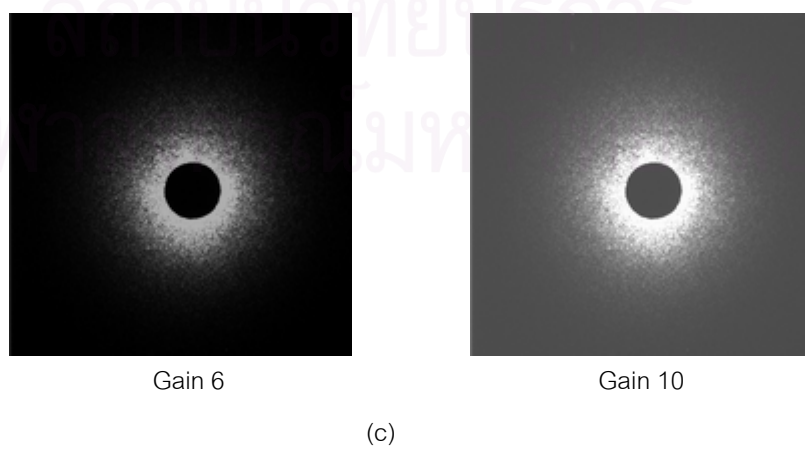
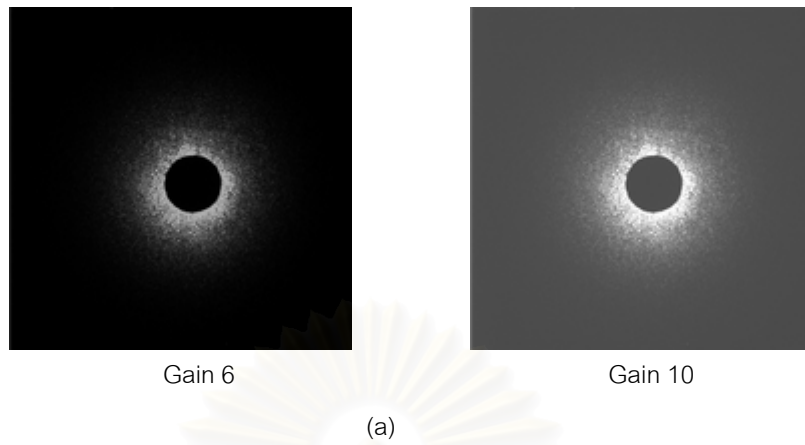
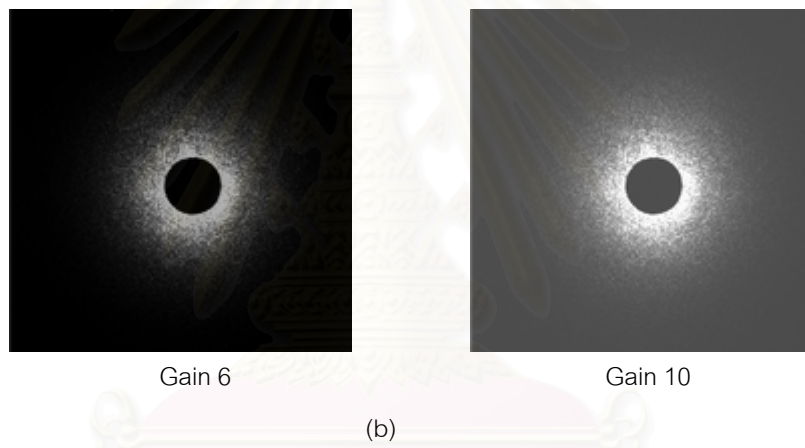


Figure 5.7 : Scattering light photographs of pure polypropylene 5 and their blends of LCC and GMS.

Pure Polypropylene 6



Polypropylene 6 / 1% LCC



Polypropylene 6 / 1% GMS

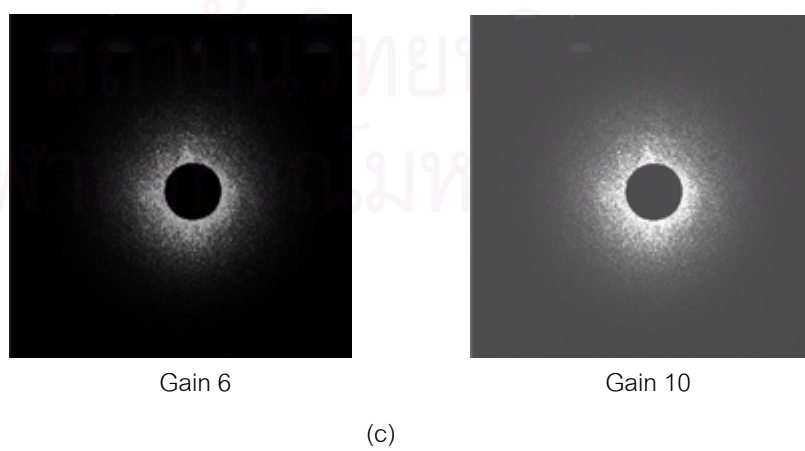
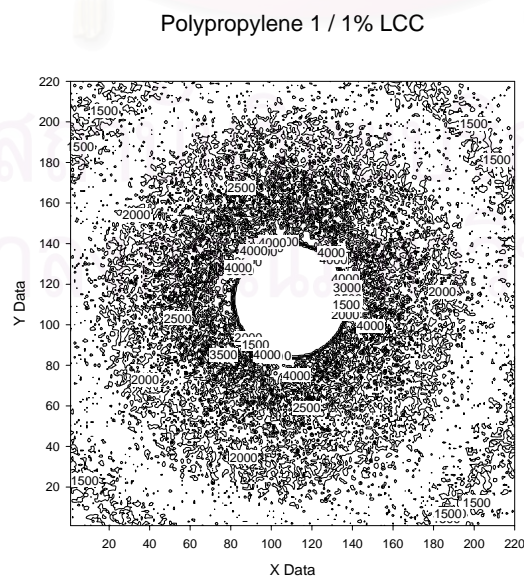
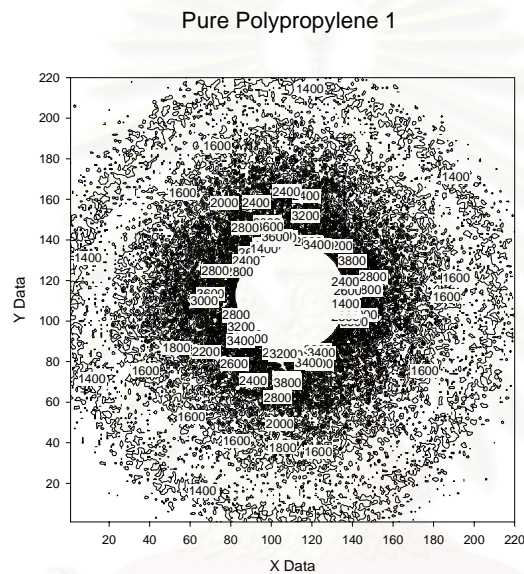


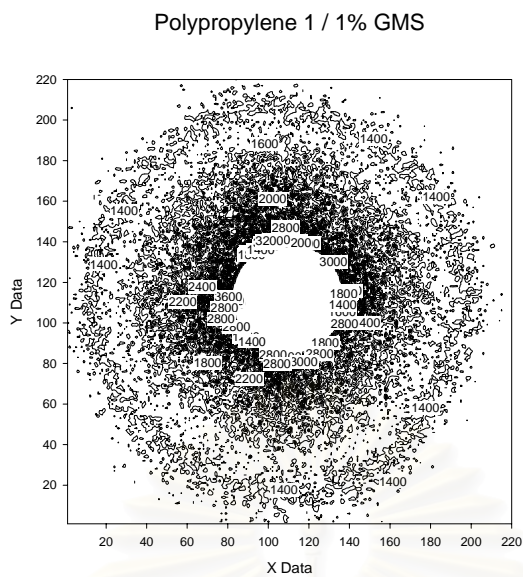
Figure 5.8 : Scattering light photographs of pure polypropylene 6 and their blends of LCC and GMS.

From these scattered light photographs, the best gain is gain 10 because the intensity data are bright enough and suit to transfer into digital intensity data.

5.2.2 Digital Intensity data

The static light scattering apparatus can provide digital intensity data for every pixels. For one light scattering photograph, it contains 48,400 data points of digital intensity and it can be plot as show in Figure 5.9.





(c)

Figure 5.9 : Scattered light contour graphs of (a) Pure Polypropylene 1, (b) Polypropylene 1 / 1% LCC and (c) Polypropylene 1 / 1% GMS

From Figure 5.9, the data points are processed as shown in the schematic diagram (Figure 5.10) in order to obtain smooth contour lines.

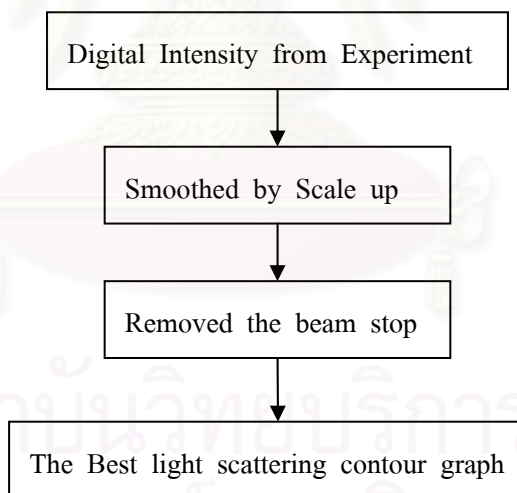


Figure 5.10 : Schematic diagram of smoothing procedure

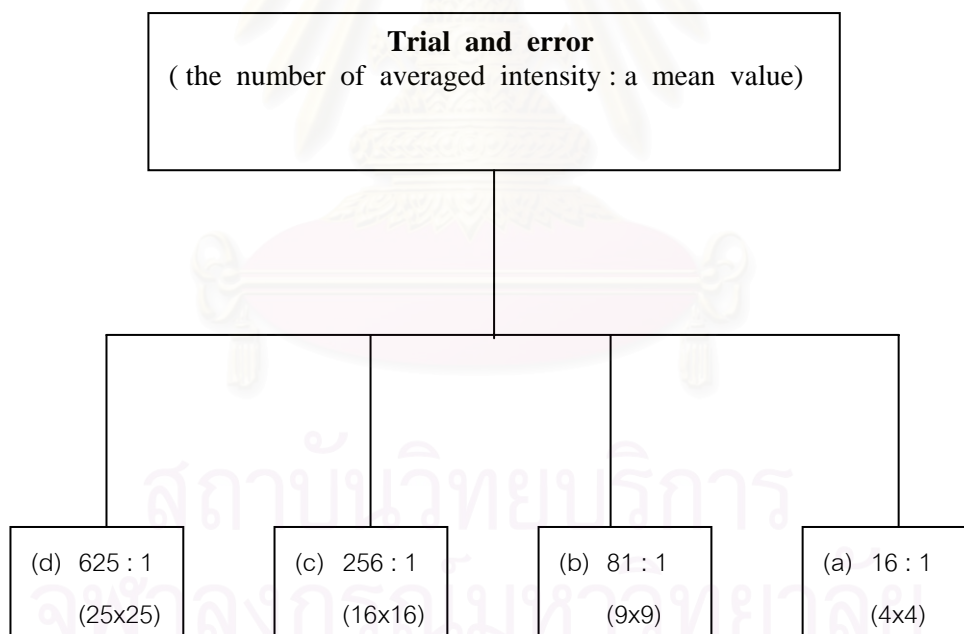
This procedure is auto - running by using sub - programming which can be run within 3 minutes.

5.2.2.1 Smoothing Digital Intensity Data

Digital intensity data are smoothed by using the average of intensity data to get better contour graphs that are clear and the characteristics of their curvatures are the same.

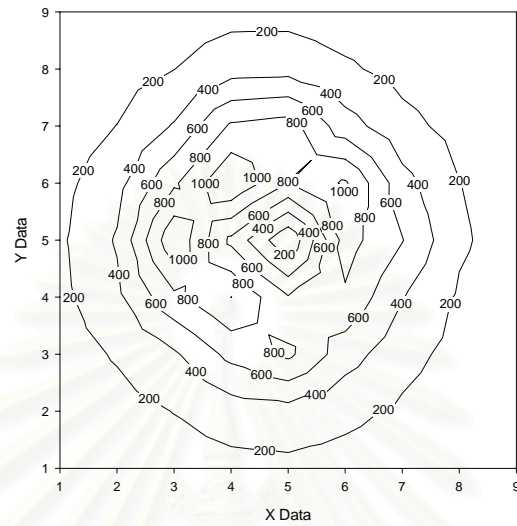
In searching the standard procedure , many trials and errors were done by varying the number of intensity data , which are averaged , and collected in details.

The detail of that trial can be concluded as follow ,



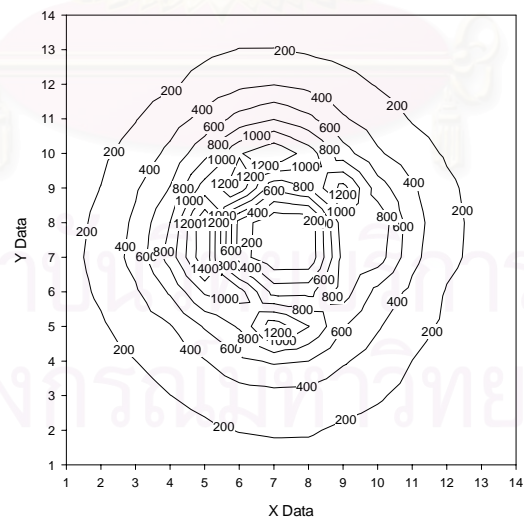
Result from trial and error are shown as contour graphs.

Pure Polypropylene 1



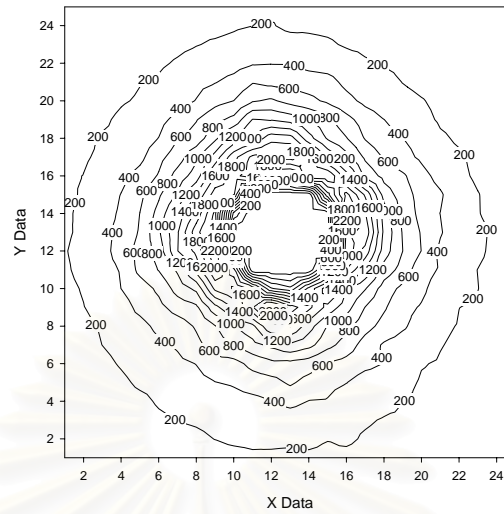
(a) 625 : 1 (25x25)

Pure Polypropylene 1



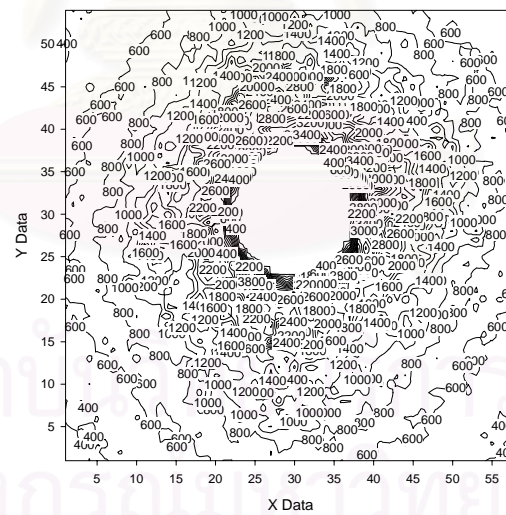
(b) 256 : 1 (16x16)

Pure Polypropylene 1



(c) 81 : 1 (9x9)

Pure Polypropylene 1

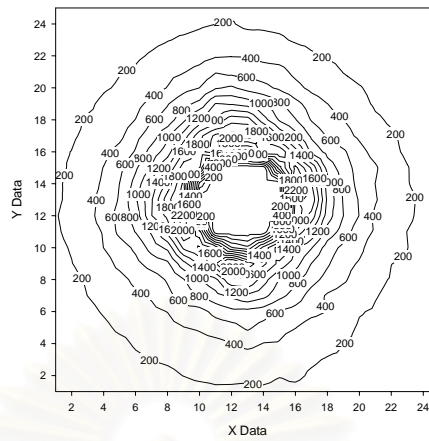


(d) 16 : 1 (4x4)

Figure 5.11 : Contour graphs of trial and error in smoothing intensity data

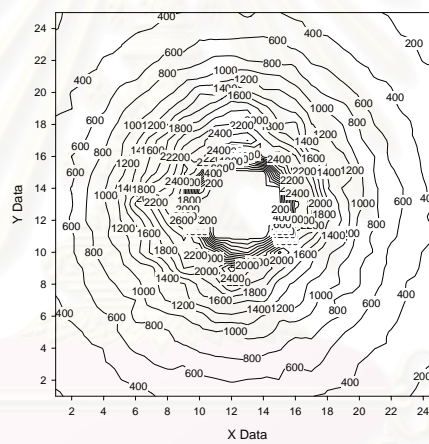
From these results, the best result is 81 : 1 because the graph fit with the scale and it is not too small to collect the important detail as well as its contour line can be distinguishable.

Pure Polypropylene 1



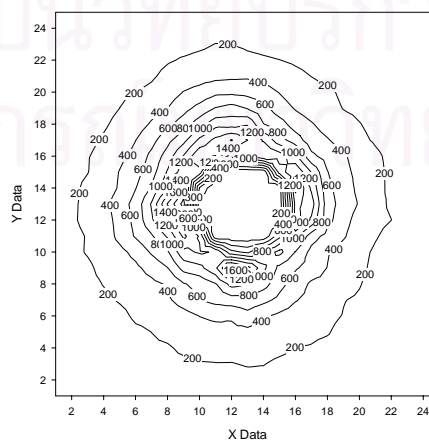
(a)

Polypropylene 1 / 1% LCC



(b)

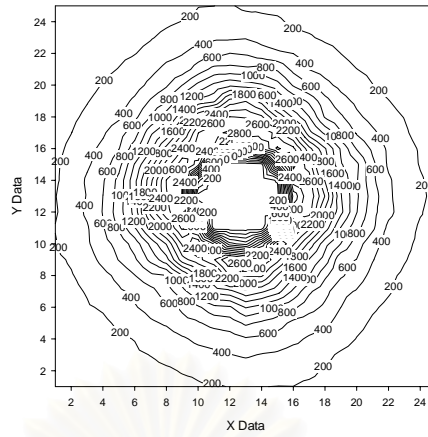
Polypropylene 1 / 1% GMS



(c)

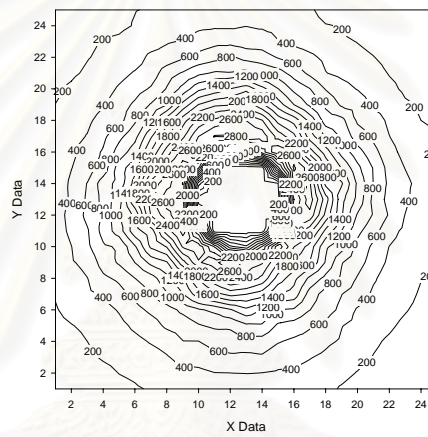
Figure 5.12 : Smoothed contour graphs of (a) pure polypropylene 1, (b) polypropylene1 /1% LCC and (c) polypropylene 1 / 1% GMS blends

Pure Polypropylene 2



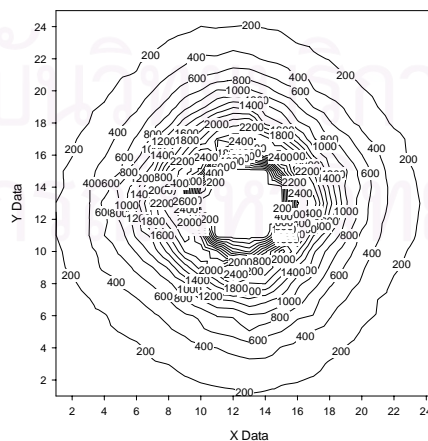
(a)

Polypropylene 2 / 1% LCC



(b)

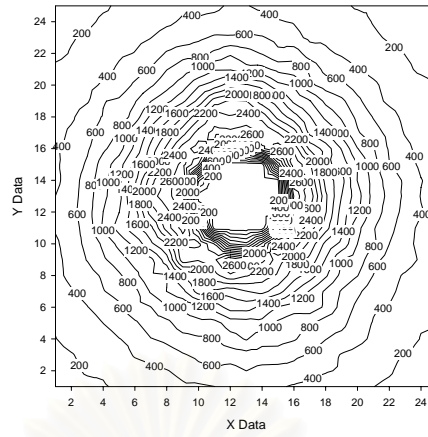
Polypropylene 2 / 1% GMS



(c)

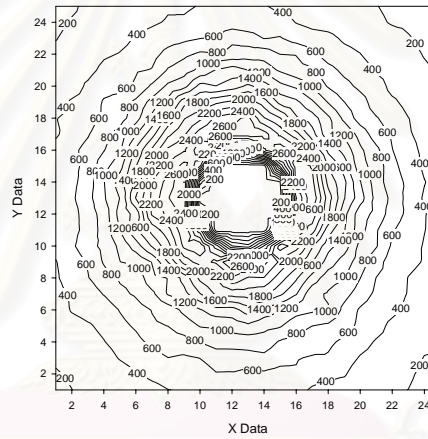
Figure 5.13 : Smoothed contour graphs of (a) pure polypropylene 2, (b) polypropylene 2 / 1% LCC and (c) polypropylene 2 / 1% GMS blends

Pure Polypropylene 3



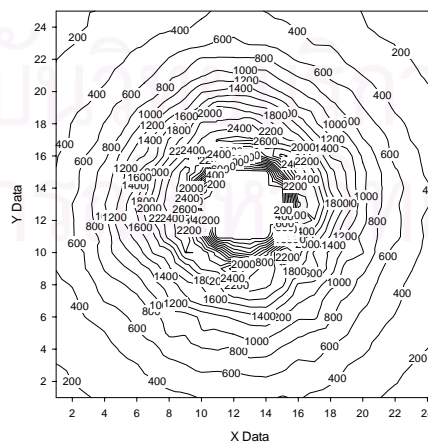
(a)

Polypropylene 3 / 1 % LCC



(b)

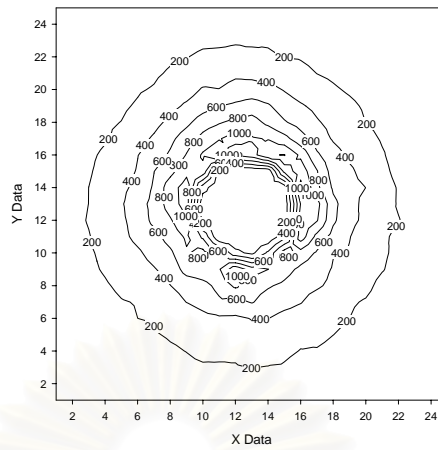
Polypropylene 3 / 1 % GMS



(c)

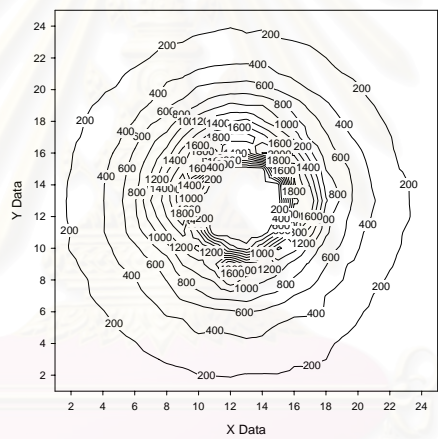
Figure 5.14 : Smoothed contour graphs of (a) pure polypropylene 3, (b) polypropylene 3 / 1% LCC and (c) polypropylene 3 / 1% GMS blends

Pure Polypropylene 4



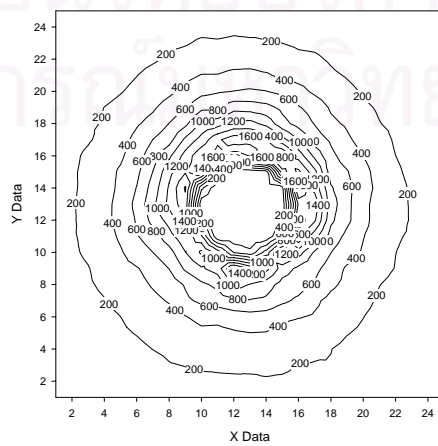
(a)

Polypropylene 4 / 1 % LCC



(b)

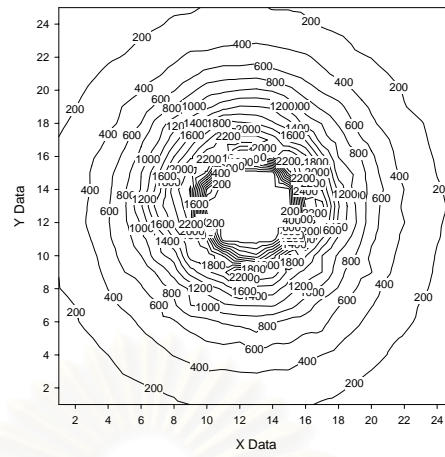
Polypropylene 4 / 1 % GMS



(c)

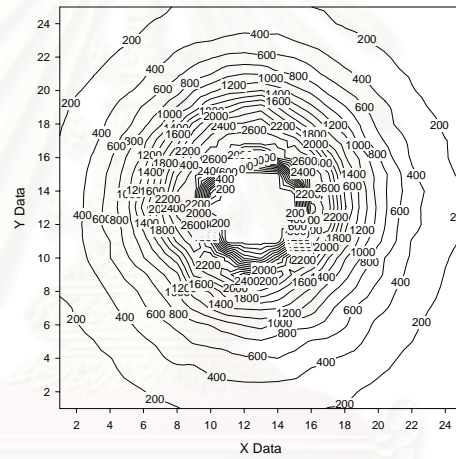
Figure 5.15 : Smoothed contour graphs of (a) pure polypropylene 4, (b) polypropylene 4 /1% LCC and (c) polypropylene 4 / 1% GMS blends

Pure Polypropylene 5



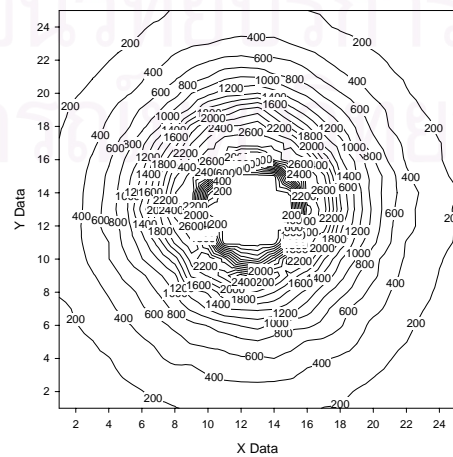
(a)

Polypropylene 5 / 1% LCC



(b)

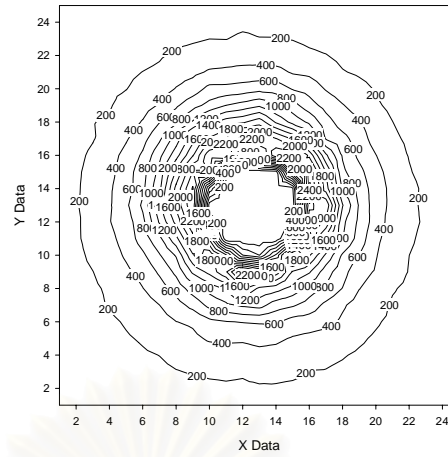
Polypropylene 5 / 1% GMS



(c)

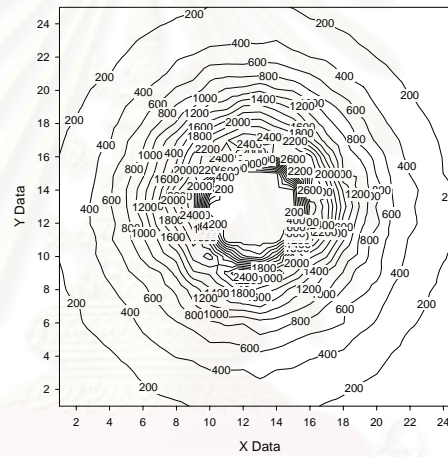
Figure 5.16 : Smoothed contour graphs of (a) pure polypropylene 5, (b) polypropylene 5 / 1% LCC blends and (c) polypropylene 5 / 1% GMS blends

Pure Polypropylene 6



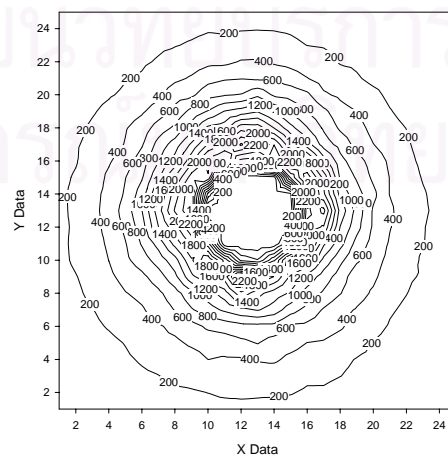
(a)

Polypropylene 6 / 1 % LCC



(b)

Polypropylene 6 / 1% GMS



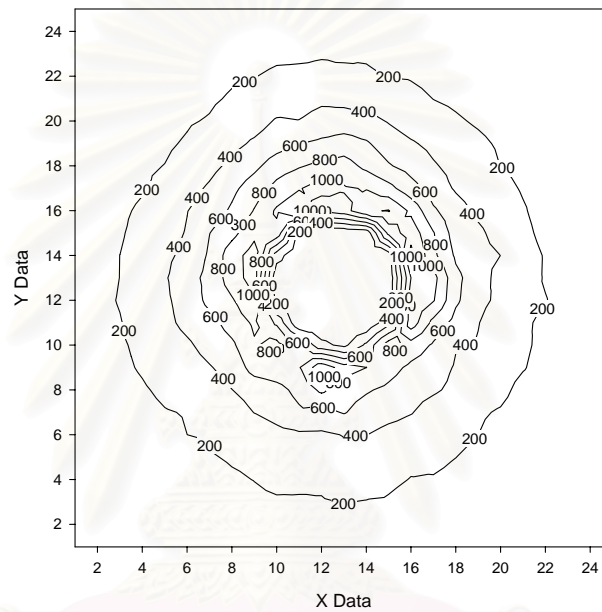
(c)

Figure 5.17 : Smoothed contour graphs of (a) pure polypropylene 6, (b) polypropylene 6 / 1% LCC and (c) polypropylene 6 / 1% GMS blends

5.2.2.2 Removing the beam stop

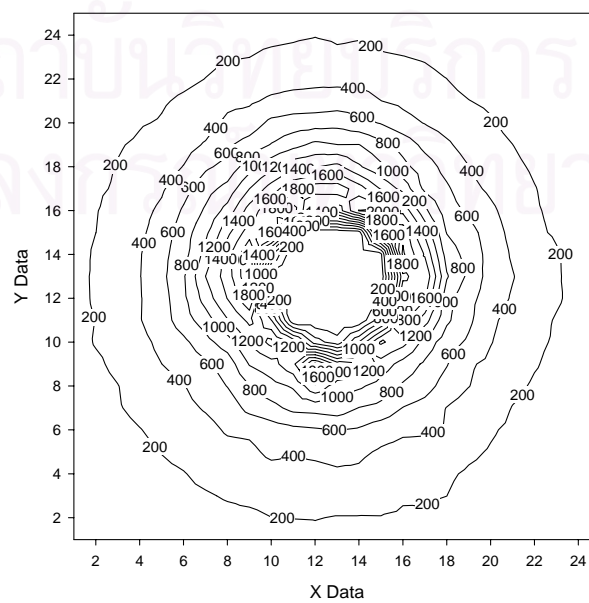
At the center of each contour graph, it shows a small circle of the beam stop which comes from placing a coin at the center of the scene to protect the lens of the CCD Camera from the incident beam. Because the intensity data at this area do not arise from the light scattering of sample so they should be adjusted by using average intensity data from the outermost edge of the circle in this area. Adjusted results are shown in Figure 5.18.

Pure Polypropylene 4



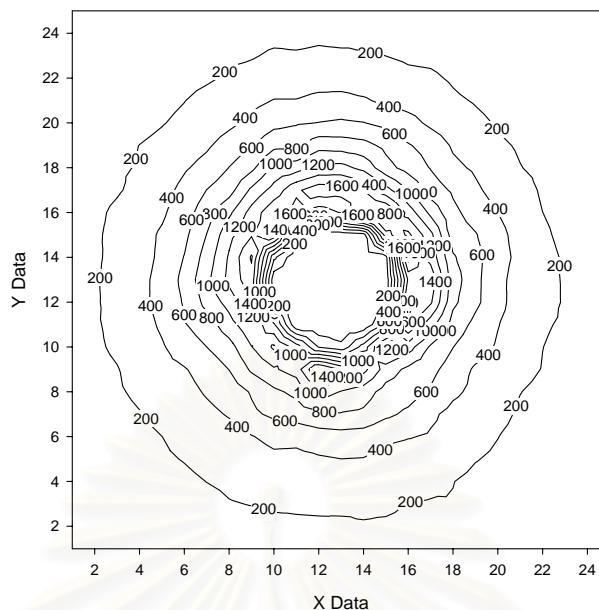
(a)

Polypropylene 4/ 1 % LCC



(b)

Polypropylene 4 / 1 % GMS



(c)

Figure 5.18 : Contour graphs of (a) pure polypropylene 4 (b) polypropylene 4 / 1% LCC and (c) polypropylene 4 / 1%GMS

According to the intensity data, it was found that the crystals of polypropylenes that were synthesized by metallocene catalyst in different polymerization times will differently scatter laser beams, that is to say polypropylene obtained in higher polymerization time can better scatters laser beams. For Ziegler-Natta-synthesized polypropylene, PP5 (melt flow index = 11) has the highest light scattering. And when addition of low molar mass liquid crystal chemical (LCC) or glycerol monostearate (GMS) was operated, there have some changes in crystalline structure. In the case of addition of low molar mass liquid crystal chemical, the scattering light photographs were brighter. It was indicated that the crystal of these blends can scatter laser beams more than pure polypropylene crystal, angles of light scattering extend, because of the enhancement of crystallinity. But the blends of polypropylene and GMS do not have apparent tendency of increasing light scattering. Namely in the case of metallocene-synthesized polypropylene, the blends scatter laser beam less than pure polypropylene, but the blends of Ziegler-Natta-synthesized polypropylenes and GMS scatter laser beam better than pure polypropylene. These results require further investigation from results of DSC and XRD.

From the obtained results, it is sufficient to indicate that the blend of polypropylene and low molar mass liquid crystal chemical have the highest crystallinity in all of polypropylenes because of the best light scattering. However, in the case of GMS addition it is necessary to prove this suggestion by other accurated analytical techniques to support these results.

5.3 Differential Scanning Calorimetry (DSC)

Results of DSC experiments, obtained on samples heated, cooled and heated again at $10\text{ }^{\circ}\text{C} / \text{min}$ from the temperature of -20 to $200\text{ }^{\circ}\text{C}$, are presented in Table 5.3. Melting temperatures of polypropylenes produced using Ziegler-Natta are significantly higher than melting temperature of metallocene-synthesized polypropylene, because of the different molecular weight of each polypropylenes. Actually molecular weight of metallocene-synthesized polypropylene is higher than molecular weight of Ziegler-Natta-synthesized polypropylene in the heterogeneous polymerization system. However the obtained metallocene-synthesized polypropylenes were produced in homogeneous polymerization system, therefore molecular weight of metallocene-synthesized polypropylene is lower than molecular weight of Ziegler-Natta-synthesized polypropylene. Effects of low molar mass liquid crystal chemical addition on melting temperature (T_m) in various molecular weight isotactic polypropylene can be found. For polypropylene synthesized by

Sample	Catalyst	Polymerization time (min)	Melt flow index	T_m 1 st heating ($^{\circ}\text{C}$)	T_c ($^{\circ}\text{C}$)	T_m 2 nd heating ($^{\circ}\text{C}$)	
PP1	Pure	Metallocene	60	n.d.	141.53	106.56	136.3
	LC				140.84	106.11	135.67
	GMS				135.52	102.72	132.05
PP2	Pure	Metallocene	90	n.d.	142.03	106.13	136.2
	LC				136.95	104.31	134.3
	GMS				138.48	103.24	134.18
PP3	Pure	Metallocene	120	n.d.	139.35	102.74	134.89
	LC				135.64	102.54	132.15
	GMS				135.18	102.94	131.93
PP4	Pure	Ziegler-Natta	n.d.	20	169.36	114.05	165.02
	LC				166.42	118.77	166.44
	GMS				163.59	118.43	163.57
PP5	Pure	Ziegler-Natta	n.d.	11	171.86	113.88	166.05
	LC				164.56	118.5	164.51
	GMS				163.78	118.47	164.56
PP6	Pure	Ziegler-Natta	n.d.	2	170.14	111.49	167.99
	LC				166.38	116.25	166.66
	GMS				166.28	116.68	165.51

Table 5.3 : Melting temperature and Crystallization temperature of polypropylene and their blends.

metallocene catalyst (PP1 , PP2 and PP3) the first heated and the second heated melting temperatures decrease about 4 °C and 2 °C, respectively. The crystallization temperature (Tc) of the low molar mass liquid crystal chemical blend remain equal to the pure polypropylene.

For polypropylene produced using Ziegler-Natta catalyst (PP4 , PP5 and PP6) , the first heated melting temperature fall around 5 °C and it has not apparent tendency of the reduction temperature from the second heated samples. The crystallization temperature from the cool down experiments will increase about 5 °C.

The influences of glycerol monostearate addition on polypropylene synthesized by metallocene catalyst (PP1 , PP2 and PP3), the first heated and the second heated melting temperature decrease about 5 °C and 3 °C , respectively. But the crystallization temperatures do not clearly change.

Sample	Catalyst	Polymerization time (min)	Melt flow index	1 st Melting lattice energy(J/g)	Lattice energy (J/g)	2 nd Melting lattice energy(J/g)	
PP1	Pure	Metallocene	60	n.d.	92.5	79.8	77.95
	LC				71.88	57.36	60.26
	GMS				68.49	53.46	58.15
PP2	Pure	Metallocene	90	n.d.	89.64	84.2	83.15
	LC				88.09	72.96	77.89
	GMS				88.29	67.24	76.44
PP3	Pure	Metallocene	120	n.d.	89.1	78.94	80.36
	LC				93.29	58.94	71.57
	GMS				113.08	61.08	70.65
PP4	Pure	Ziegler-Natta	n.d.	20	101.18	107.77	109.83
	LC				117.87	94.23	100.4
	GMS				108.66	97.09	96.55
PP5	Pure	Ziegler-Natta	n.d.	11	91.66	102.08	101.52
	LC				108.37	99.05	97.58
	GMS				107.93	98.48	99.6
PP6	Pure	Ziegler-Natta	n.d.	2	99.5	100.85	102.07
	LC				108.74	89.06	89.9
	GMS				94.03	91.41	94.69

Table 5.4 : Melting lattice energy and Lattice energy of polypropylene and their blends.

For polypropylene produced using Ziegler-Natta catalyst (PP4, PP5 and PP6) the first heated and the second heated melting temperature decrease about 6 °C and 2 °C, respectively. The crystallization temperature increase around 5 °C.

It is also found that if polymer is passed many cycles of heating, the melting temperature will decrease and both of low molar mass liquid crystal chemical and glycerol monostearate blends can also reduce crystalline lattice energy and crystalline melting lattice energy.

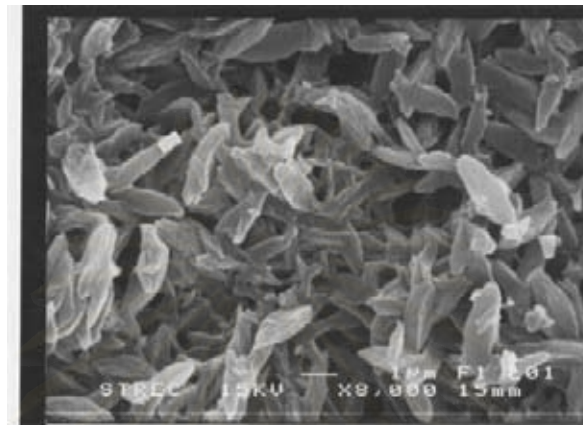
From these results, they are summarized that low molar mass liquid crystal chemical and glycerol monostearate slightly decrease melting temperature of polypropylene. Because low molar mass liquid crystal chemical and GMS reduce melt viscosity of the blends (S.Wacharawichanant *et al.* 2004), crystal of the blends will melt easier, therefore melting phenomena can occur at lower temperature. Glycerol monostearate can also have more effects on melting temperature rather than low molar mass liquid crystal polymer for both synthesis catalyst systems.

Low molar mass liquid crystal chemical and glycerol monostearate do not apparently effect crystallization temperatures for polypropylene synthesized using metallocene catalyst. On the other hand, for polypropylene synthesized by ziegler-natta catalyst, crystallization temperature of the glycerol monostearate blend significantly increase. Because low molar mass liquid crystal chemical and glycerol monostearate are able to enhance molecular mobility (S.Wacharawichanant *et al.* 2004) and to accelerate crystallization, therefore crystallization is able to occur at higher temperature.

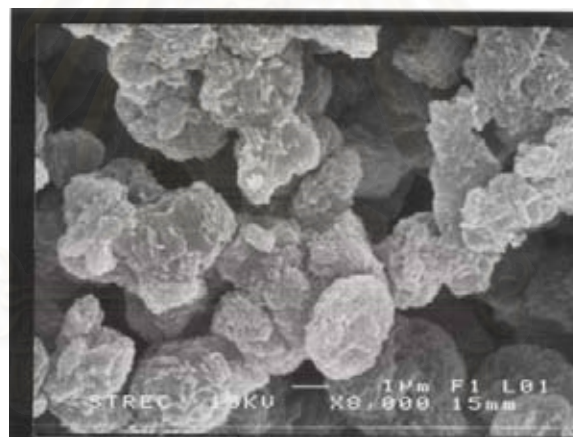
These significant differences of crystallization temperatures, when low molar mass liquid crystal chemical and glycerol monostearate were added, due to high molecular weights of Ziegler-Natta-synthesized polypropylenes. On the other hand, for metallocene-synthesized polypropylenes, their differences of crystallization temperatures compared to pure polymer are slightly change because of their lower molecular weights than the Ziegler-Natta polypropylene.

5.4 Scanning Electron Microscopy (SEM)

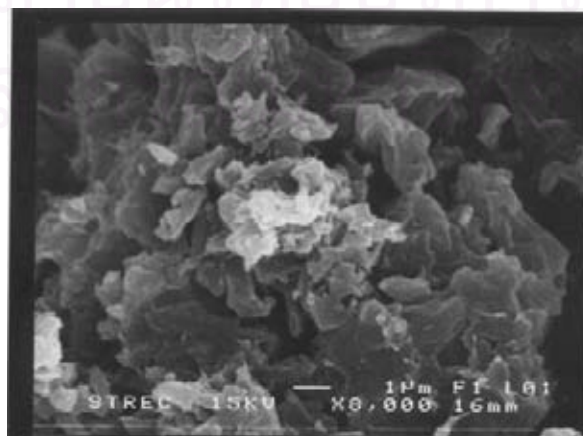
The additives and all polypropylene product in this study were observed by scanning electron microscopy (SEM) to determine its morphology as exhibited in Figure 5.19.



(a) Pure Polypropylene 1



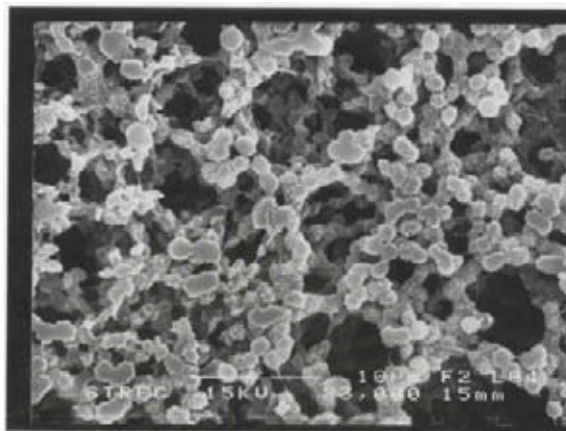
(b) Pure Polypropylene 2



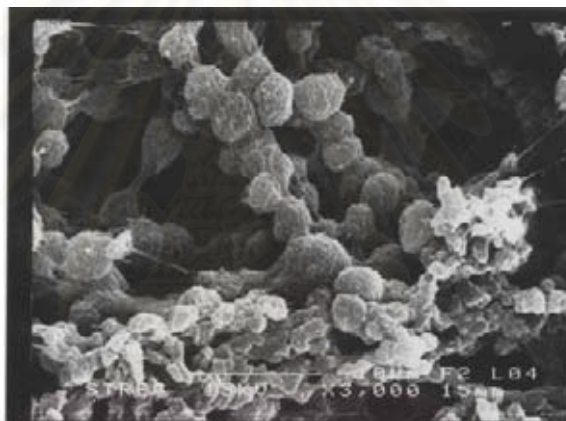
(c) Pure Polypropylene 3

Figure 5.19 : SEM Photographs of polypropylene that synthesized by metallocene

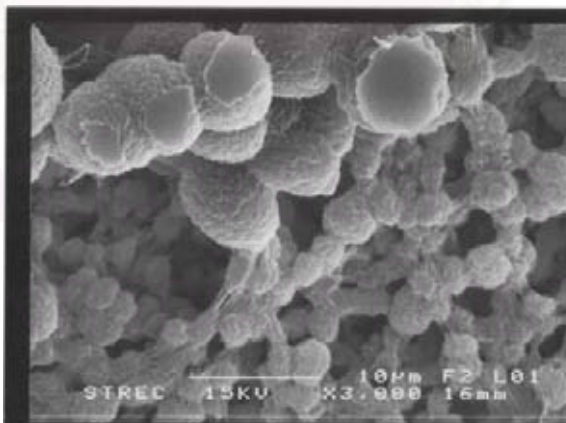
From the Figure 5.19 ,it shows that polypropylene 1,2 and 3 (PP1,PP2,PP3) synthesized by the various polymerization times , will show the different morphologies.



(a) Pure Polypropylene 1



(b) Polypropylene 1/ 1 % LCC



(c) Polypropylene 1 / 1% GMS

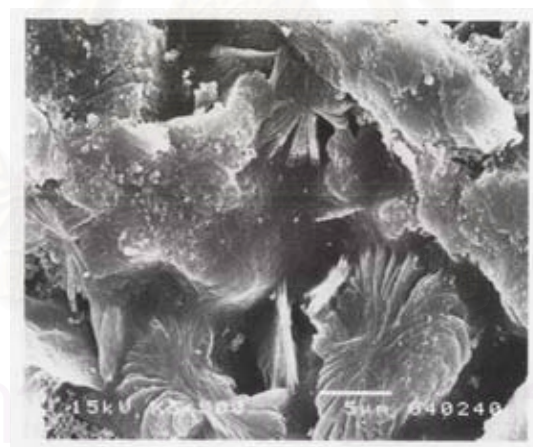
Figure 5.20 : SEM Photographs of polypropylene that synthesized by metallocene and their blends.

In the case of spherulite observation ,before investigating the morphology of this system by SEM , sample surface is etched in order to reveal spherulite morphologies of crystalline polymer by using permanganic etching technique.

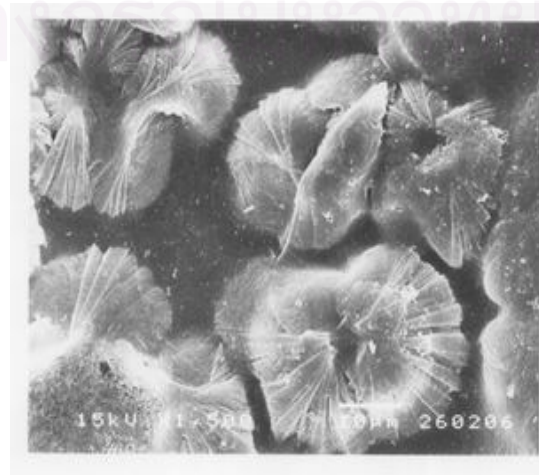
Permanganic etching technique is the best method for polypropylene etching. In this study, the solution of potassium permanganate in concentrated sulfuric acid 3.5 % weight by volume was used as etchant. There are two steps of etching method [Marsha, S. 1998]. To search the optimum etching time by vary etching time 5, 10, 15 and 20 minutes for each step. From that trial and error, the optimum etching time of each step is 10 minutes at the temperature of 60 °C because the etching surface of sample can clearly show spherulite morphologies. Results of spherulite morphologies of the blends at all blends from SEM are shown in Figure 5.21-5.23.



(a) Pure Polypropylene 4

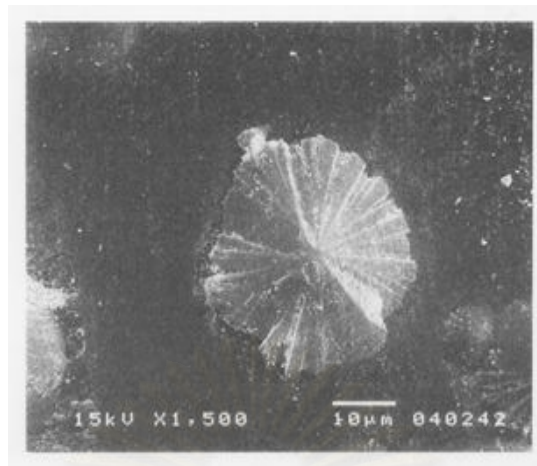


(b) Polypropylene 4 / 1% LCC

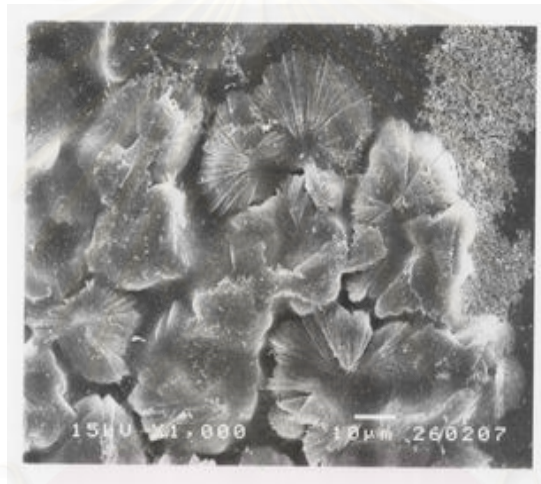


(c) Polypropylene 4 / 1% GMS

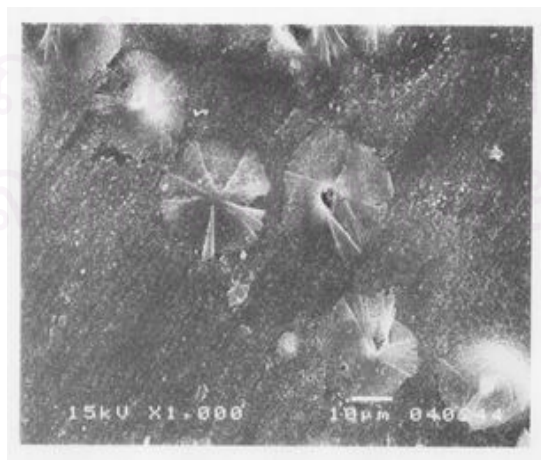
Figure 5.21 : SEM Photographs of spherulites of polypropylene 4 and their blends.



(a) Pure Polypropylene 5

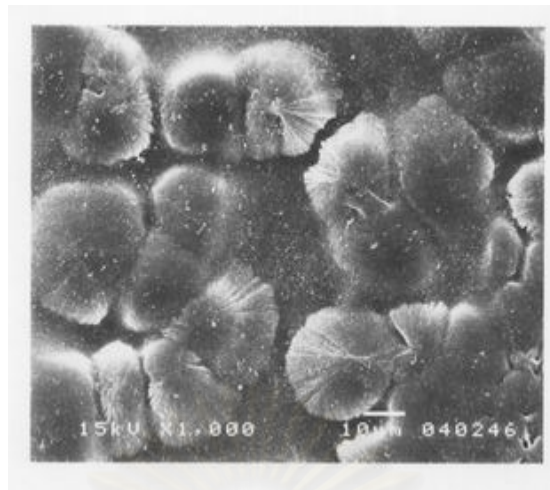


(b) Polypropylene 5 / 1% LCC



(c) Polypropylene 5 / 1% GMS

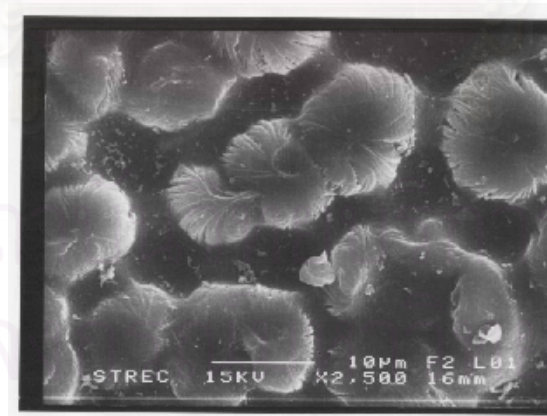
Figure 5.22 : SEM Photographs of spherulites of polypropylene 5 and their blends.



(a) Pure Polypropylene 6



(b) Polypropylene 6 / 1% LCC



(c) Polypropylene 6 / 1% GMS

Figure 5.23 : SEM Photograph of spherulites of polypropylene 6 and their blends.

From the SEM photographs , it found that the addition of low molar mass liquid crystal chemical and glycerol monostearate do not clearly effect to the size of spherulite.

5.5 X-Ray Diffraction (XRD)

This results in a so-called surface plot. The important peaks characteristic of the α phase can be found at scattering angles 2θ of 14° (110), 17° (040), 18.5° (130), 21° (111) and 22° (131 and 041). The crystallinity is determined by measuring the integrated area of the crystalline reflections and the integrated of the non-crystalline background and comparing the two [G. Farrow, 1961].

$$\% \text{ Crystallinity} = \frac{\text{Area of crystalline fraction}}{\text{Area of crystalline fraction} + \text{Area of amorphous fraction} * (y)}$$

where y is a factor, necessary to correct for the non-coincidence of the centres of gravity of amorphous and crystalline reflections. From high temperature X-ray diffraction photographs of variety of polypropylenes are shown in Figure 5.24

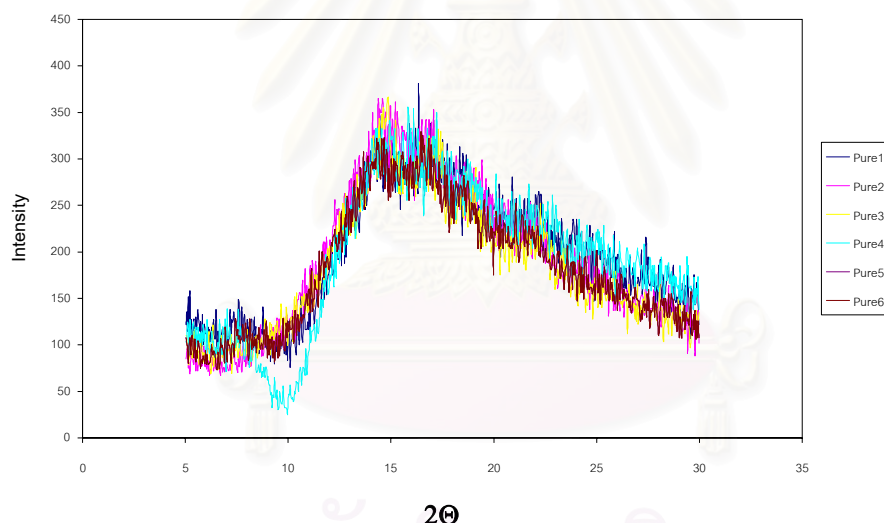


Figure 5.24 : X-ray diffractograms of amorphous reflection of polypropylene

The curves from the sample of polypropylenes is asymmetrical in shape, it can be seen that there are small differences in shape for each curves. Therefore to measure crystallinity of unoriented polypropylene specimens by X-ray diffraction. The average of these curves has been used as the standard curve for crystallinity measurements.

X-ray diffractograms of each polypropylenes and its blends were shown in Figure 5.25-5.42 .

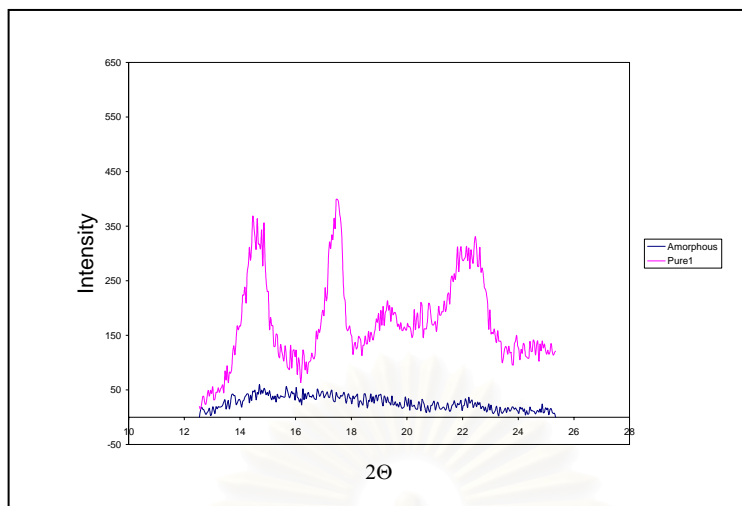


Figure 5.25 : X-ray diffractogram of pure polypropylene 1

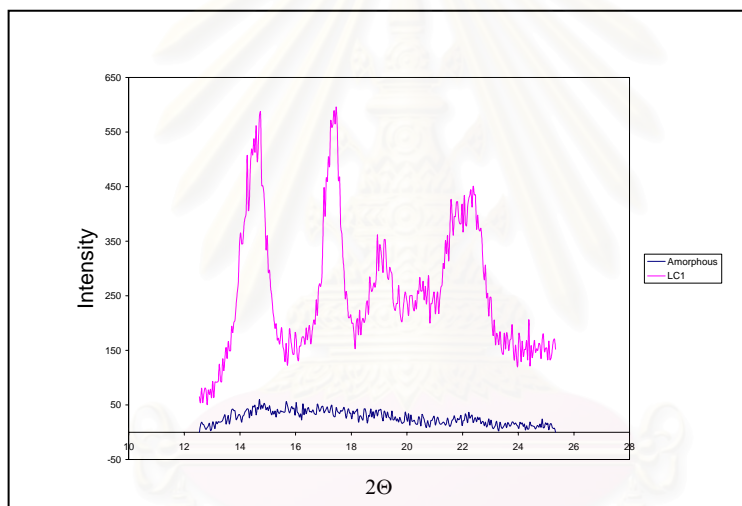


Figure 5.26 : X-ray diffractogram of polypropylene 1 / 1% LCC

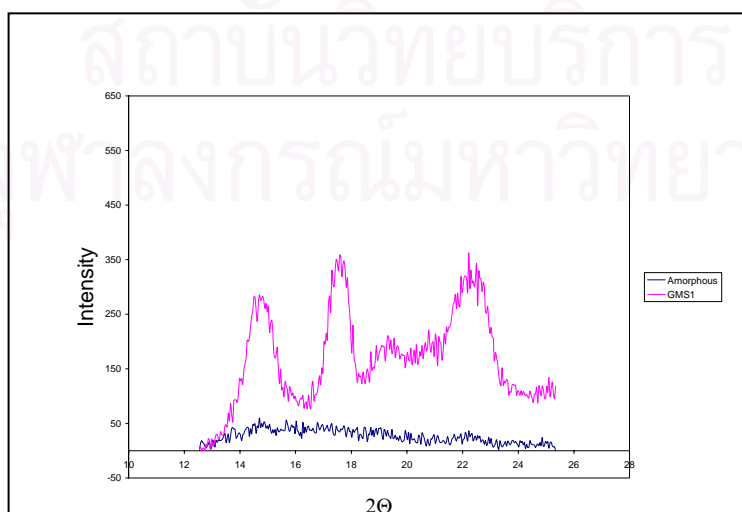


Figure 5.27 : X-ray diffractogram of polypropylene 1 / 1% GMS

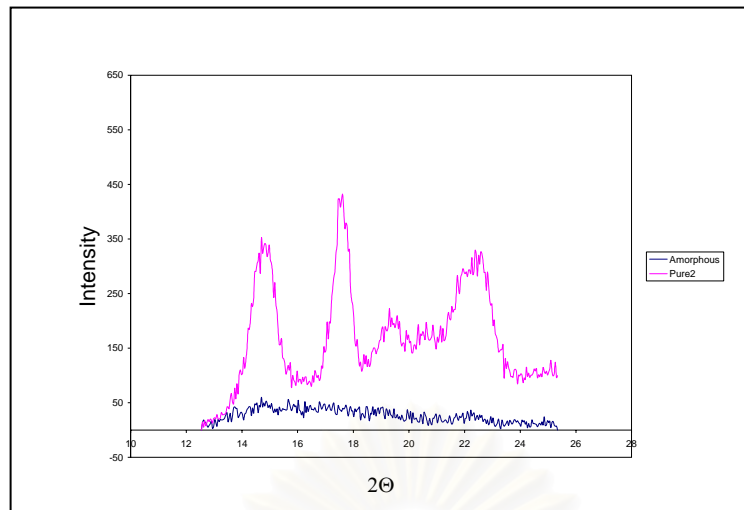


Figure 5.28 : X-ray diffractogram of pure polypropylene 2

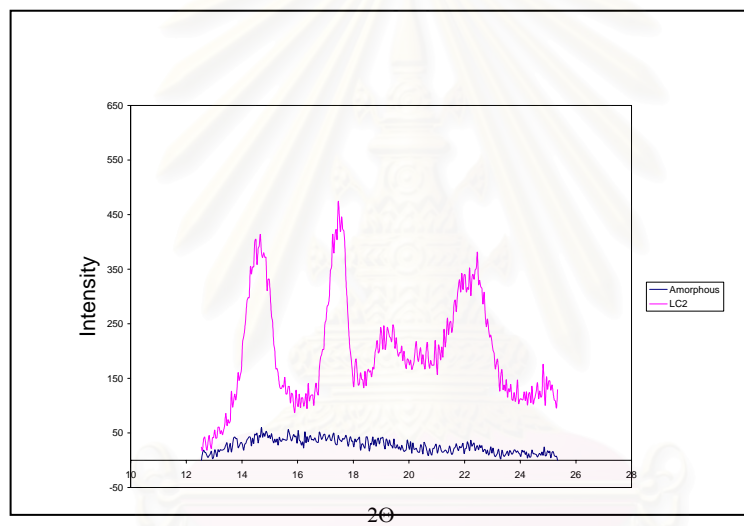


Figure 5.29 : X-ray diffractogram of polypropylene 2 / 1% LCC

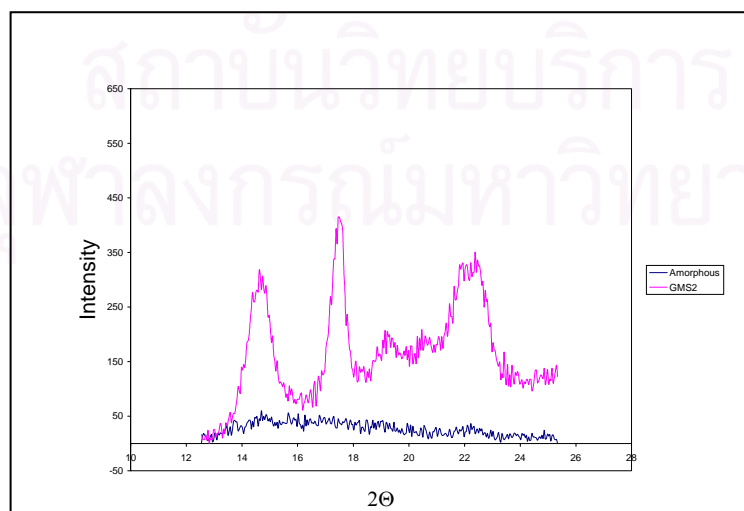


Figure 5.30 : X-ray diffractogram of polypropylene 2 / 1% GMS

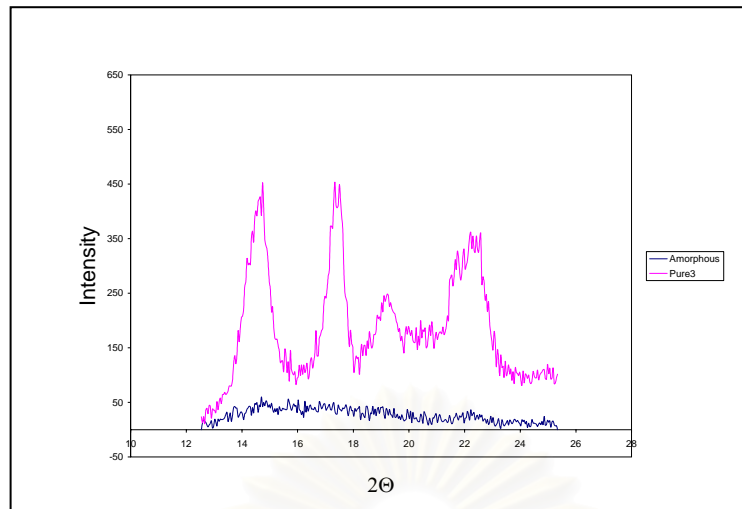


Figure 5.31 : X-ray diffractogram of pure polypropylene 3

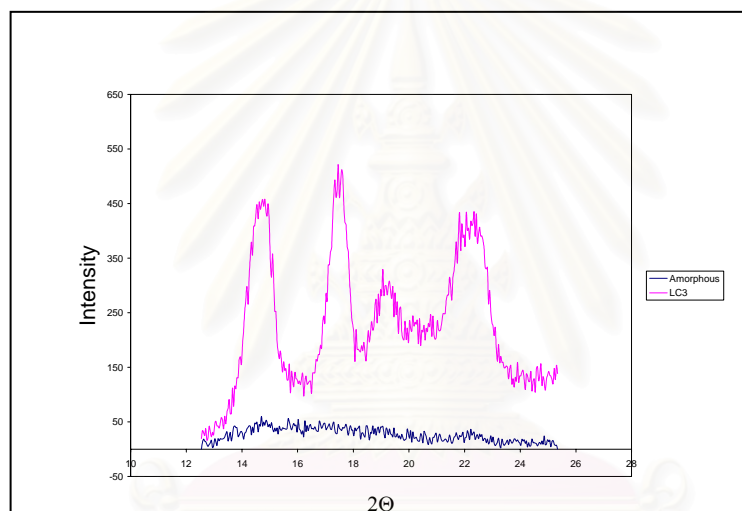


Figure 5.32 : X-ray diffractogram of polypropylene 3 / 1% LCC

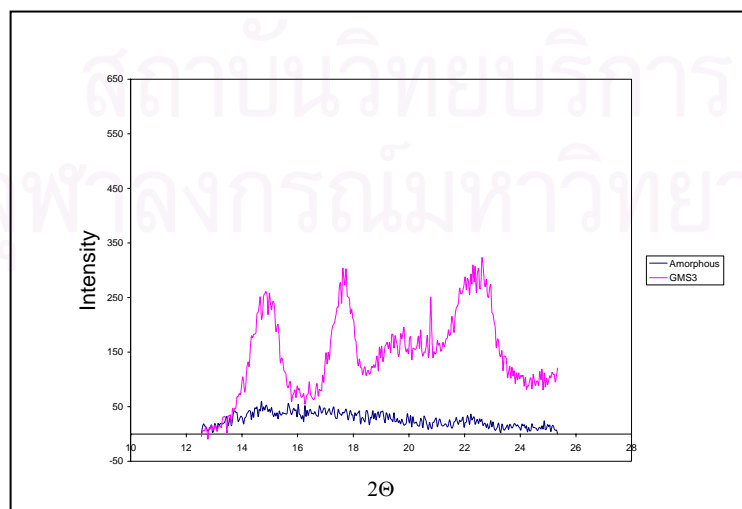


Figure 5.33 : X-ray diffractogram of polypropylene 3 / 1% GMS

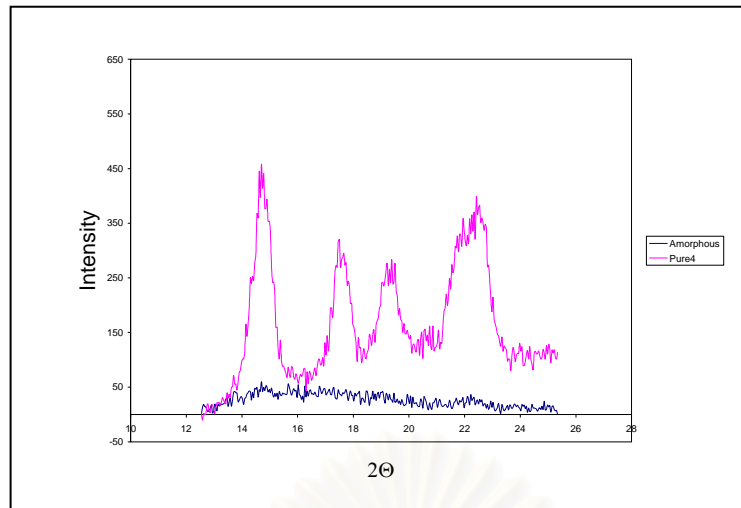


Figure 5.34 : X-ray diffractogram of pure polypropylene 4

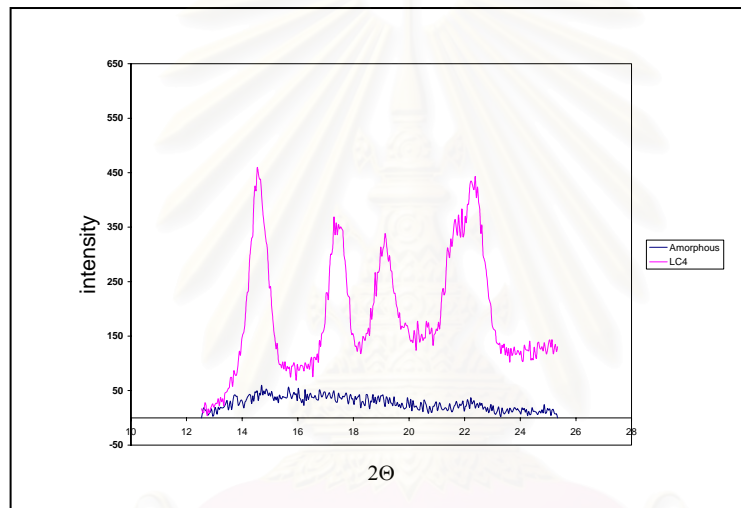


Figure 5.35 : X-ray diffractogram of polypropylene 4/ 1% LCC

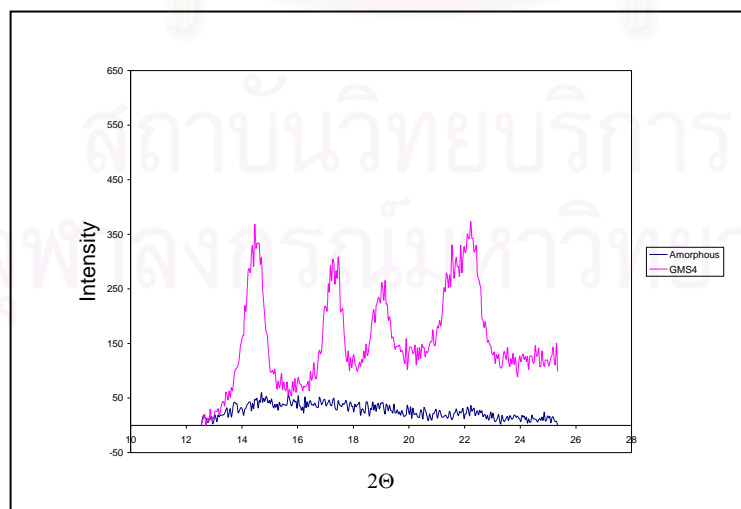


Figure 5.36 : X-ray diffractogram of polypropylene 4 / 1% GMS

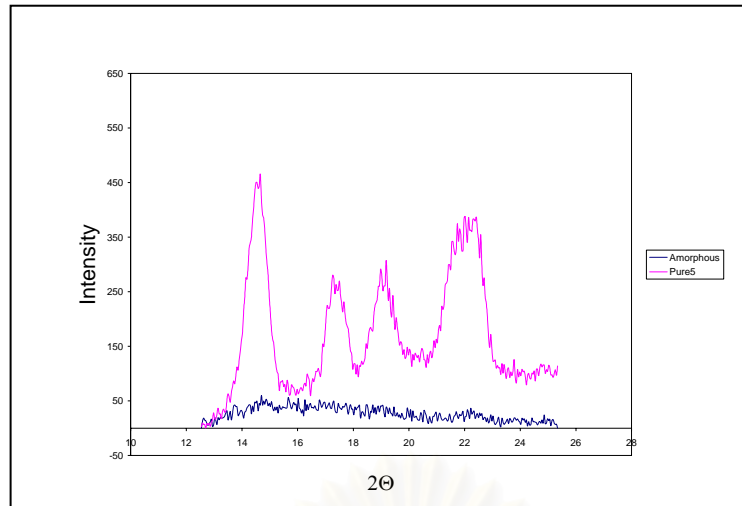


Figure 5.37 : X-ray diffractogram of pure polypropylene 5

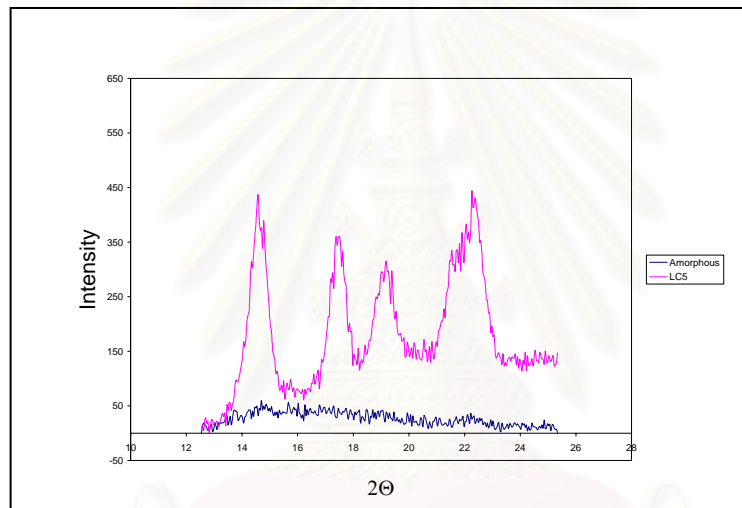


Figure 5.38 : X-ray diffractogram of polypropylene 5 / 1% LCC

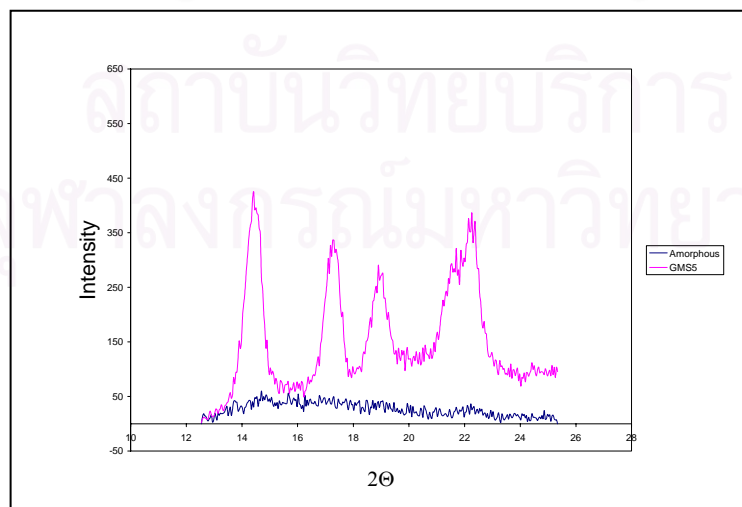


Figure 5.39 : X-ray diffractogram of polypropylene 5 / 1% GMS

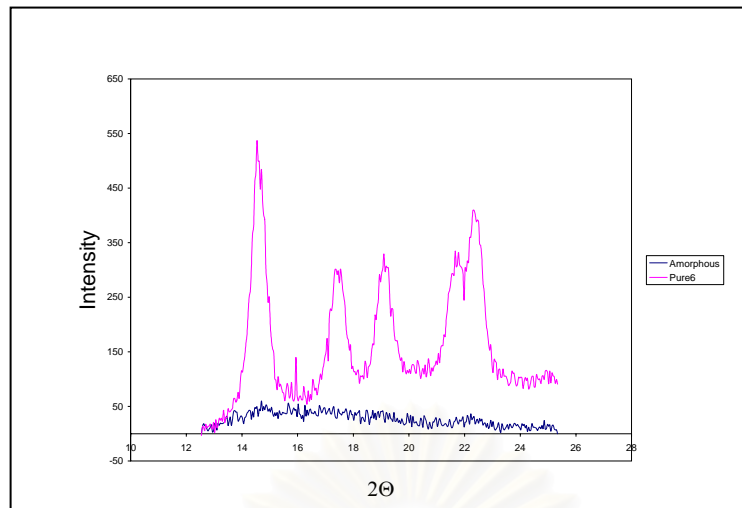


Figure 5.40 : X-ray diffractogram of pure polypropylene 6

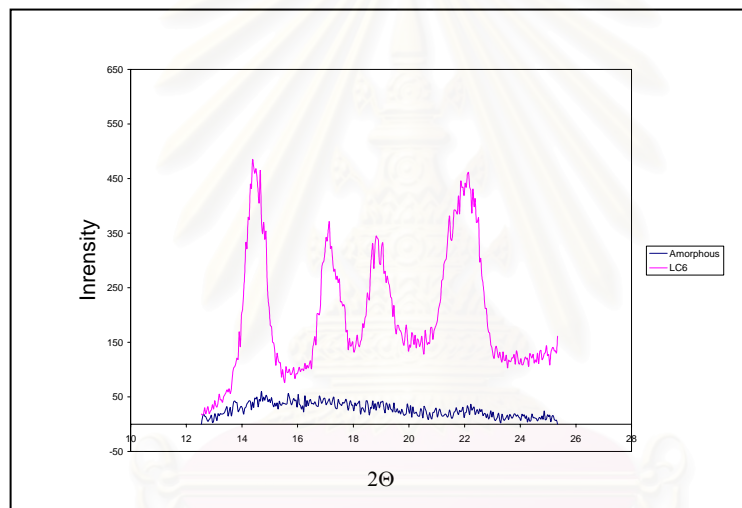


Figure 5.41 : X-ray diffractogram of polypropylene 6 / 1% LCC

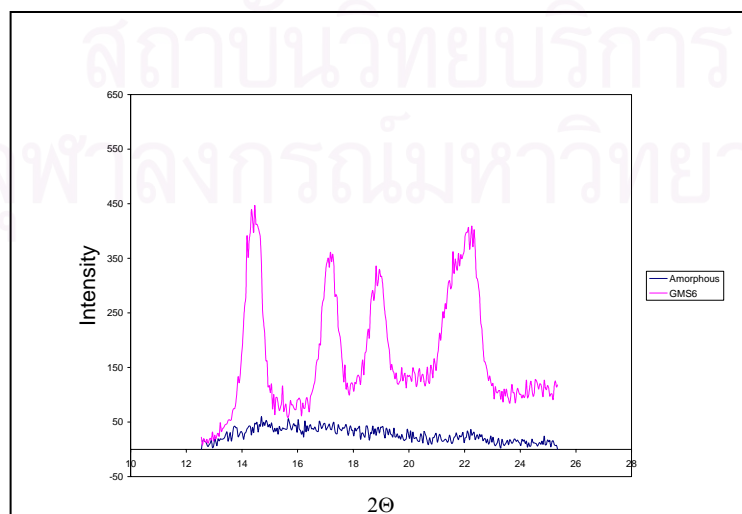


Figure 5.42 : X-ray diffractogram of polypropylene 6 / 1% GMS

Sample		Catalyst	Polymerization time (min)	Melt flow index	% Crystallinity
PP1	Pure	Metallocene	60	n.d.	83.83
	LC				86.24
	GMS				82.01
PP2	Pure	Metallocene	90	n.d.	84.23
	LC				86.47
	GMS				83.93
PP3	Pure	Metallocene	120	n.d.	84.69
	LC				86.92
	GMS				84.37
PP4	Pure	Ziegler-Natta	n.d.	20	83.89
	LC				85.89
	GMS				83.01
PP5	Pure	Ziegler-Natta	n.d.	11	84.36
	LC				85.26
	GMS				82.47
PP6	Pure	Ziegler-Natta	n.d.	2	83.40
	LC				86.56
	GMS				82.92

Table 5.5 : % Crystallinity of polypropylenes and their blends .

From the data of % crystallinity in Table 5.5 , it is indicated that metallocene-synthesized polypropylene produced in different polymerization time , which has different crystallinity. Namely metallocene-synthesized polypropylene produced in higher polymerization time , which has higher crystallinity. In the case of Ziegler-Natta – synthesized polypropylene , PP5 (melt flow index = 11) has the highest crystallinity.

When low molar mass liquid crystal chemical was added into the matrix of polypropylene , crystallinity moderately raised about 2-3 % . For the blends of polypropylene and GMS , crystallinity slightly decreased .

Comparison of two analytically characteristic results between SALS and XRD , the results of crystallinity correspond to the light scattering results , namely polypropylene obtained in higher polymerization time , which can better scatters laser

beams , it will have higher crystallinity. Ziegler-Natta – synthesized polypropylene has the best light scattering , it has highest crystallinity. In the case of additive effect , for metallocene-synthesized polypropylene (PP1 , PP2 and PP3) the results of crystallinity also correspond to the light scattering results. They are meant that low molar mass liquid crystal chemical increases crystallinity of the blend , which will scatter laser beams better than pure polypropylene ,while GMS decreases crystallinity of the blend , which will scatter beams less than pure polypropylene.

For Ziegler-Natta – synthesized polypropylenes (PP4 , PP5 and PP6) , low molar mass liquid crystal chemical increases crystallinity of the blend , therefore the crystal of the blend scatters laser beam better than pure polypropylene. But in the case of GMS addition , the results of XRD contradict to the light scattering results , namely crystallinity of the blend decreases , but the crystal of the blend scatter laser beam better than pure polypropylene. Because of the size of the spherulite did not change accordingly to the percent crystallinity.



สถาบันวิทยบริการ
จุฬาลงกรณ์มหาวิทยาลัย

CHAPTER VI

Conclusions and Recommendations

For the study of light scattering behaviors, melting and crystallization temperature, morphology and crystallinity of polypropylene and the blends of LCC or GMS, in this chapter, the conclusions and recommendations for further studies will be focused.

6.1 Conclusions

The conclusions of this study are shown as follows:

1. Polypropylene produced using metallocene catalyst (PP1, PP2 and PP3) which were synthesized by higher polymerization times, were obtained with the higher activities and shown the different morphologies.

2. Polypropylene produced using metallocene catalyst (PP1, PP2 and PP3), which were synthesized by higher polymerization times, have better light scattering. And Ziegler-Natta -synthesized polypropylene (PP4, PP5 and PP6) that have different melt flow index, can differently scatter laser beams.

3. There are some changes in the crystalline structure when low molar mass liquid crystal polymer was added into polypropylene metric. Namely the crystal of polypropylene-1% low molar mass liquid crystal chemical (LCC) blend can scatter beams better than the crystal of pure polypropylene.

4. For effects of GMS addition, light scattering of metallocene-synthesized polypropylenes were less. But in the case polypropylene synthesized by Ziegler-Natta catalyst, light scattering of the blends were better than pure polypropylene but less than LCC blends.

5. If polymer is passed many cycles of heating, the melting temperature will be slightly decrease.

6. Low molar mass liquid crystal chemical (LCC) and glycerol monostearate (GMS) in the blends are able to slightly reduce melting temperature. Glycerol monostearate have more pronounced effects.

7. In the case of Ziegler-Natta -synthesized polypropylene (PP4 , PP5 and PP6) , low molar mass liquid crystal chemical (LCC) and glycerol monostearate (GMS) can significantly increase crystallization temperatures because the molecule of melted polypropylene can move faster , crystallization is easier to occur.

8. Metallocene-synthesized polypropylene produced in higher polymerization time , it has higher crystallinity.

9. Low molar mass liquid crystal chemical (LCC) can moderately raise crystallinity of the blend. But GMS slightly decrease crystallinity of the blend.

10. In the case of metallocene-synthesized polypropylene , the results of crystallinity correspond to the light scattering results. That is to say low molar mass liquid crystal chemical increases crystallinity of the blend , which will scatter beams rather than pure polypropylene , while GMS decreases crystallinity of the blend , so it will scatter laser beams less than pure polypropylene.

11. In the case of metallocene-synthesized polypropylene , the results of crystallinity contradict to the light scattering results.

6.2 Recommendations for further studies

The recommendations for further studies are as follows :

1. It might be further investigated effects of the content of LCC and GMS in the blend on light scattering behavior , melting temperature , crystallization temperature and crystallinity.

2. It should be interesting to study the kinetic of crystalline polymers by using small angle light scattering technique.

3. It should be investigated the other additives , which blend with crystalline polymer by using small angle light scattering and X-ray diffraction technique.

References

- A.E.M. Keijzers, J.J. van Aartsen, and W. Prins . J. Am. Chem. Soc. 90 , 12 (1968) : 3107-3113.
- Bergman, J.S., Coates , G. W.,Chen. H., Giannelis, E. P. ,Thoas, M. G.,
Chem.Commun. 21 (1999) : 2179.
- Busico , V., Cipullo , R., Progr. Polym. Sci. 26 , 3 (2001) : 443.
- Corradini , P., Guerra , G., Cavallo , I., Moscardi , G., Vacatello , M., Fink, G.,
Mulhaupt , R., and Brintzinger , H Ziegler Catalysts Springer ,
Berlin,(1995).
- Del Duca , D. ,Moore , E. P., End-Use Properties , in Polymer Handbook , Moore,
E. P., Editor., Hanser : Munchen. (1996) , p 237.
- Demus, D., et al ,Handbook of liquid crystals volume. 2A : low molecular weight
liquid crystals. (n.p.): Wiley-VCH (1998).
- D.Hlavata' and Z.Hora'k , Eur.Polym. J. 30 , 5 (1993) : 597-600.
- Ewen , J.A. Mechanisms of stereochemical control in propylene polymerizations
with soluble group 4B metallocene / methylalumoxane catalysts. J. Am.
Chem. Soc. 106 (1984) : 6355-6364.
- Farrow , G. and Preston , D. Brit. J. appl.Phys. 11 (1960) : 353.
- F. Javier Torre , M. Milagros Corta'zar , M. A' ngeles Go'mez, Gary Ellis,
Carlos Marco . Polymer 44 (2003) : 5209-5217.
- Hlatky, G. G. Metallocene catalysts for olefin polymerization. Coordination
Chemistry Reviews 181 (1999) : 243-296.
- Jerome Maugey , Patrick Navard. Polymer 43 (2002) : 6829-6837.
- Kilwon Cho, D. Nabi Saheb, Hoichang Yang, Byoung Kang, Joonkyung Kim,

Sang-Soo Lee . Polymer 44 (2003) : 4053–4059.

Long , N. J. Metallocene : An introduction to sandwich complexes London : Blackwell Science , (1998).

Morgan, A. B., Gilman, J. W., Jackson, C. L., Macromol. Chem. Phys. 202 (2001) : 2239.

Nobuo Kawahara , Shin-ichi Kojoh , Shingo Matsuo, Hideyuki Kaneko , Tomoaki Matsugi, Yoshihisa Toda, Akira Mizuno, Norio Kashiwa . Polymer 45 (2004) : 2883–2888.

Natta ,G., Pino , P., Nazzanti , G., Giannini ,U.,Namtica , E., and Peraldo , M.Chim. E. Ind.(Milan) 39 (1957) :19.

Oertel , C. G., Applications of polypropylene ,in Polypropylene Handbook,Moore , E. P.,Editor., Hanser : Munchen. (1996) p 349.

S.Wacharawichanant , S.Thongyai , S.Tanodekaew , J.S. Higgins , N.Clarke. Pollymer 45 (2004) : 2201-2209.

Sayant Saengsuwan , Sauvarop Bualek-Limcharoen , Geoffrey R. Mitchell , Robert H. Olley. Polymer 44 (2003) : 3407–3415.

Sayant Saengsuwan , Geoffrey R. Mitchell , Sauvarop Bualek-Limcharoen. Polymer 44 (2003) : 5951–5959.

Scheirs, J., and Kaminsky , W. Metallocene-based Polyolefins : Preparation, properties and technology Volume 1.(n.p.): John Wiley & Sons ,(1999).

Sinn , H., and Kaminsky , W. Adv. Inorg.Chem. 18 (1980) : 99-149.

Shaofeng Ran , Benjamin S. Hsiao , Pawan K. Agarwal , Manika Varma-Nair. Polymer 44 , 8 (2003) : 2385-2392.

Sherman , L. M., Plasticstechnology , May (2002).

Sperling, L.H. Introduction to Physical Polymer Science 3rd ed. New York : John Wiley & Son , (2001).

Stein, R.S. ; and Hotta, T. Light scattering from oriented polymer films. Journal of Applied Physics. 35 , 7 (1964) : 2237-2242.

Stien, R.S., Cronauer, J., and Zachmann, H.G. Real time scattering measurements of the crystallization of polymers and their blends. Journal of Molecular Structure. 383 (1996) : 19-22.

S.Vleeshouwers . Polymer 38 , 13 (1997) : 3213-3221.

T. Xu , H. Lei , C.S. Xie . Materials and Design 24 (2003) : 227–230.

Wolfsberger , A.,Gahleitner , M. , Wachholder, M. Kunststoffe 92 , 10 (2002) : 44.

Zhi-Gang Wang , Benjamin S. Hsiao ,S. Srinivas ,Gary M. Brown, Andy H. Tsou , Stephen Z.D. Cheng , Richard S. Stein. Polymer 42 (2001) : 7561-7566.

สถาบันวิทยบริการ
จุฬาลงกรณ์มหาวิทยาลัย



Appendices

สถาบันวิทยบริการ
จุฬาลงกรณ์มหาวิทยาลัย

Appendix A : The light scattering measurement and etching

The standard methods of the light scattering measurement and etching are as follows :

1. The investigation light scattering behavior ;

- 1.1 The laser beam passed through the sample which was mounted between two polarizers. Using the illumination of light from gain 6 and gain 10, collect 48,400 digital intensity data from light scattering photographs.
- 1.2 To get the better contour graph of light scattering. From digital intensity data, we smoothed data by using average data. We average 81 data to be 1 data. Totally we got 625 averaged data.
- 1.3 Since we put a coin at the center of the screen, called beam stop, to protect the laser beam which has high intensity passed through the CCD camera directly, the contour graph at the center is very poor. So we modified averaged intensity data at the center of the contour graph of light scattering by adjusting data in the area of a coin to a new data which was closer to data around the outermost rim of a coin.

2. Etching ;

In this work, we made two steps of etching by using 20 ml of the solution of potassium-permanganate in conc. Sulfuric acid 3.5 % weight by volume, as the etchant. First etching, the sample was etched for 10 minutes, then washed by water for 5 minutes and then washed by acetone for 5 minutes. Second etching, the same sample was etched for 10 minutes in the new prepared etchant. Then the sample was washed by water for 10 minutes and then washed by acetone for 10 minutes. The thickness of the sample is 1 mm.

Appendix B : The data of DSC characterization

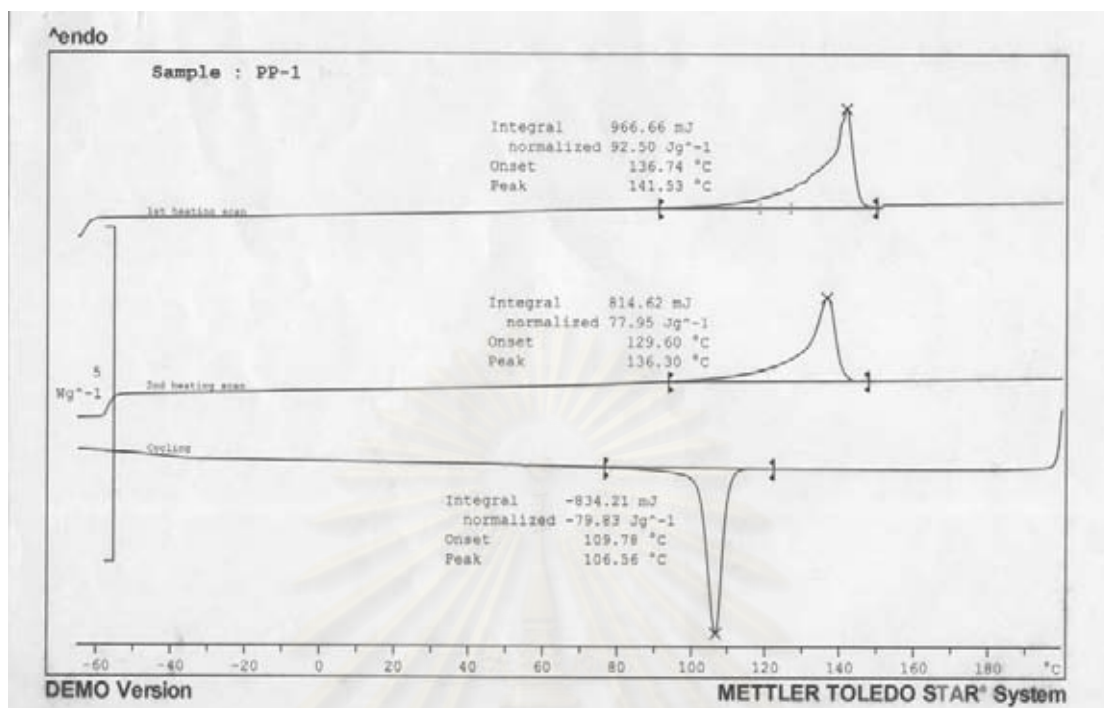


Figure B-1 : DSC curve of Pure Polypropylene 1

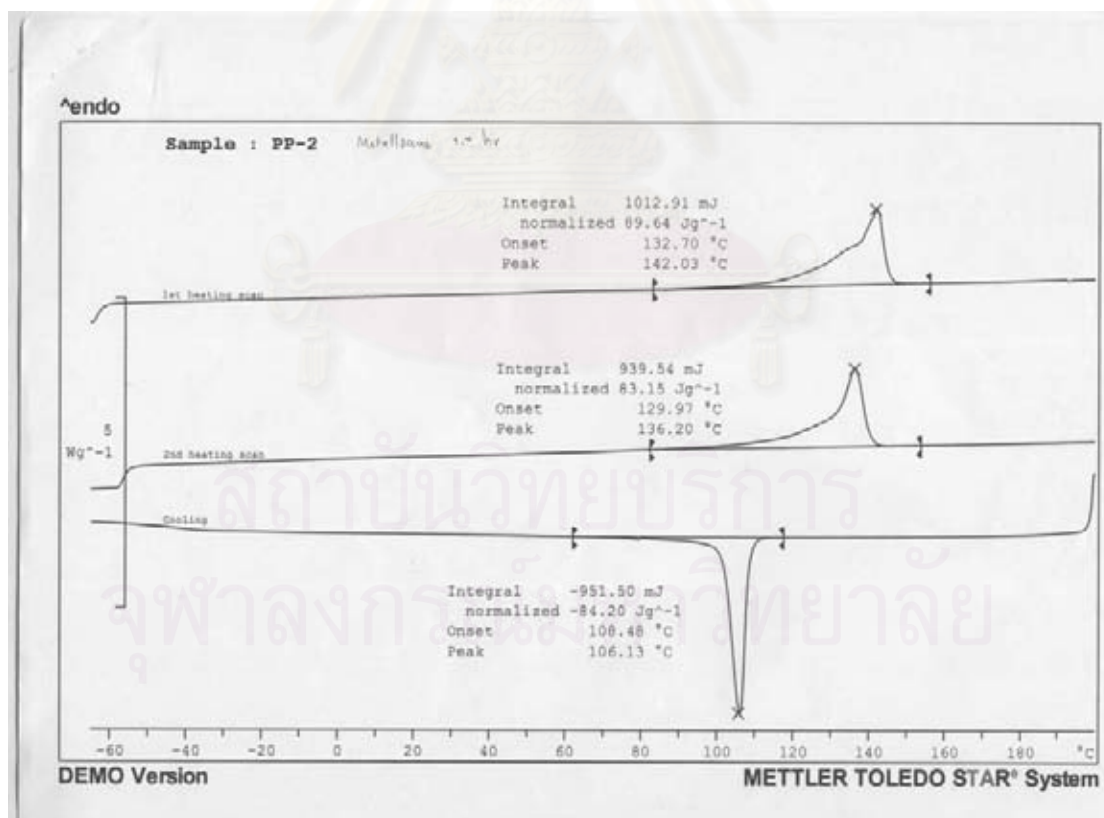


Figure B-2 : DSC curve of Pure Polypropylene 2

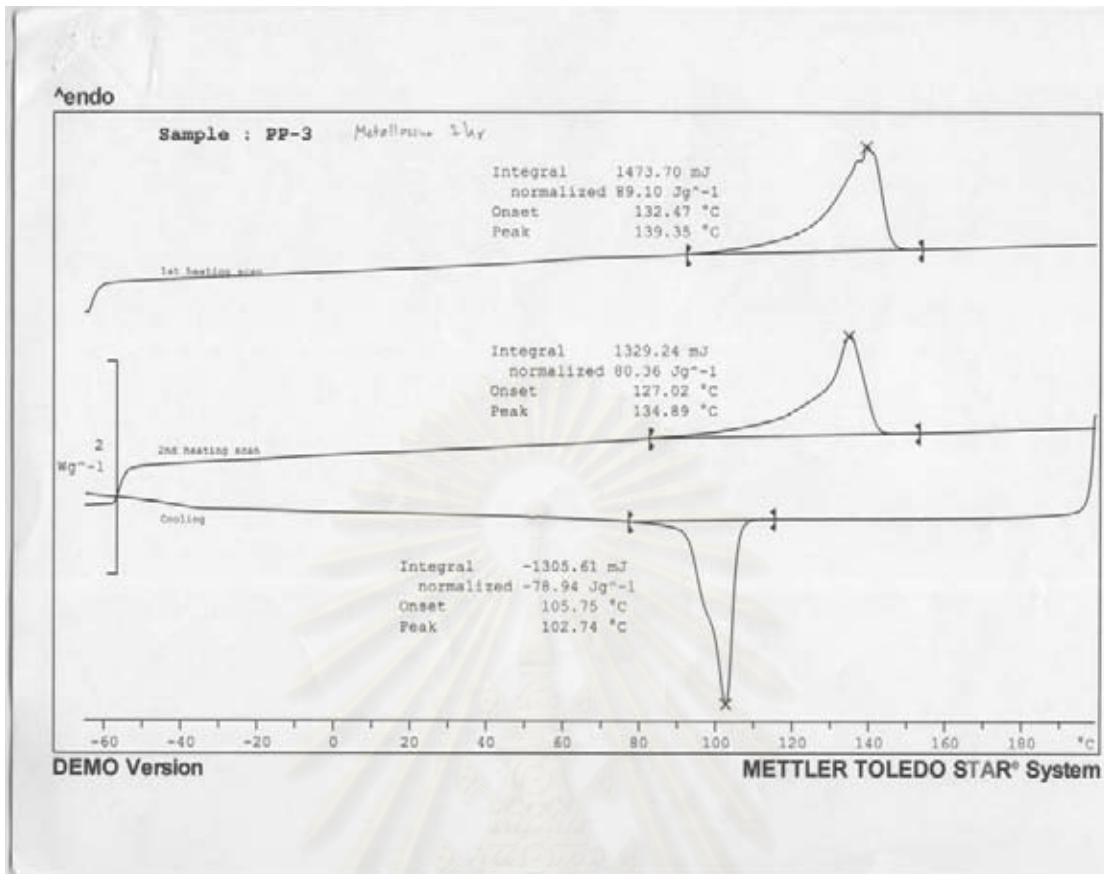


Figure B-3 : DSC curve of Pure Polypropylene 3

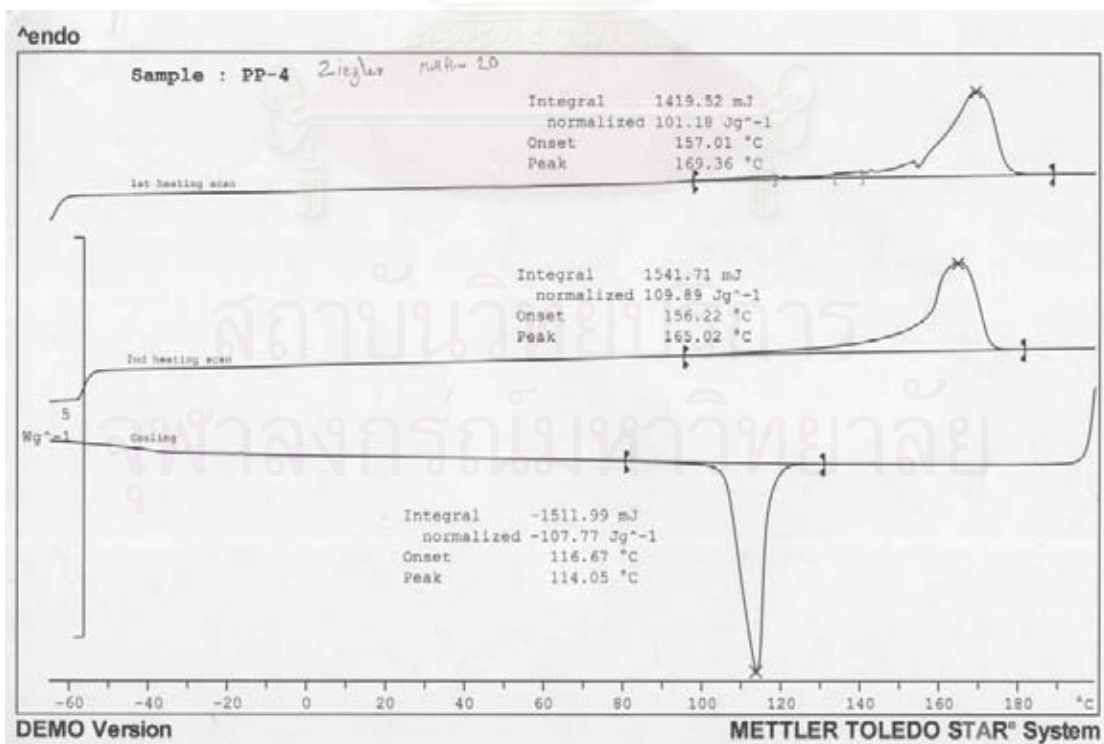


Figure B-4 : DSC curve of Pure Polypropylene 4

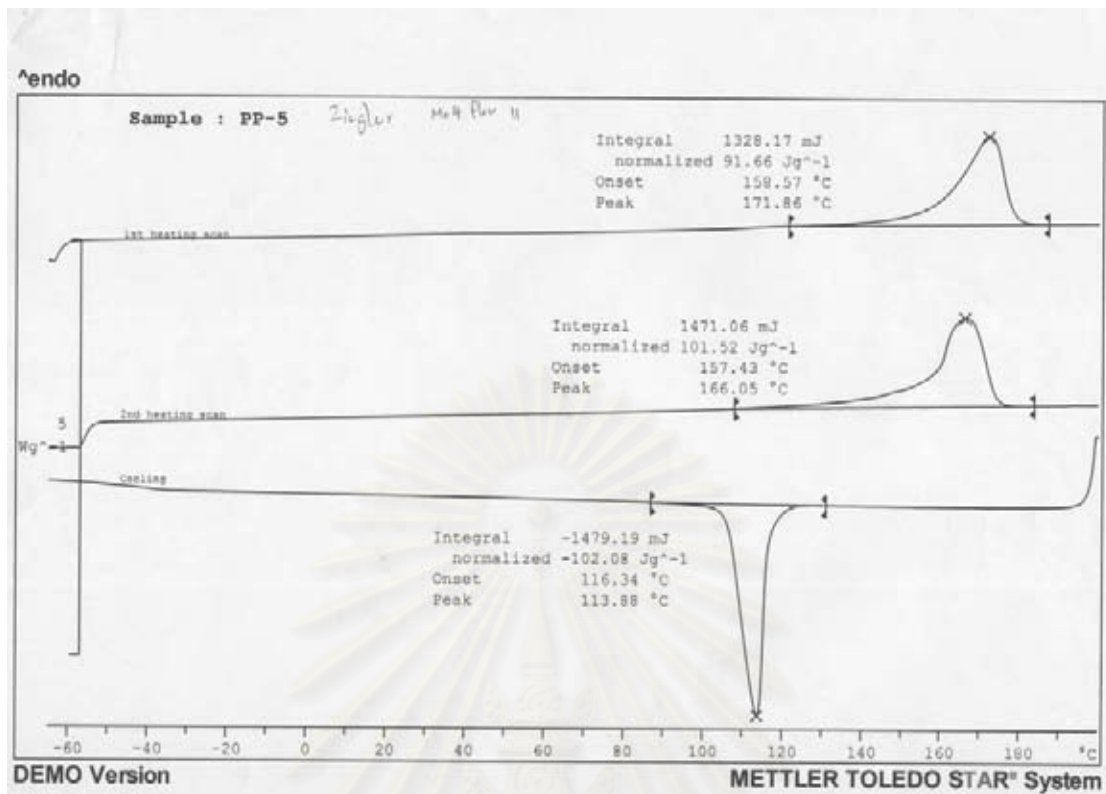


Figure B-5 : DSC curve of Pure Polypropylene 5

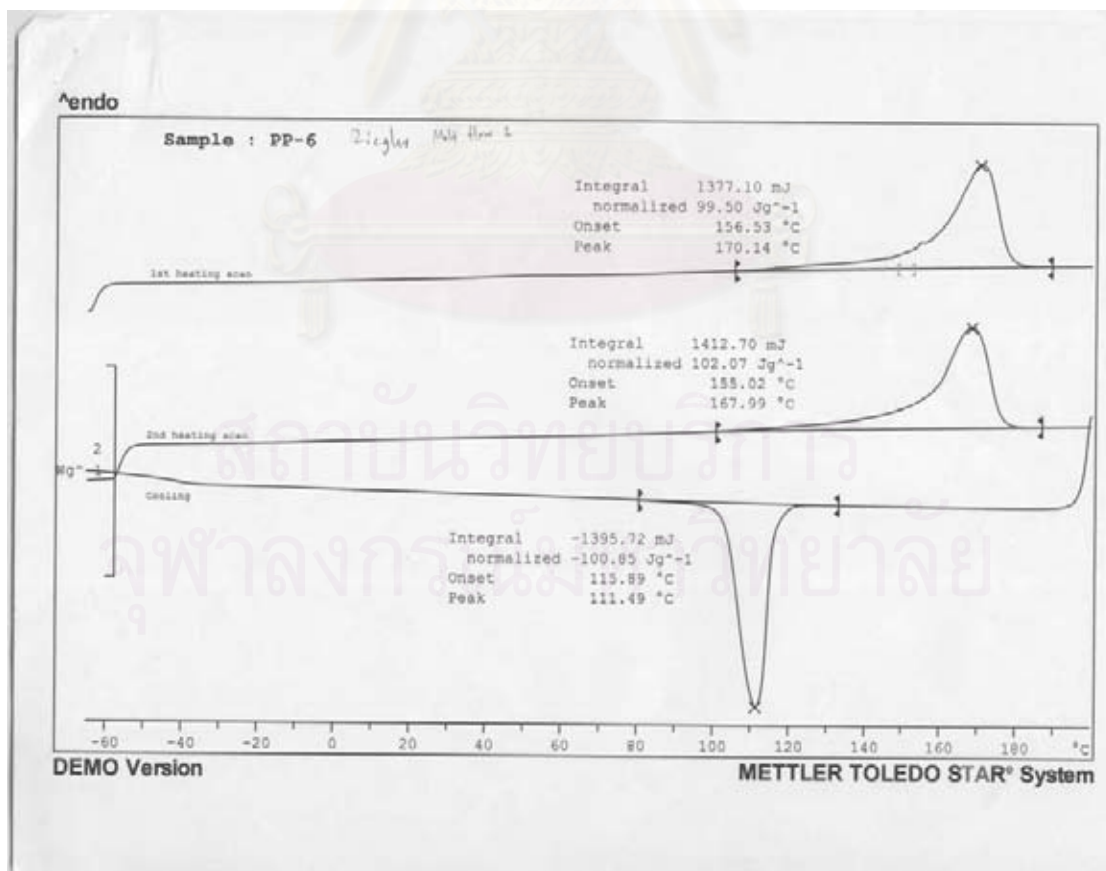


Figure B-6 : DSC curve of Pure Polypropylene 6

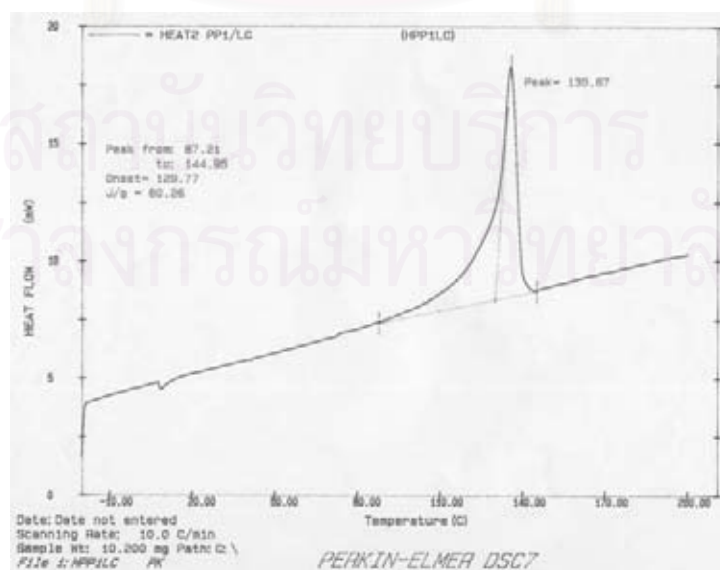
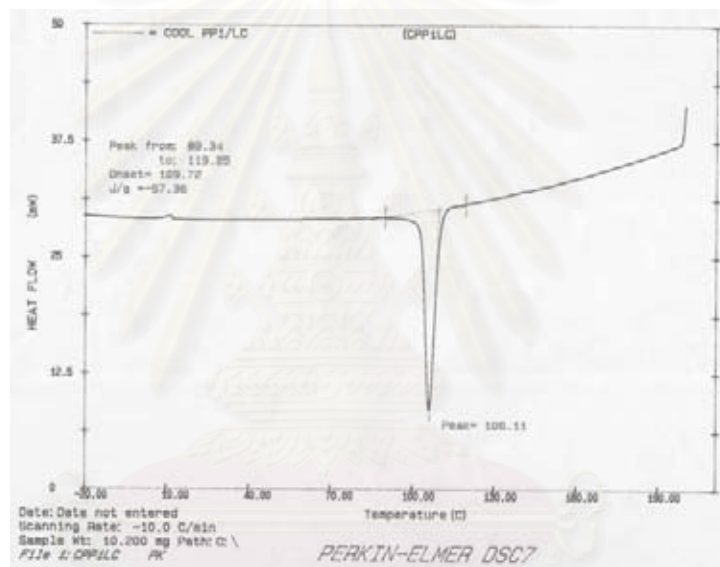
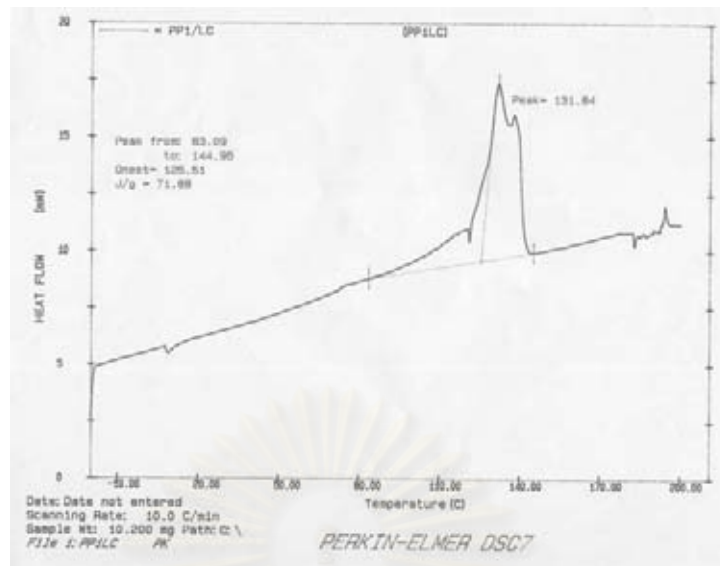


Figure B-7 : DSC curve of Polypropylene 1/1% LCC

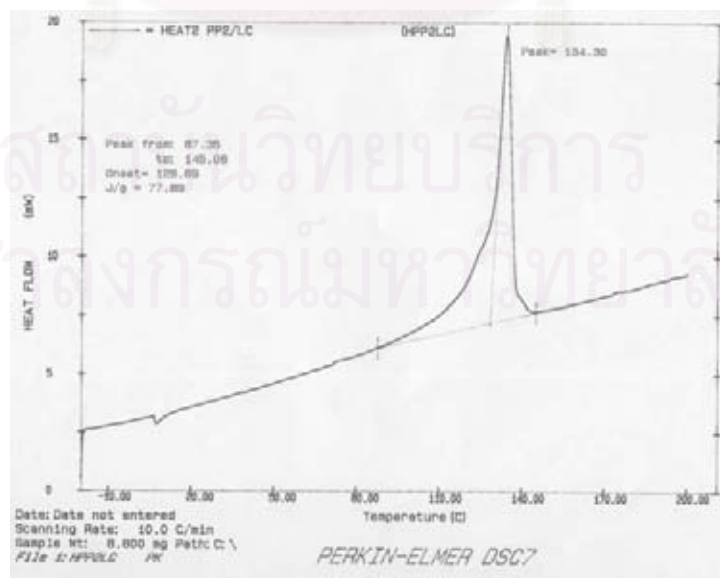
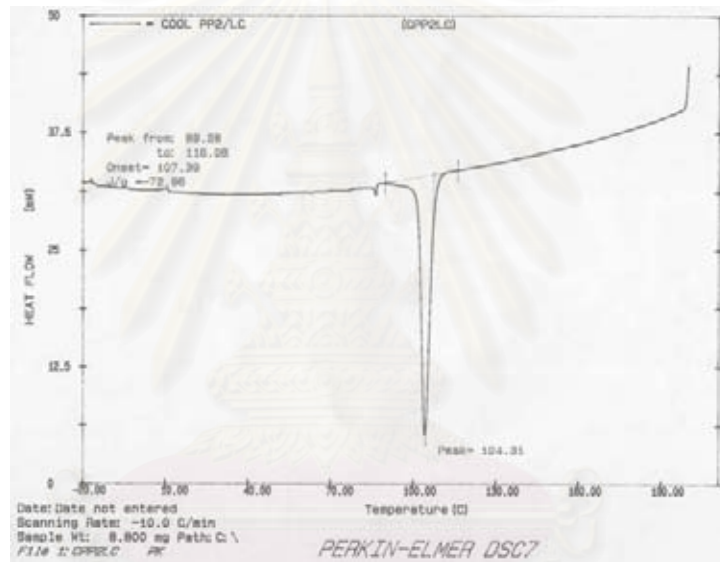
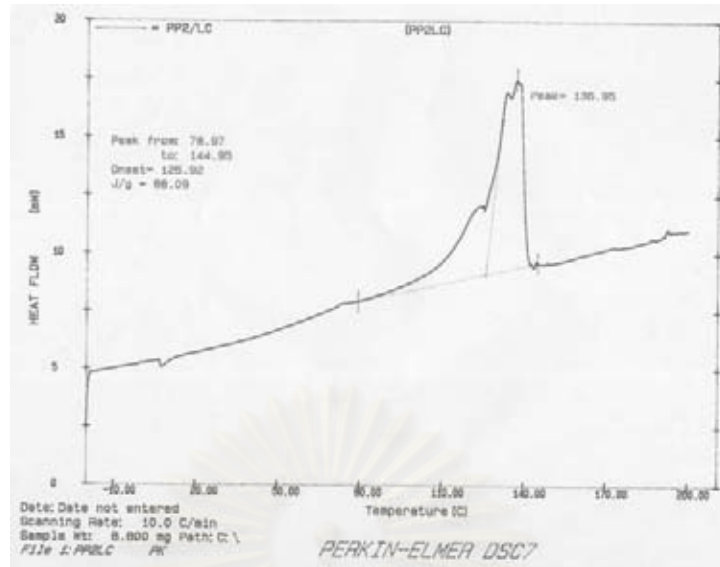


Figure B-8 : DSC curve of Polypropylene 2/1% LCC

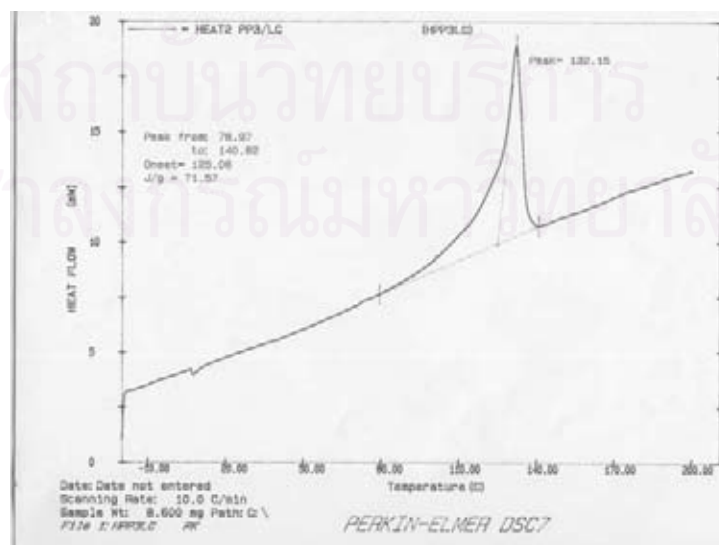
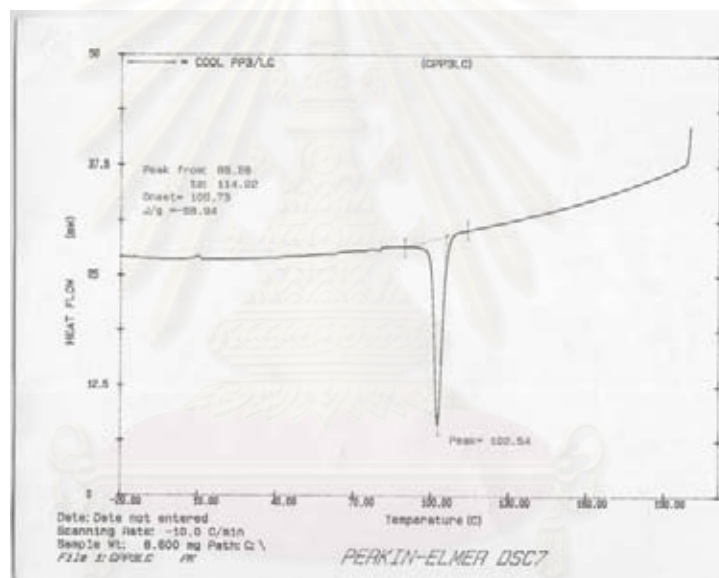
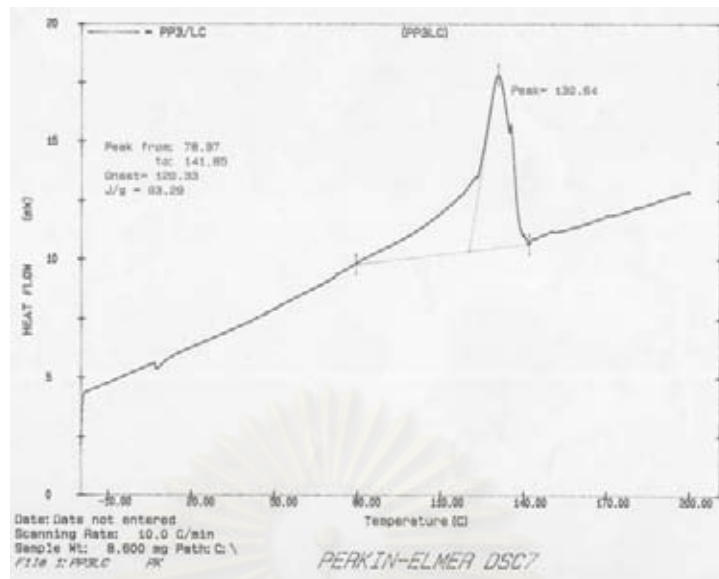


Figure B-9 : DSC curve of Polypropylene 3/1% LCC

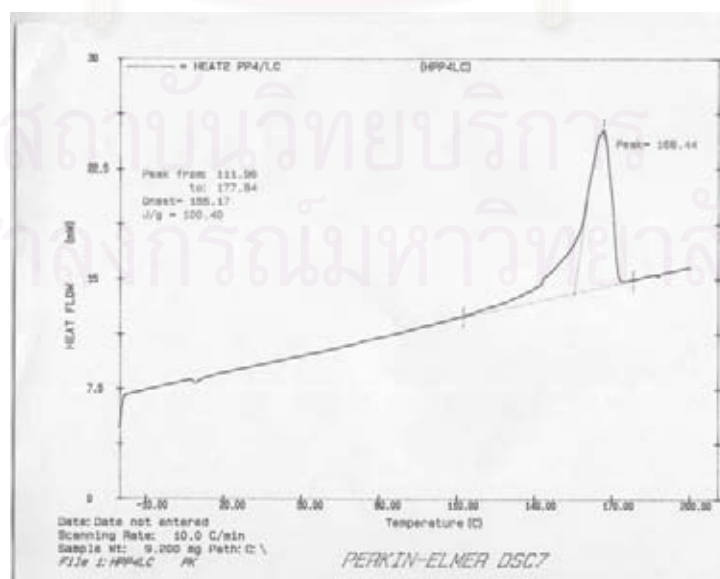
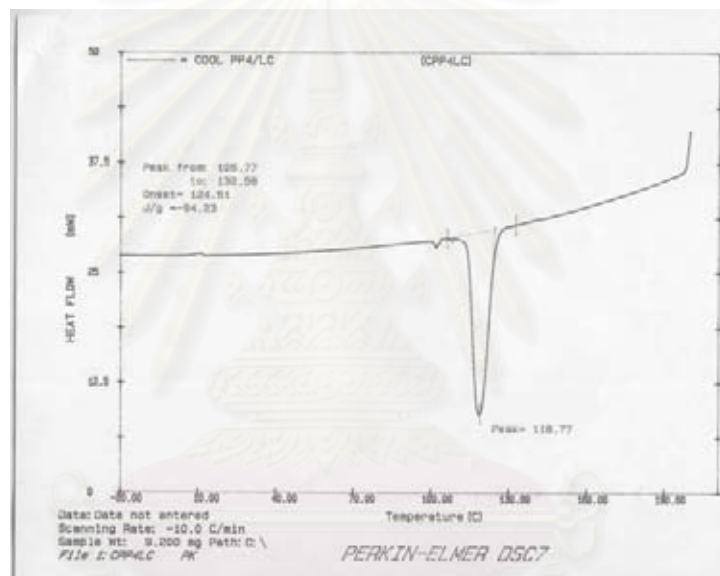
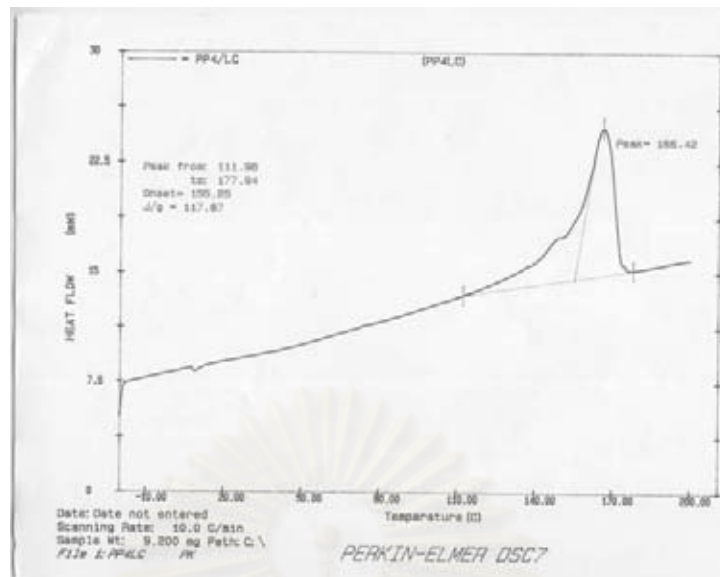


Figure B-10 : DSC curve of Polypropylene 4/1% LCC

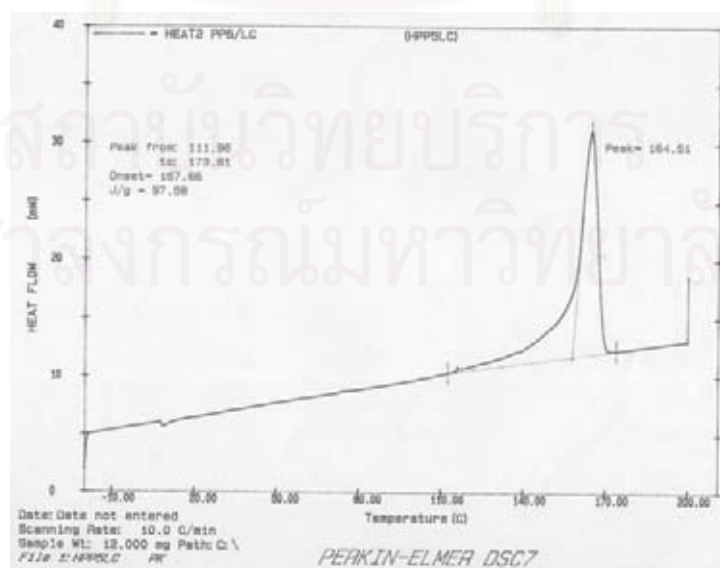
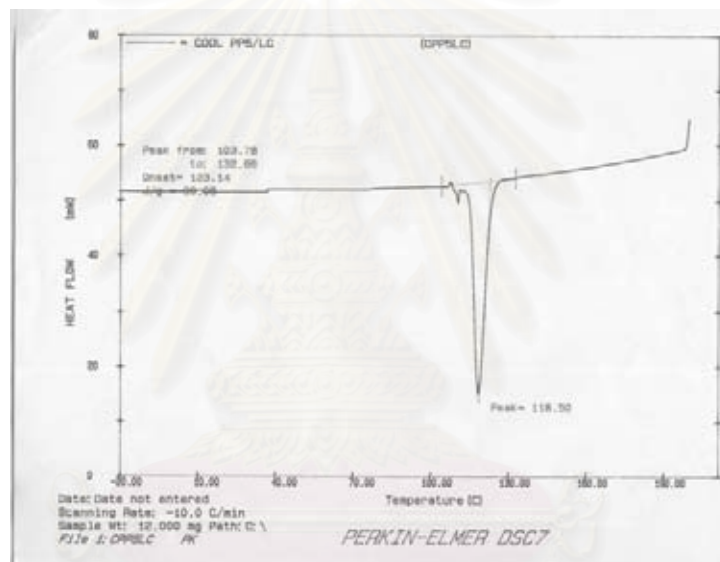
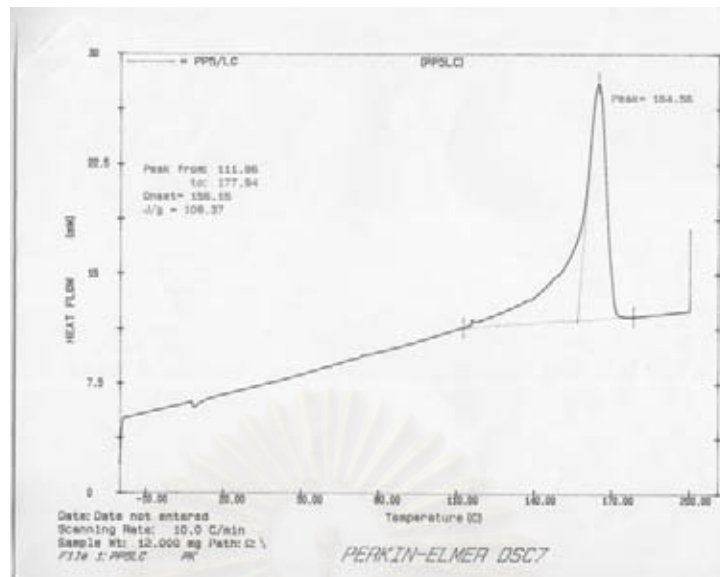


Figure B-11 : DSC curve of Polypropylene 5/1% LCC

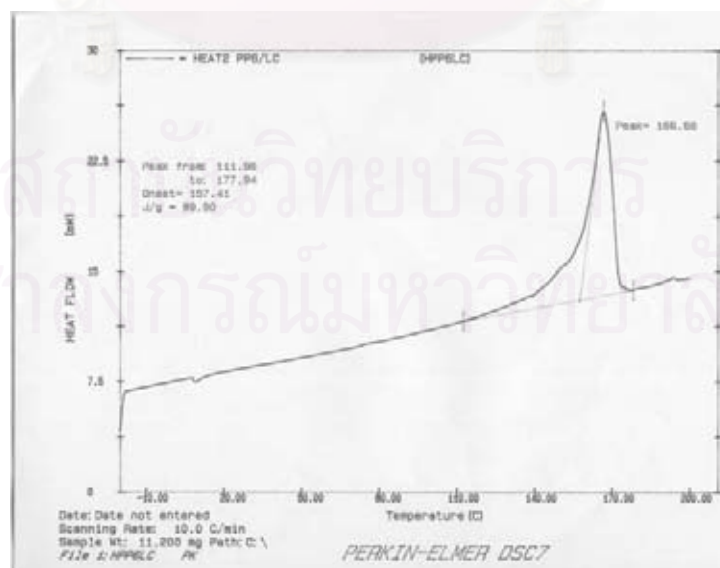
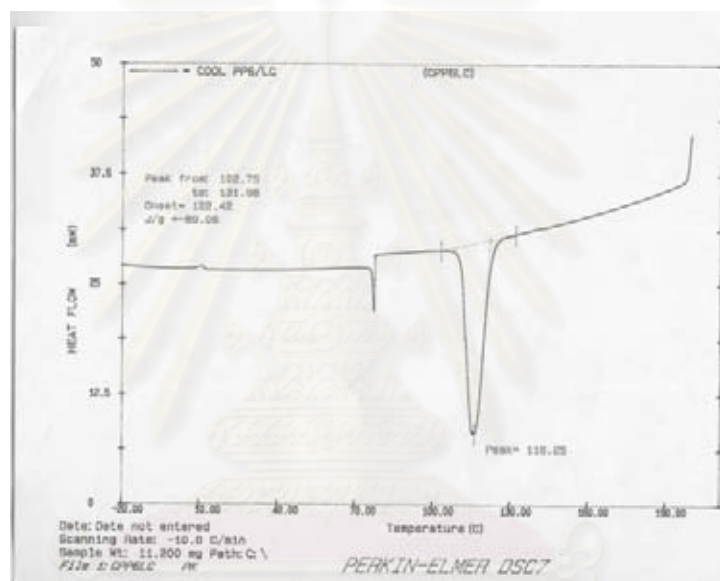
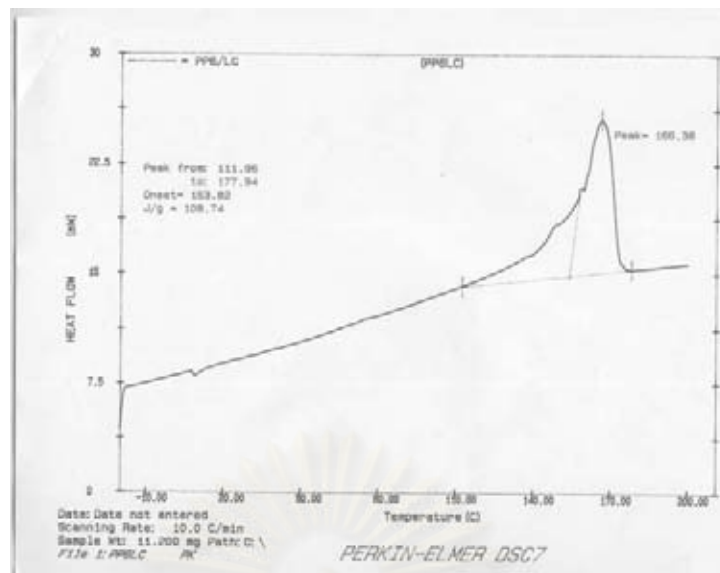


Figure B-12 : DSC curve of Polypropylene 6/1% LCC

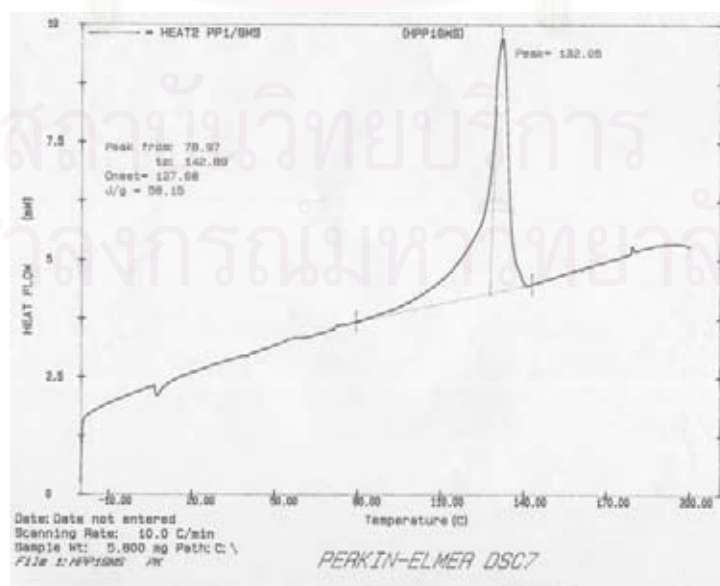
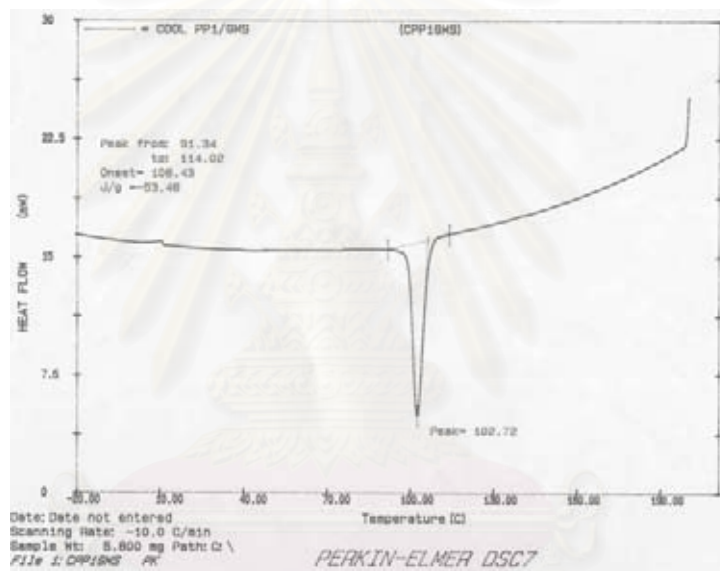
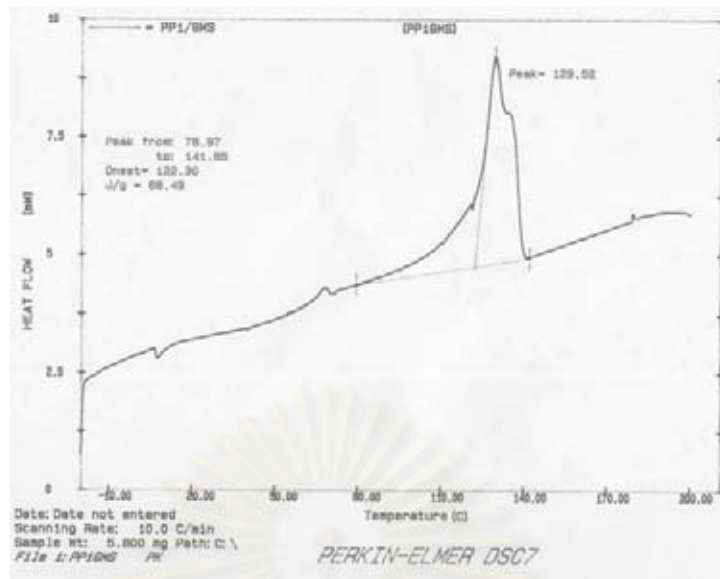


Figure B-13 : DSC curve of Polypropylene 1/1%GMS

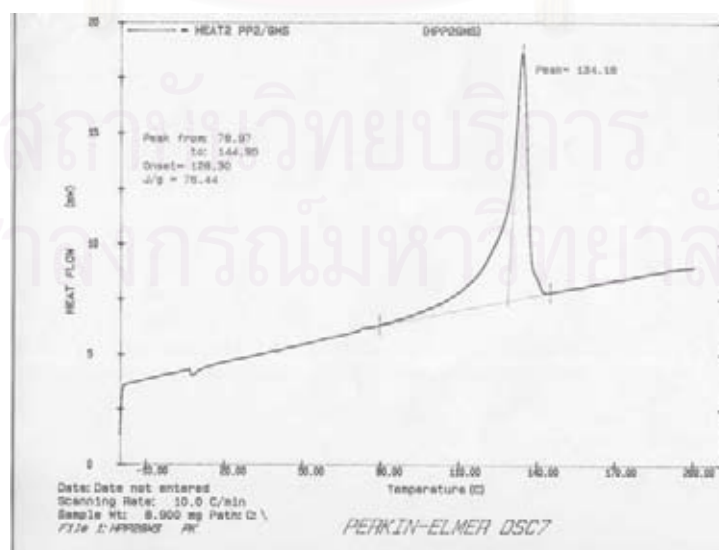
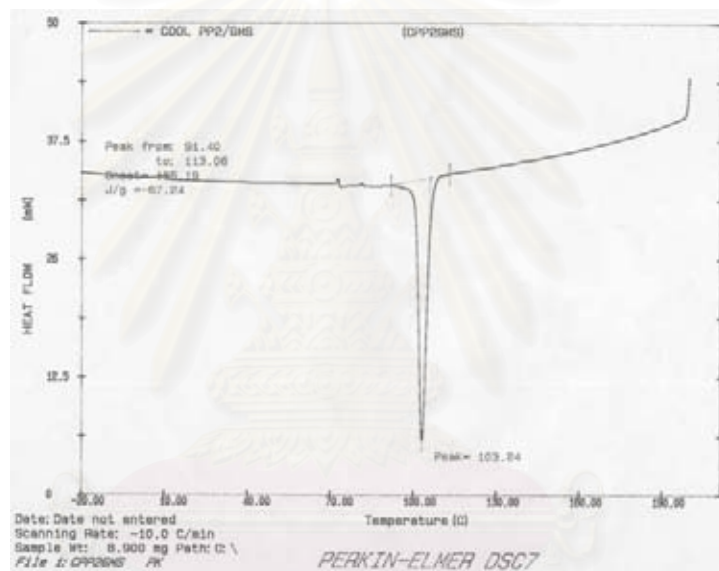
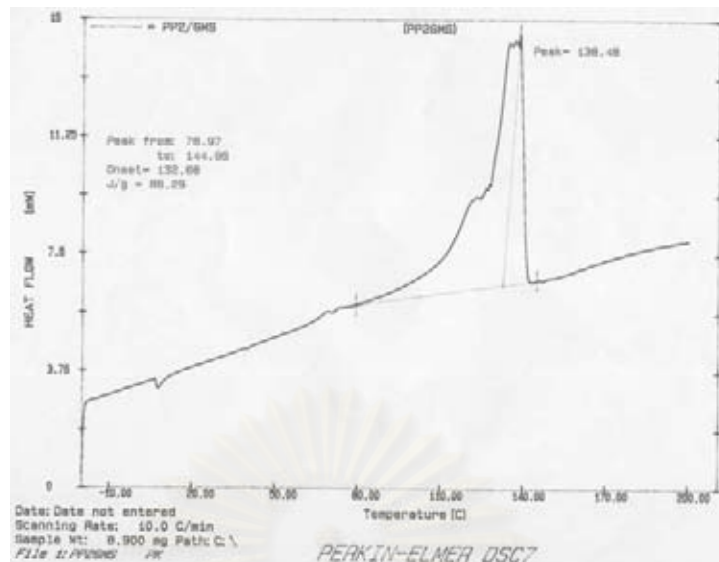


Figure B-14 : DSC curve of Polypropylene 2/1%GMS

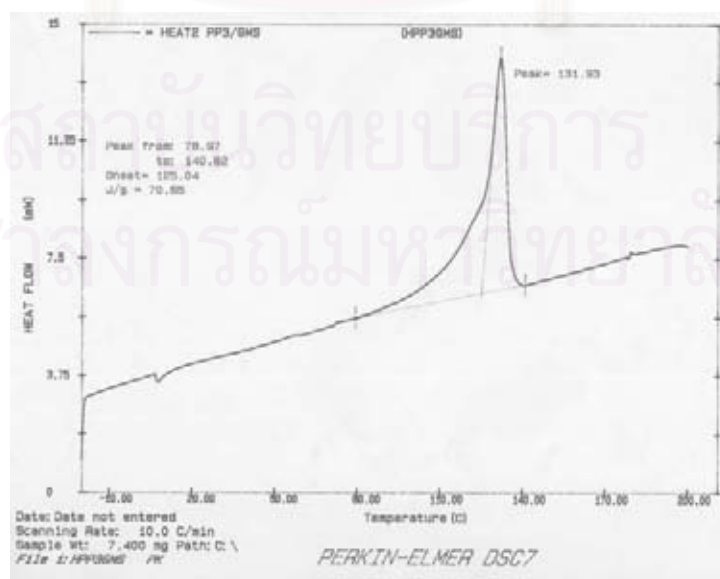
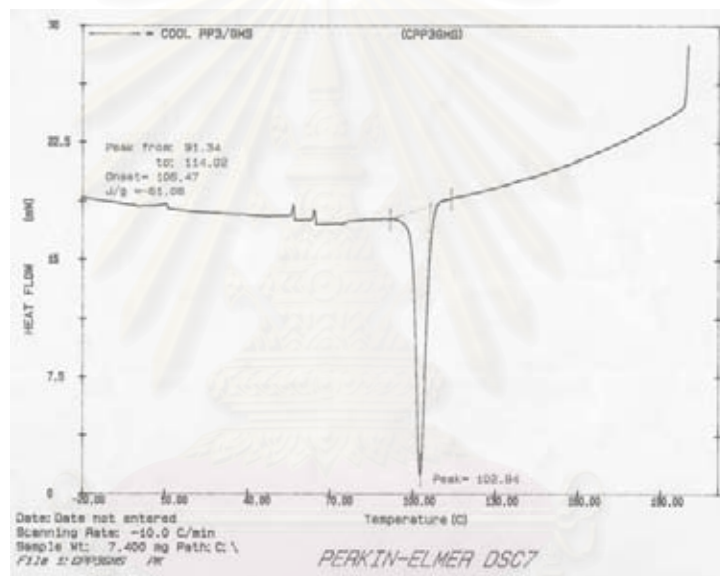
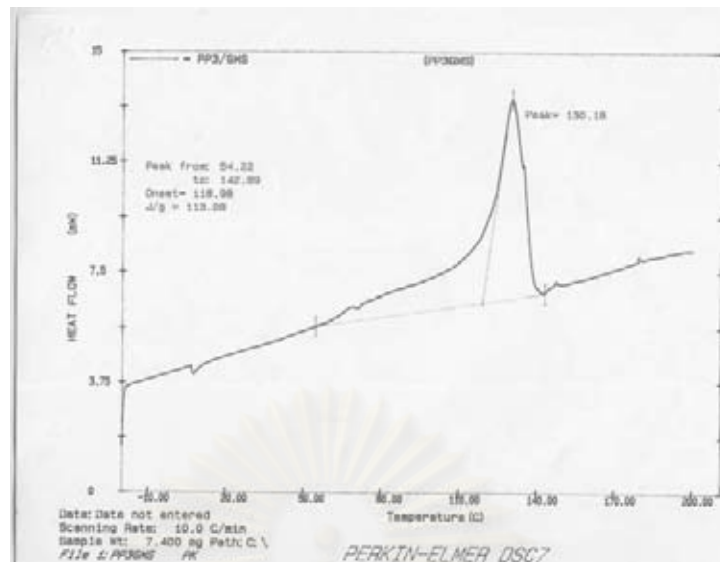


Figure B-15 : DSC curve of Polypropylene 3/1%GMS

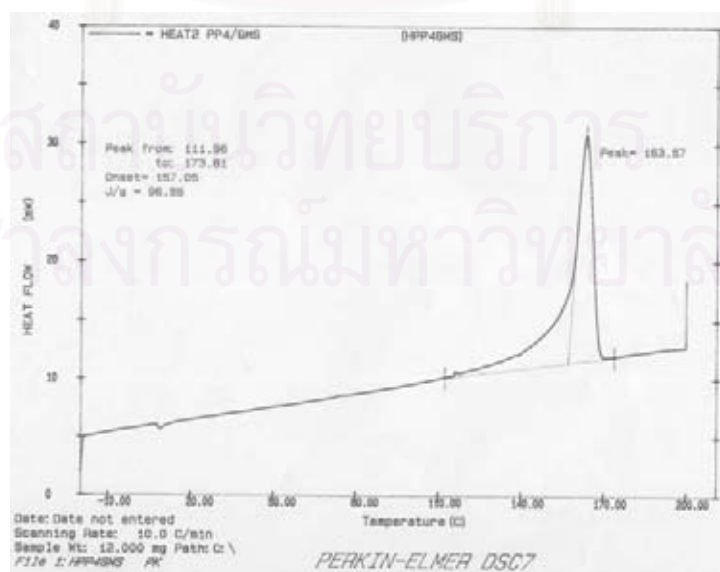
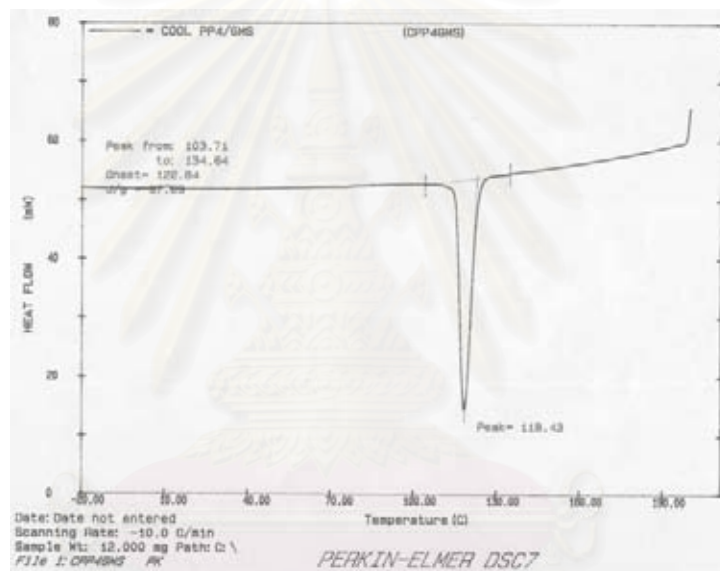
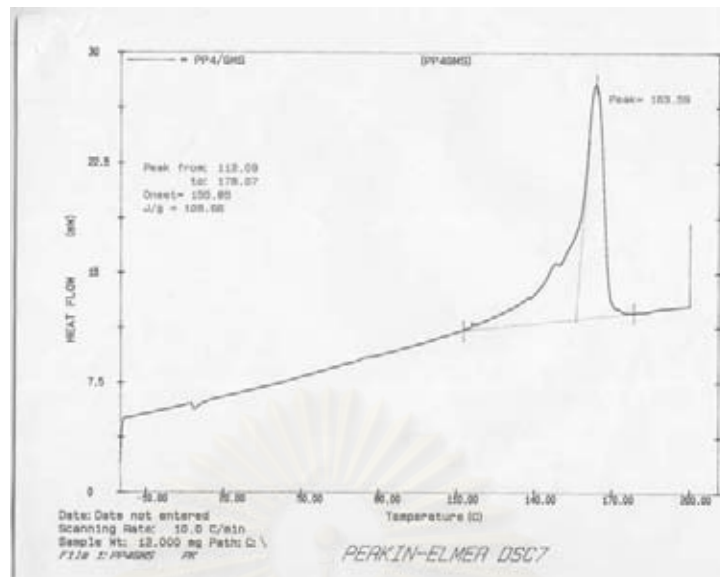


Figure B-16 : DSC curve of Polypropylene 4/1%GMS

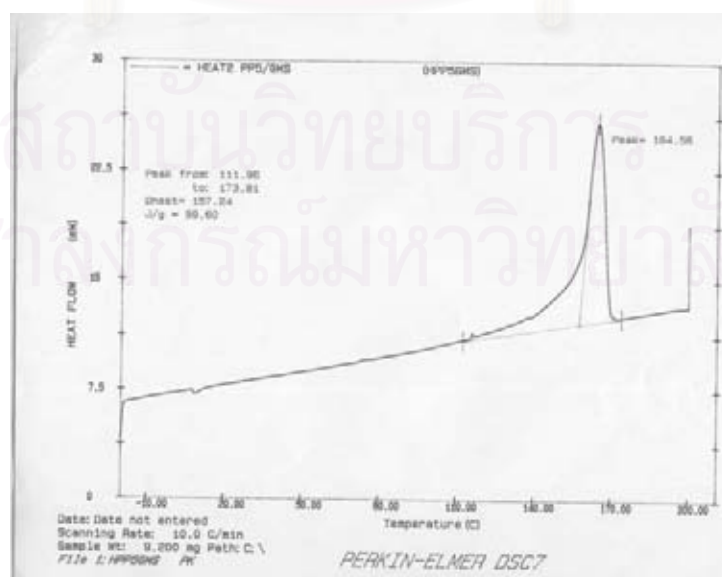
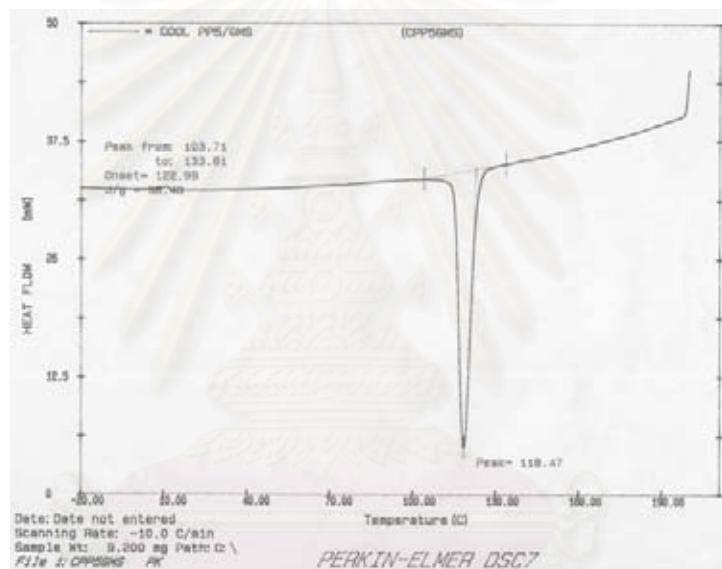
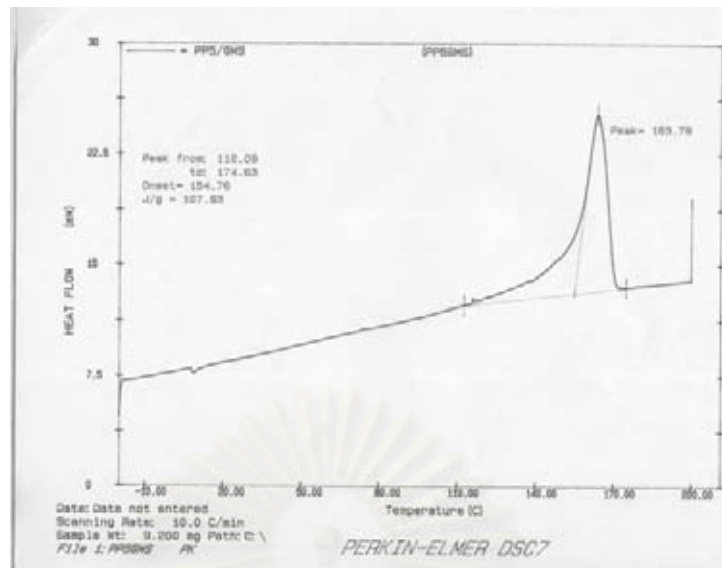


Figure B-17 : DSC curve of Polypropylene 5/1%GMS

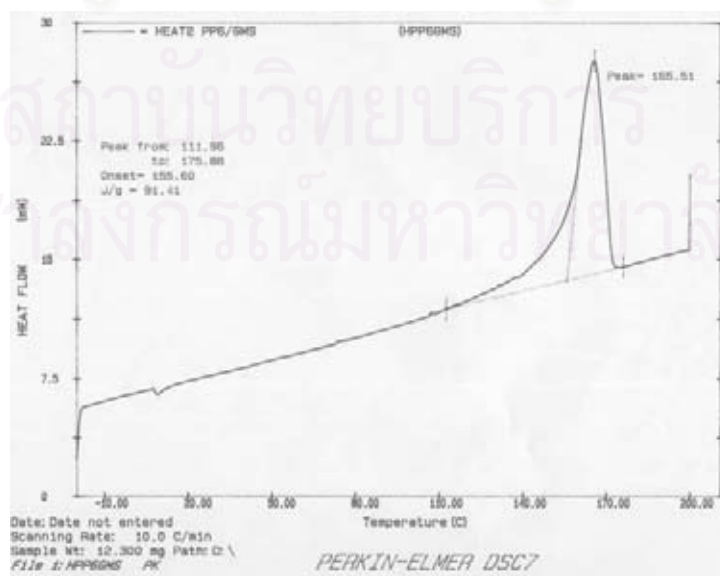
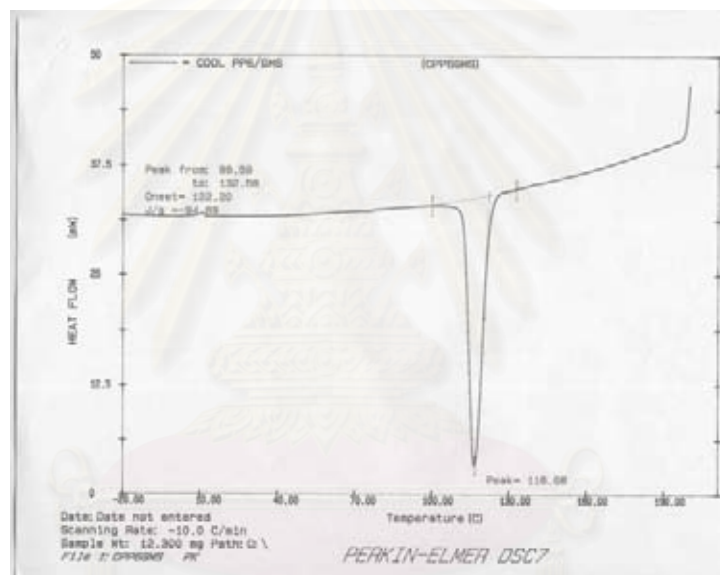
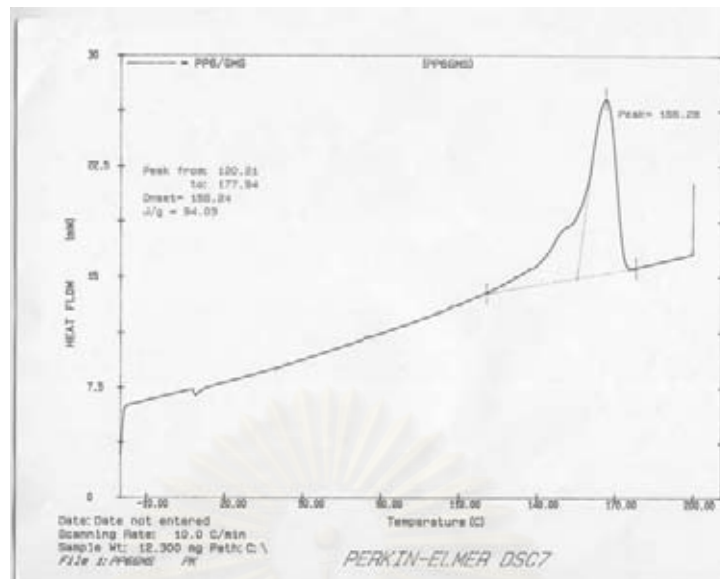


Figure B-18 : DSC curve of Polypropylene 6/1%GMS

Appendix C : The data of XRD characterization

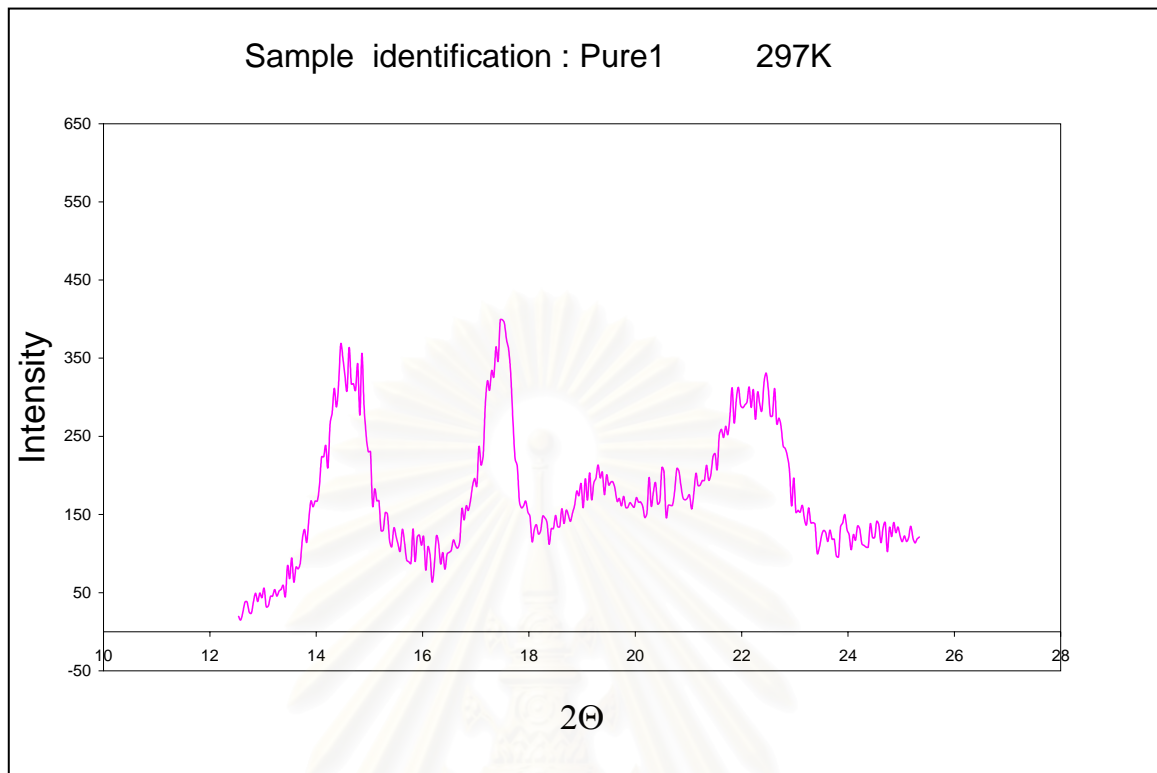


Figure C-1 : Amorphous curve of pure polypropylene1

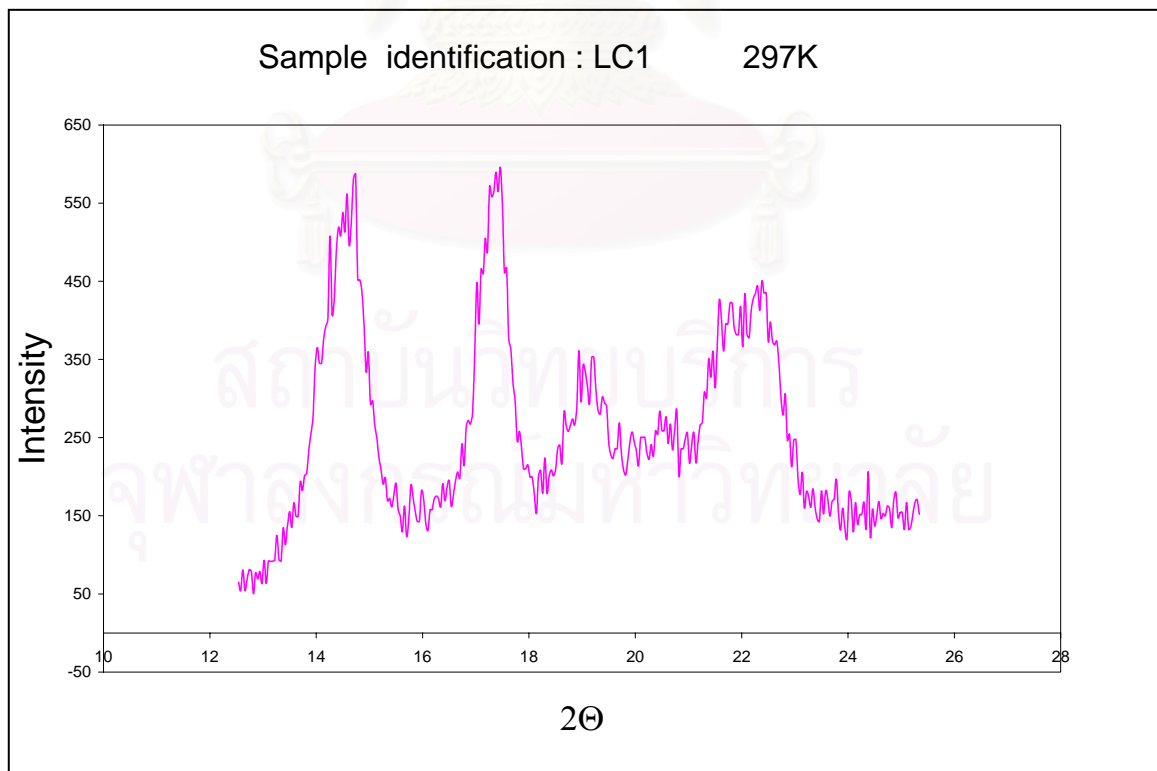


Figure C-2 : Amorphous curve of polypropylene1/1%LCC

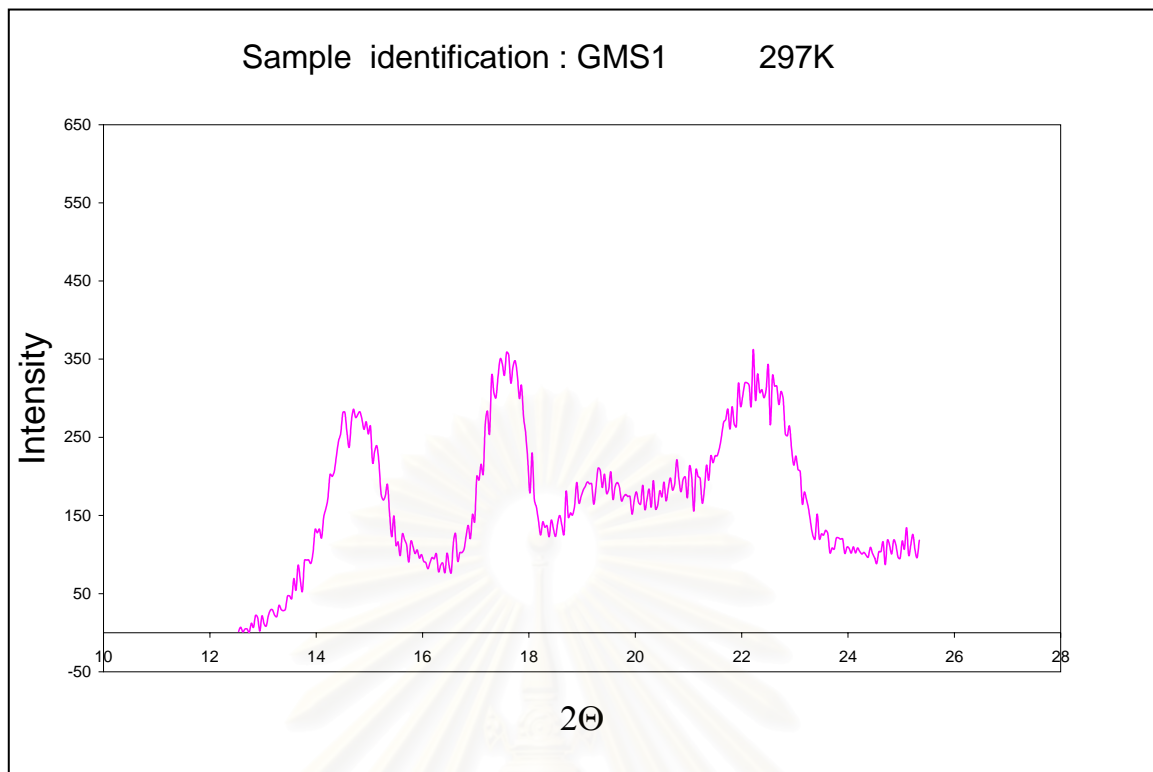


Figure C-3 : Amorphous curve of polypropylene1/1%GMS

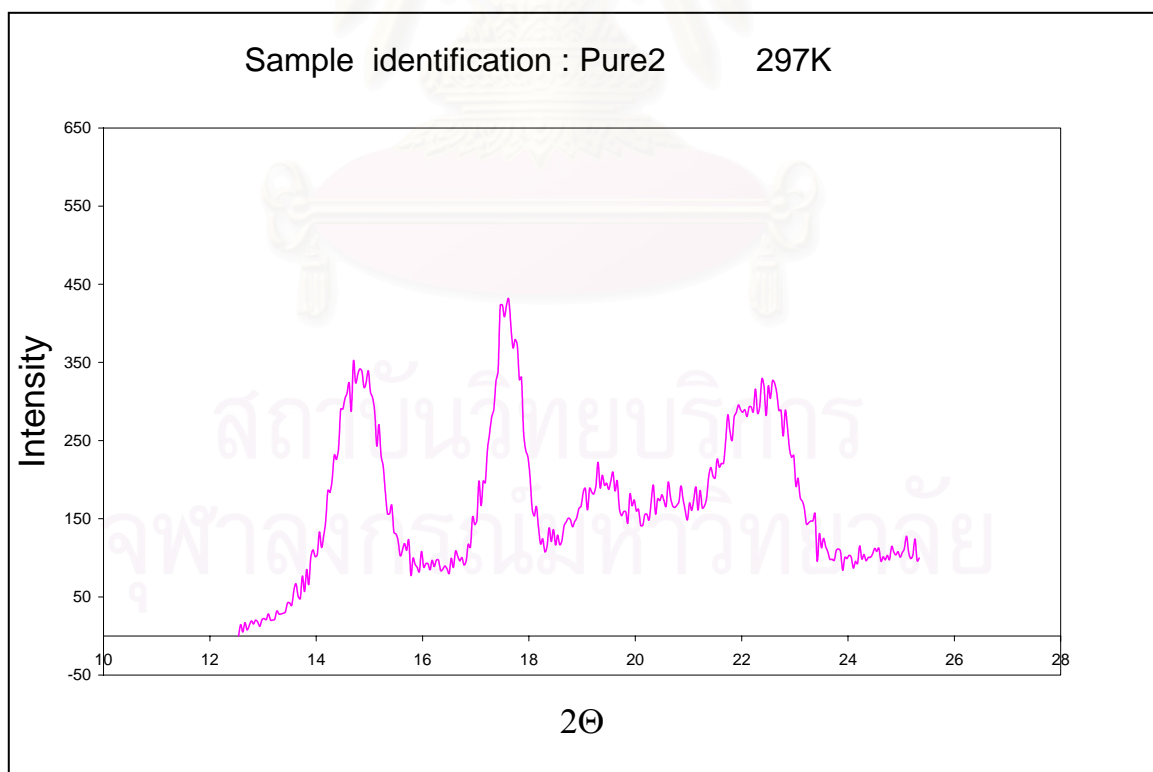


Figure C-4 : Amorphous curve of pure polypropylene2

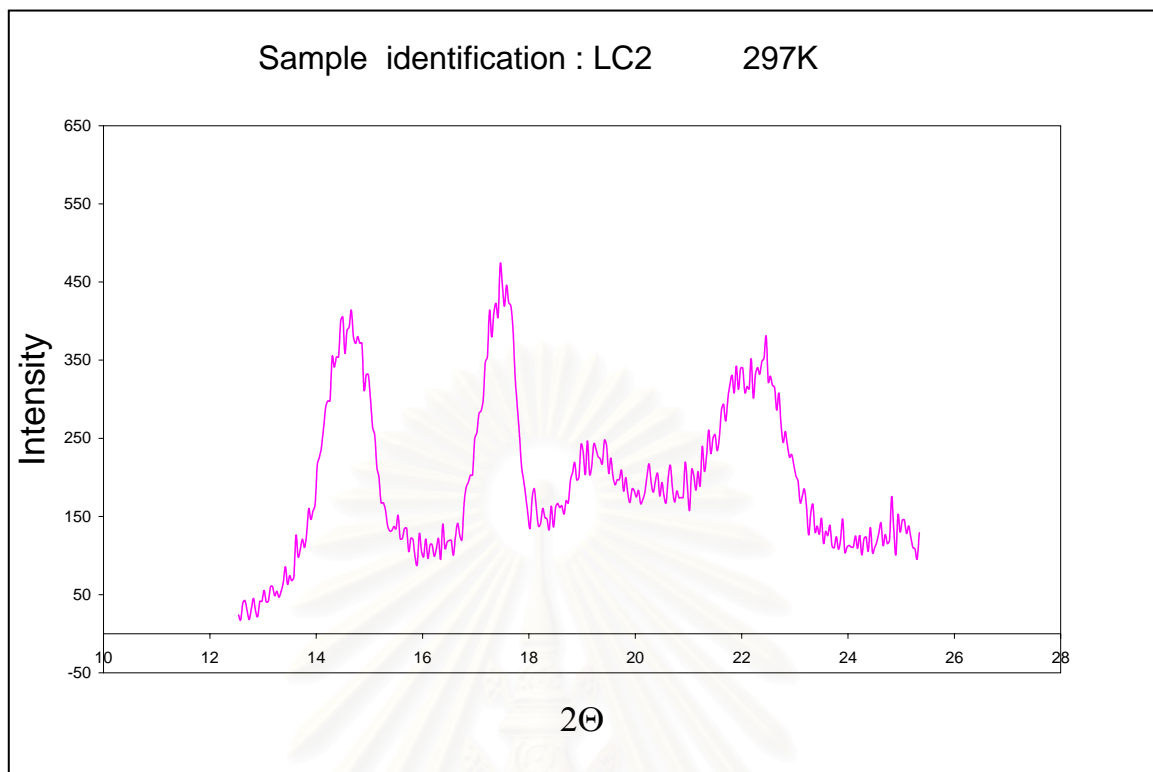


Figure C-5 : Amorphous curve of polypropylene2/1%LCC

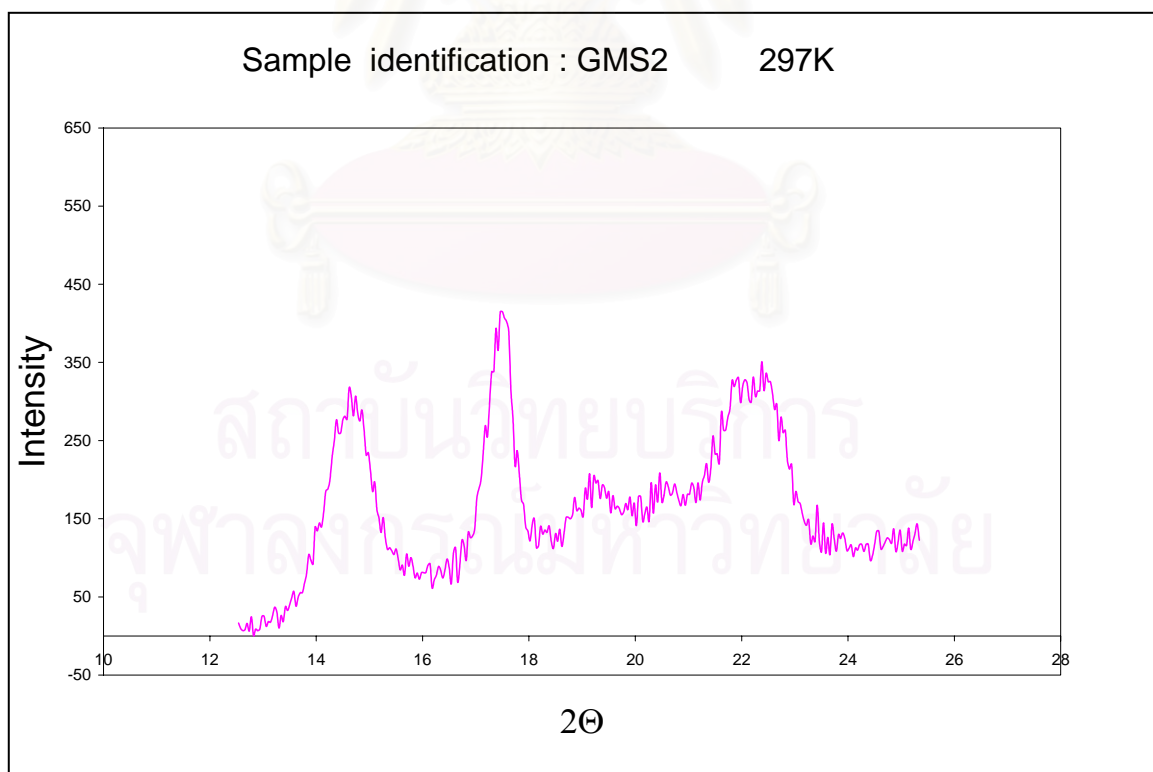


Figure C-6 : Amorphous curve of polypropylene2/1%GMS

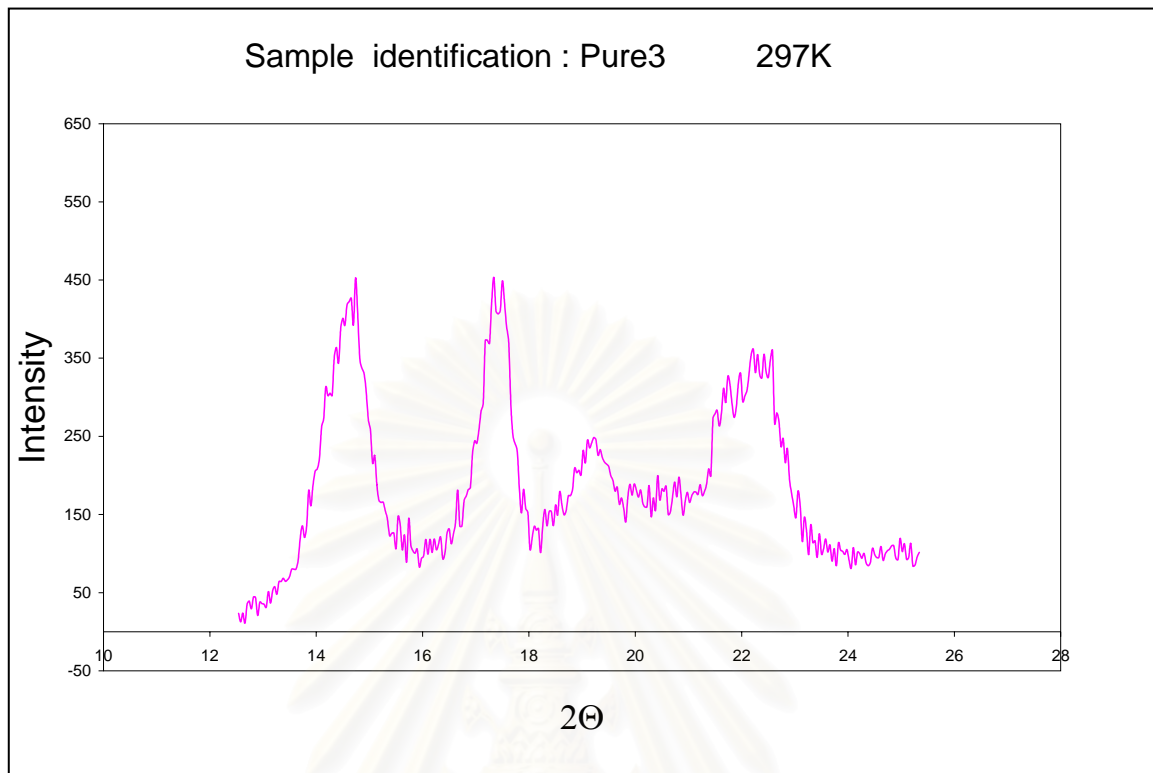


Figure C-7 : Amorphous curve of pure polypropylene3

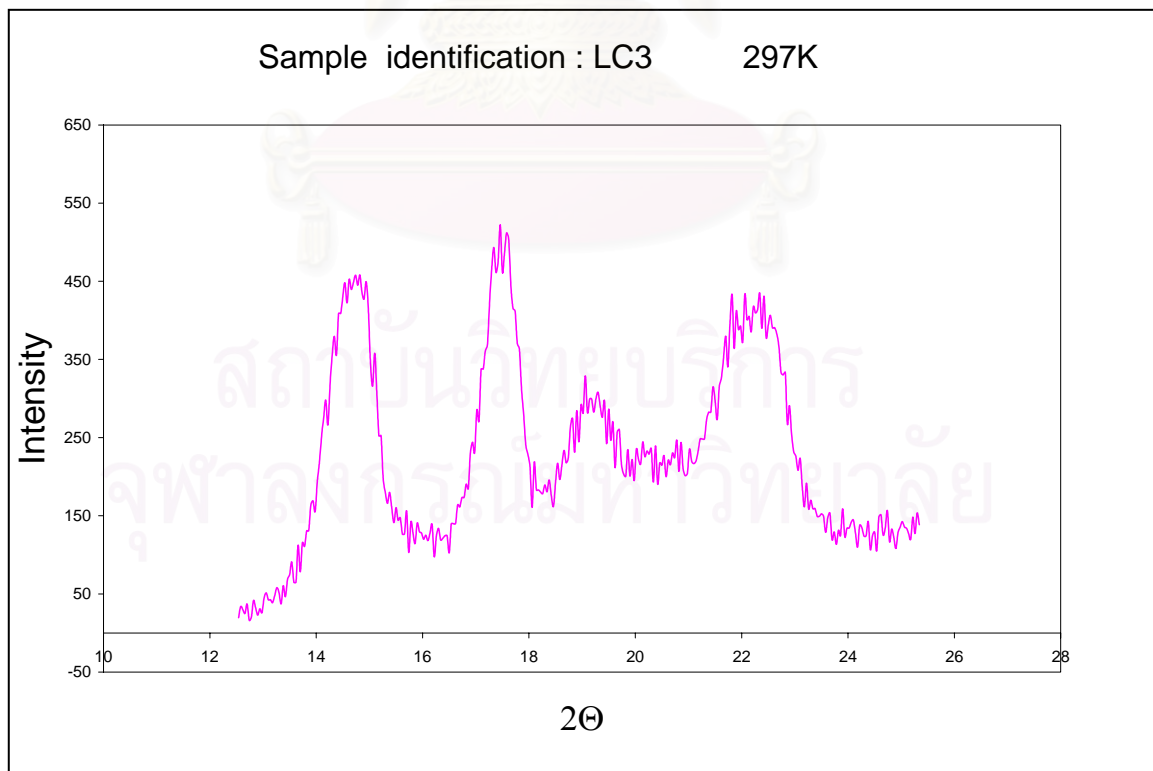


Figure C-8 : Amorphous curve of polypropylene3/1%LCC

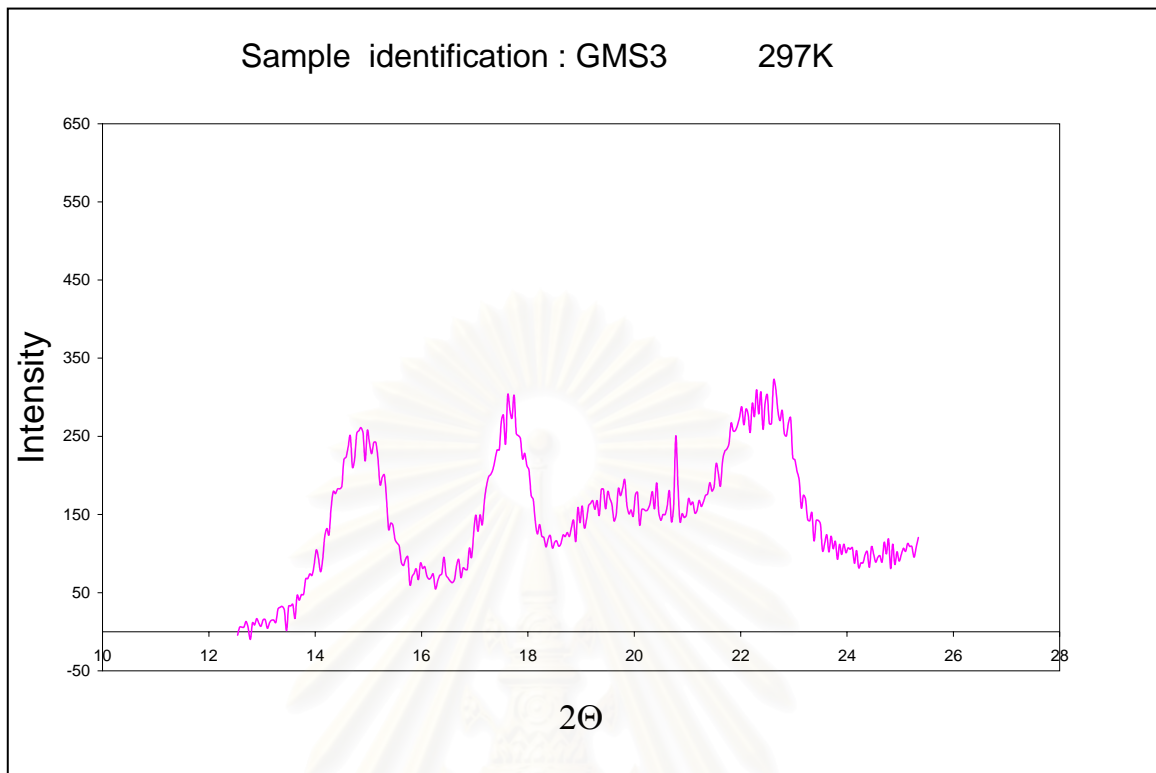


Figure C-9 : Amorphous curve of polypropylene3/1%GMS

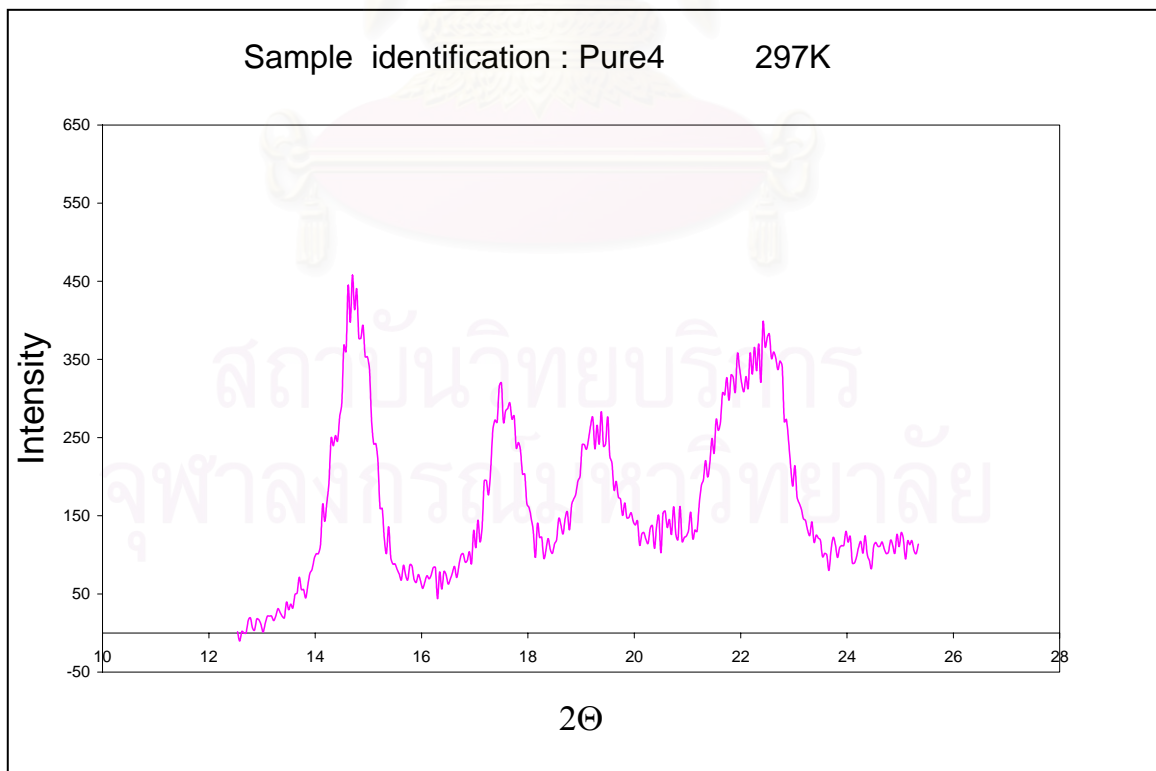


Figure C-10 : Amorphous curve of pure polypropylene4

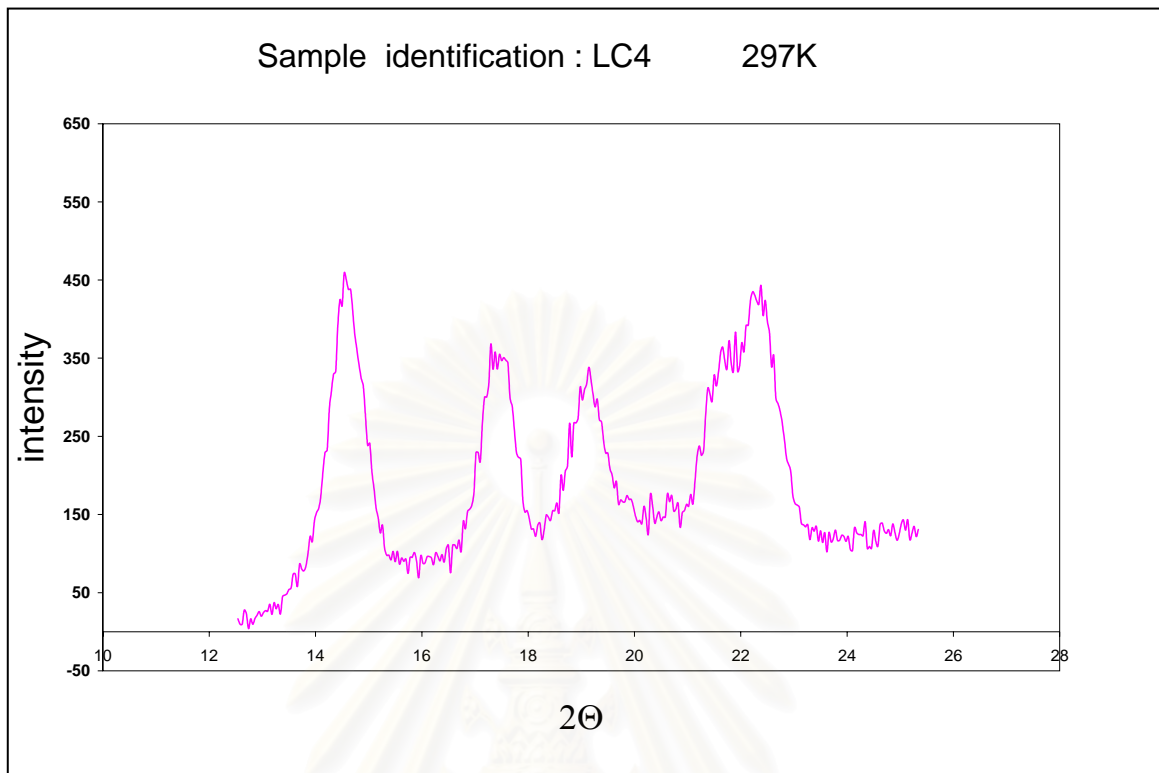


Figure C-11 : Amorphous curve of polypropylene4/1%LCC

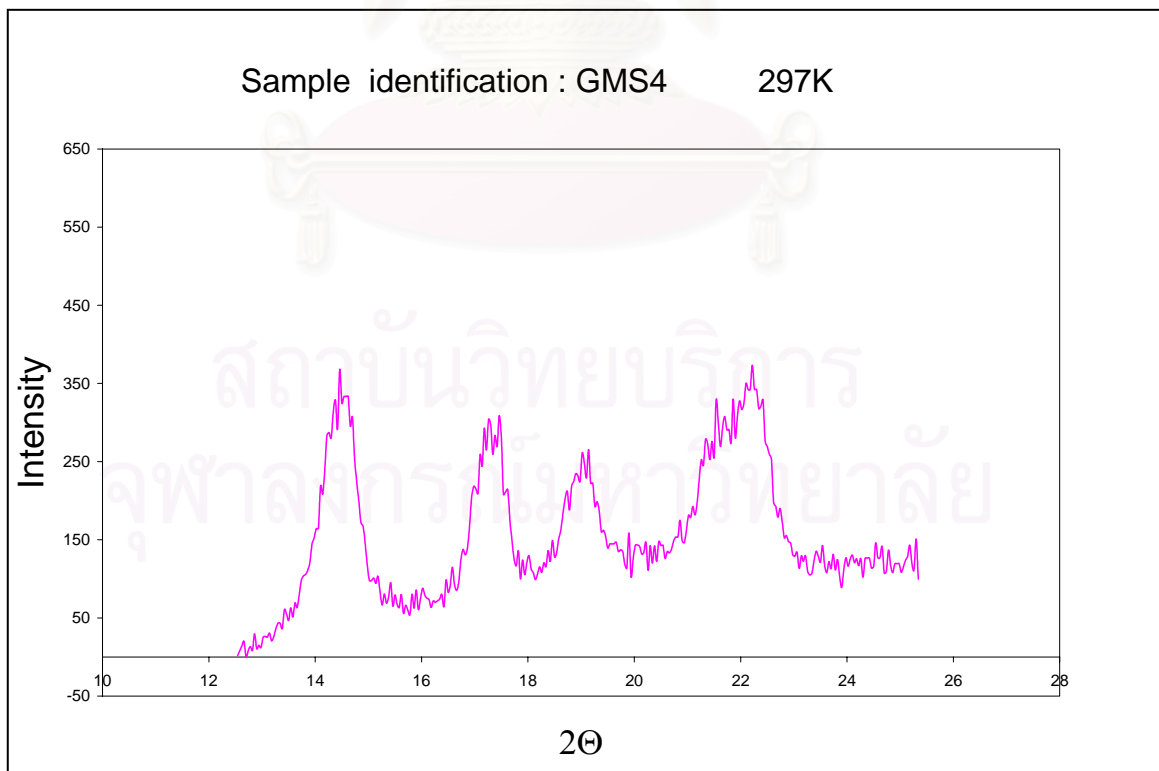


Figure C-12 : Amorphous curve of polypropylene4/1%GMS

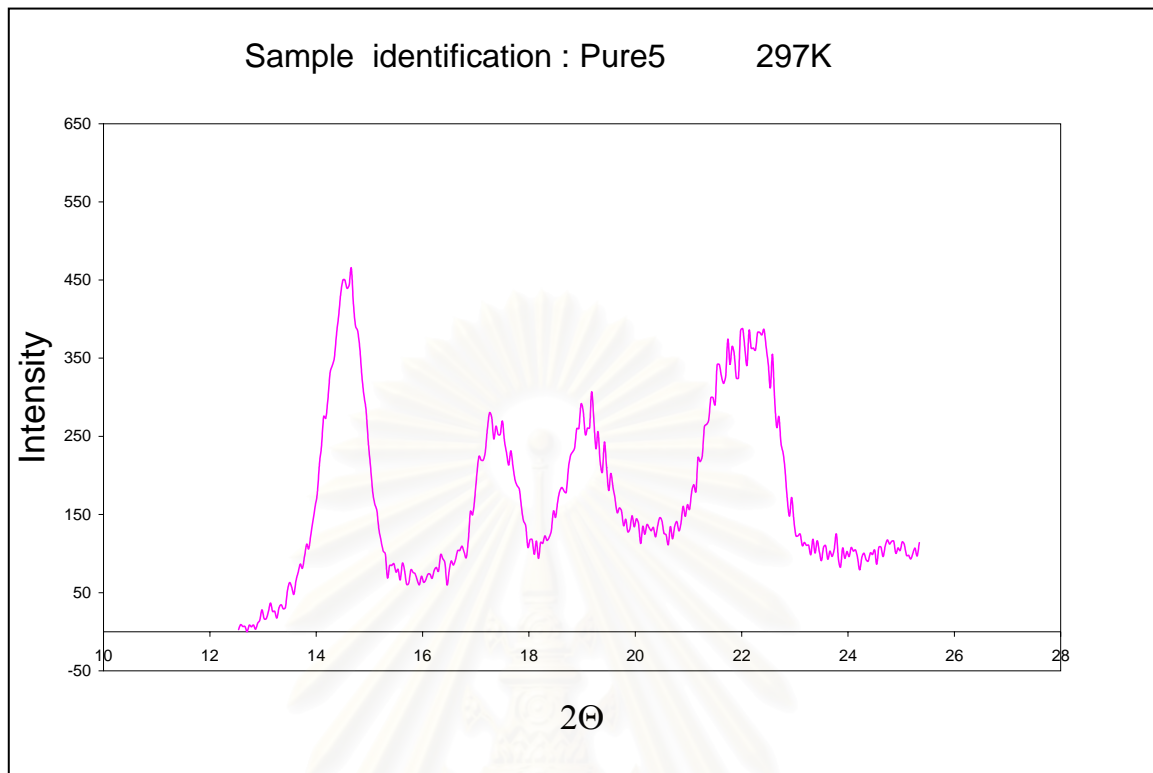


Figure C-13 : Amorphous curve of pure polypropylene5

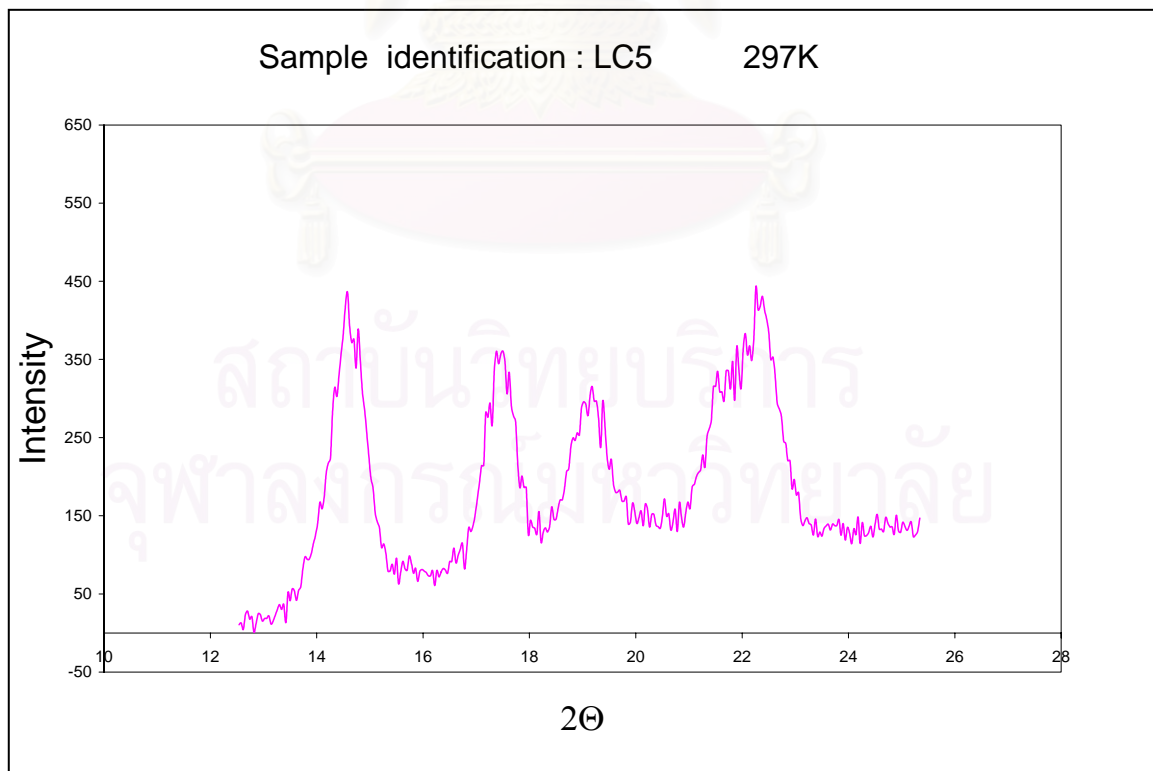


Figure C-14 : Amorphous curve of polypropylene5/1%LCC

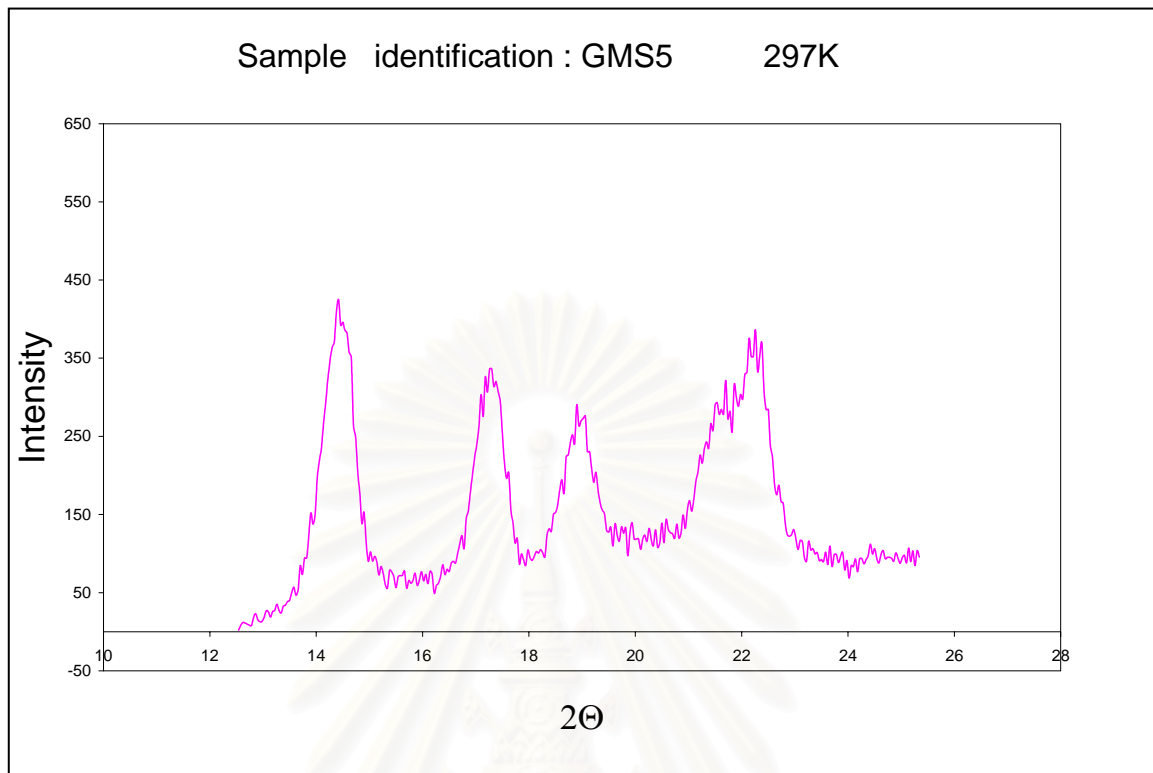


Figure C-15 : Amorphous curve of polypropylene5/1%GMS

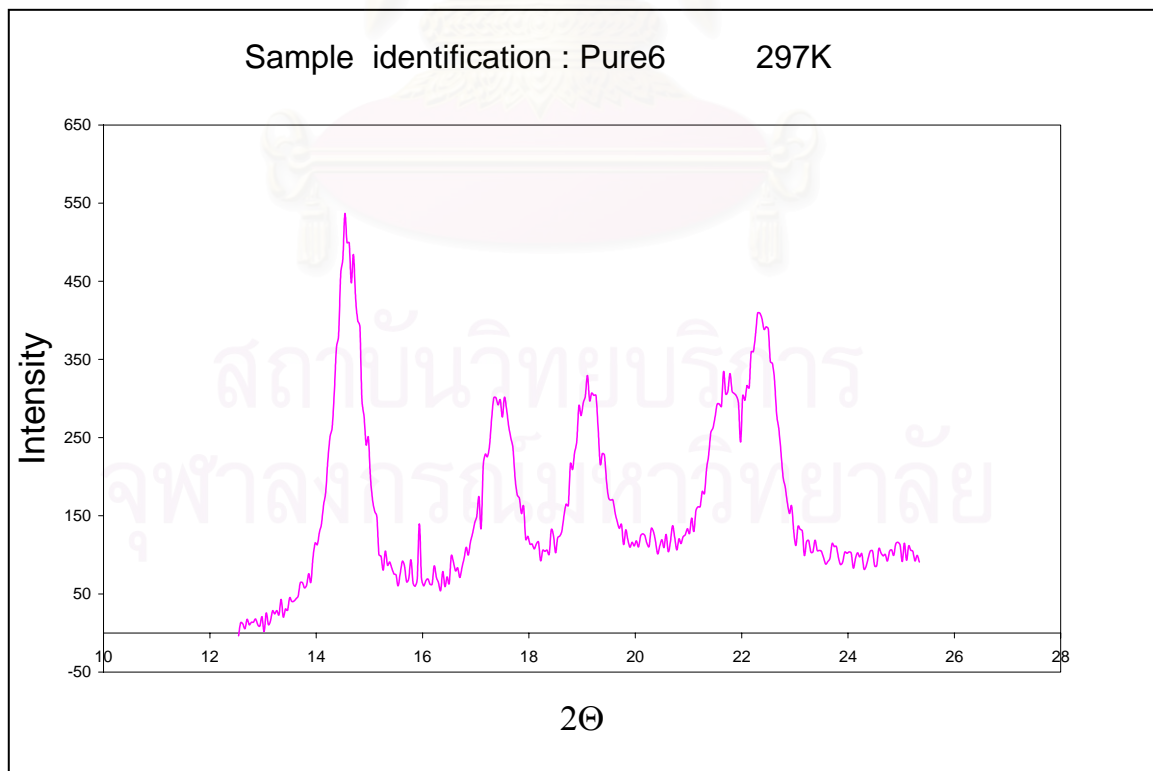


Figure C-16 : Amorphous curve of pure polypropylene6

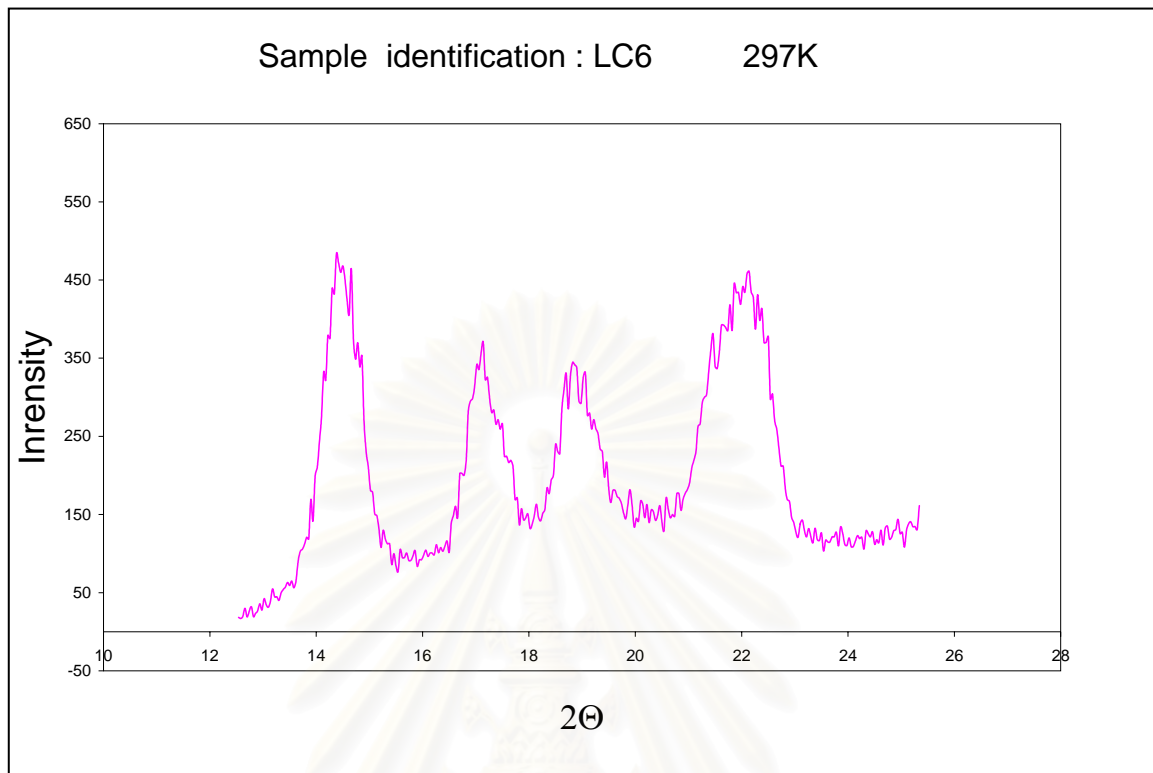


Figure C-17 : Amorphous curve of polypropylene6/1%LCC

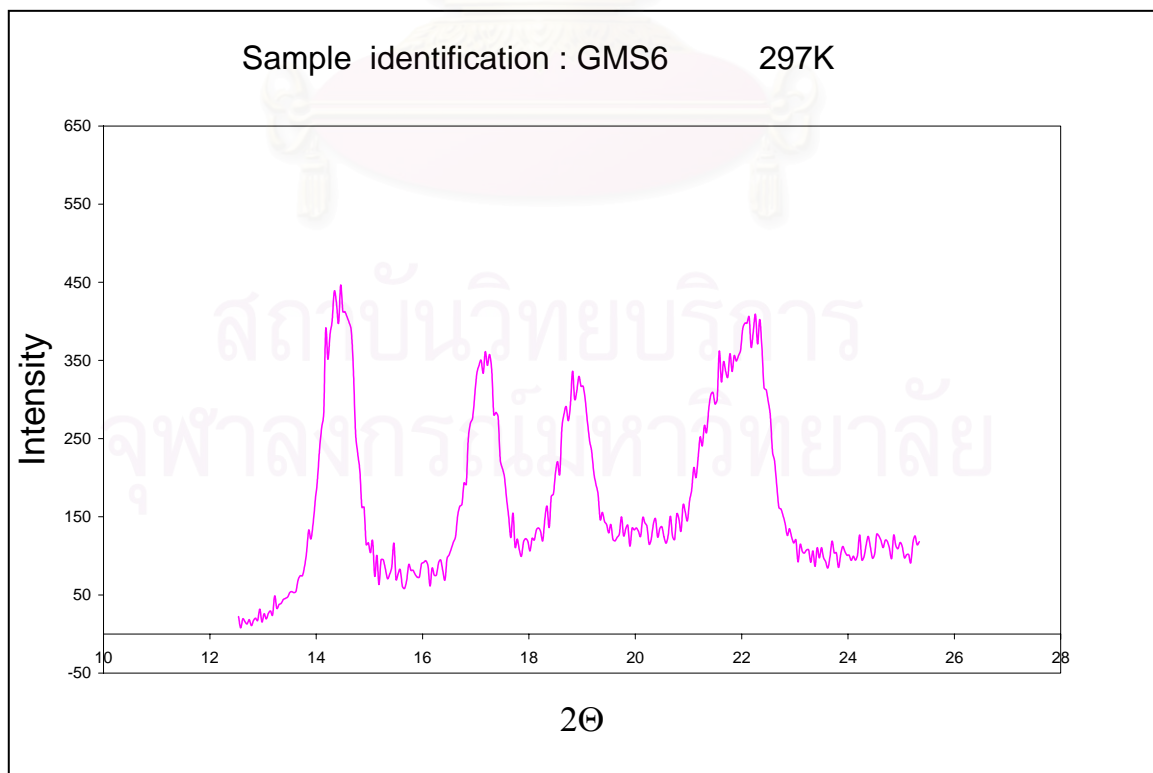


Figure C-18 : Amorphous curve of polypropylene6/1%GMS

Vita

Mr. Eakkalak Singnoo was born in Songkhla , Thailand in May 19, 1978. He received the Bachelor Degree of Engineering in Chemical Engineering from Department of Chemical Engineering , Faculty of Engineering , Prince of Songkhla University in 2000. He entered the Mater degree of Engineering in Chemical Engineering Program at Chulalongkorn University in 2002.



สถาบันวิทยบริการ
จุฬาลงกรณ์มหาวิทยาลัย